REMOTE SENSING APPLICATIONS IN FORESTRY

MONITORING FOREST LAND FROM HIGH ALTITUDE AND FROM SPACE

by

Personnel of the
Remote Sensing Research Work Unit

Pacific Southwest Forest and Range Experiment Station
Forest Service, U. S. Department of Agriculture

Final Report 30 September 197

A report of research performed under the auspices of the

Forestry Remote Sensing Laboratory,
School of Forestry and Conservation
University of California
Berkeley, California

A Coordination Task Carried Out in Cooperation with
The Forest Service, U. S. Department of Agriculture

For

EARTH RESOURCES SURVEY PROGRAM
OFFICE OF SPACE SCIENCES AND APPLICATIONS
NATIONAL AERONAUTICS AND SPACE ADMINISTRATION

REMOTE SENSING APPLICATIONS IN FORESTRY

MONITORING FOREST LAND FROM HIGH ALTITUDE AND FROM SPACE

by

Personnel of the
Remote Sensing Research Work Unit

Pacific Southwest Forest and Range Experiment Station
Forest Service, U. S. Department of Agriculture

Final Report 30 September 1972

NE-06- 00765-A

A report of research performed under the auspices of the

Forestry Remote Sensing Laboratory,
School of Forestry and Conservation
University of California
Berkeley, California
A Coordination Task Carried Out in Cooperation with
The Forest Service, U. S. Department of Agriculture

For

EARTH RESOURCES SURVEY PROGRAM
OFFICE OF SPACE SCIENCES AND APPLICATIONS
NATIONAL AERONAUTICS AND SPACE ADMINISTRATION

PREFACE

On October 1, 1965, a cooperative agreement was signed between the National Aeronautics and Space Administration (NASA) and the U.S. Department of Agriculture (USDA) authorizing research to be undertaken in remote sensing as related to Agriculture, Forestry and Range Management under funding provided by the Supporting Research and Technology (SR&T) program of NASA, Contract No. R-09-038-002. USDA designated the Forest Service to monitor and provide grants to forestry and range management research workers. All such studies were administered by the Pacific Southwest Forest and Range Experiment Station in Berkeley, California in cooperation with the Forestry Remote Sensing Laboratory of the University of California at Berkeley. Professor Robert N. Colwell of the University of California at Berkeley was designated coordinator of these research studies.

Forest and range research studies were funded either directly with the Forest Service or by Memoranda of Agreement with cooperating universities. The following is a list of research organizations participating in the SR&T program from October 1, 1965, until December 31, 1972.

1. Forest Service, USDA, Pacific Southwest Forest and Range Experiment Station, Berkeley, California.

2. Forest Service, USDA, Rocky Mountain Forest and Range Experiment Station, Fort Collins, Colorado.

3. School of Forestry and Conservation, University of California, Berkeley, California.

4. School of Forestry, University of Minnesota, St. Paul, Minnesota.

5. School of Natural Resources, University of Michigan, Ann Arbor, Michigan.

6. Department of Range Management, Oregon State University, Corvallis, Oregon.

This report summarizes the significant findings of this research and identifies research results which have been applied or are ready for application. In addition, the work carried on for the reporting period October 1, 1971, until December 31, 1972, is described in detail.

A listing of all research reports produced under NASA SR&T funding for forest and range studies can be found in the Appendix of this report.

TABLE OF CONTENTS

PERSONNEL

Salaries of all professional employees of the Remote Sensing Work Unit were contributed by the Forest Service. Employees at the Pacific Southwest Forest and Range Experiment Station assigned to these studies were:

Carl C. Wilson, Assistant Director

Robert C. Heller, Supervisory Research Forester and Work Unit Leader

Robert C. Aldrich, Principal Research Forester

John F. Wear, Forester

Frederick P. Weber, Research Forester

Nancy X. Norick, Mathematical Statistician

Robert W. Dana, Physicist

Wallace J. Greentree, Forestry Research Technician

Richard J. Myhre, Photographer

Kristina A. Zealear, Geographer resigned 7/1/72

Marilyn Wilkes, Programmer

Thomas H. Waite, Forestry Technician (Research)

Emanuel Moellman, Machinist (Maintenance)

Anne L. Weber, Work Unit Clerk

Mary L. Chin, Clerk-typist

Summer, part-time and Work Study employees assigned to the PSW remote sensing work unit include:

John Cole	James McSwanson
Richard Harris	Steven Ramirez
Benno Marx	William Toy

Cooperating Forest Service employees from other locations were:

Robert E. Stevens, Supervisory Forest Entomologist, Rocky Mountain Forest and Range Experiment Station, Fort Collins, Colorado.

John S. Schmid, Entomologist, Rocky Mountain Forest and Range Experiment Station, Fort Collins, Colorado.

Wilmer F. Bailey, Aerial survey specialist, Timber Management, U.S. Forest Service Region 2, Denver, Colorado.

Robert Mattson, Forester, Black Hills National Forest, Deadwood, South Dakota.

ACKNOWLEDGMENTS AND COOPERATORS

These experiments are being performed under the Earth Resources Survey Program in Agriculture/Forestry under the sponsorship and financial assistance of the National Aeronautics and Space Administration, Contract No. R-09-038-002. Research and administrative direction are provided by the Pacific Southwest Forest and Range Experiment Station. Other cooperators and their contributions are:

1. R. H. Miller, Assistant to the Administrator, ARS, coordinator for Agriculture/Forestry. Provided information and guidance on program planning and status.

2. R. N. Colwell, Professor of Forestry, and G. A. Thorley, Director, Forestry Remote Sensing Laboratory, School of Forestry and Conservation, University of California, Berkeley. Consultation and integration of forestry-NASA studies.

3. Richard P. Cook, David Stark, David Hessel, Black Hills National Forest, R-2, Spearfish and Lead, South Dakota. Provided maps, vehicles, and personnel.

4. Homestake Mining Company, Forestry Department, Spearfish, South Dakota. Permitted use of property to conduct experiment.

5. Richard Legault, Fabian Polcyn, Philip Hasell, Ed Work, Fred Thomson, and Frank Sadowski, Willow Run Laboratories, University of Michigan. Consultation, collection, and processing of multispectral scanning data.

SIGNIFICANT FINDINGS FROM SUPPORTING RESEARCH AND TECHNOLOGY STUDIES -- PERIOD OCTOBER 1, 1965 TO DECEMBER 31, 1972

A. INVENTORIES

1. Color infrared (CIR) film is the best photographic sensor to use for identifying forest and nonforest land uses from high altitudes.

2. Winter is the best season to take microscale CIR photography (1:120,000 to 1:2,500,000) for identifying broad forest types in the Southeastern United States. For example, 97 percent of all forest points were correctly identified by three interpreters, and 70 percent of the forest types on 1:420,000 CIR.

3. Based on a comparison of results from two independent studies, microscale CIR photography is useful for forest area estimates and as a basis for stratifying forest area in multistage forest inventories.

4. Multistage probability sampling as outlined in the S-065 Apollo 9 experiment for estimating timber volume demonstrated that such a system has excellent potentialities for earth resources inventories.

5. Automatic photo interpretation of forest and nonforest land uses using film density in pattern recognition techniques shows potential. However, at the present state of the art, the classification accuracies by those techniques are far too low to be useful in forest inventories.

B. STRESS

*1. A multistage probability sampling concept was developed for taking first small scale photographs, then large-scale photographs, and

---

*Research results which are being applied by forest managers.

finally ground samples to get rapid, reliable estimates of tree mortality from bark beetles.

*2. Scales as small as 1:32,000 are adequate for detection of infestations larger than 1 to 2 trees (>5 m) per infestation.

3. Determination of the rate of foliage discoloration of dying pine trees from bark beetle attack using sequential photography is facilitated by using Munsell charts and spectral analysis.

4. Neither normal color (NC) nor CIR film is useful as a previsual detector of stress in conifers.

5. Detection of discoloring trees in Western United States is as good on NC as on CIR at photographic scales of 1:15,840 or larger. At smaller scales, CIR is better.

6. Physiological studies showed that:

a. In the Black Hills in May, before foliage discoloration occurs and with full sun at midday, temperature differences were 2^{o} to 5^{o} C. greater on dying pines infested with bark beetles than on healthy pines.

b. Needle moisture, as measured by a pressure bomb, was consistently and significantly greater on dying trees than on healthy trees.

c. Vapor pressure deficit of the atmosphere, soil moisture availability, and solar radiation are important components of transpiration and should be measured.

---

*Research results which are being applied by forest managers.

d. No reliable temperature differences existed between Douglas-fir trees infested with Poria weirii and healthy firs. Spectral differences were also minimal between infected and healthy firs.

7. A digital data acquisition system for collecting 80 channels of biophysical data was developed prior to the launch of ERTS for rapid data analysis. The system is being used to check biophysical data transmitted via data collection platforms (DCP) to ERTS from these field sensors.

8. Expertise in collecting and processing multispectral scanner (MSS) data was developed in this program toward ultimate automatic photo interpretation and automatic data processing.

9. Accuracy in classifying forest stress signatures with multispectral scanners and processors varies and can be rated according to the following categories:

a. Good for separating healthy trees from discolored dead trees.

b. Good for separating conifers from hardwoods.

c. Poor (because of high omission and commission errors) for detecting stressed pines previsually, although no analysis has been done for MSS imagery taken in May 1972 with a single-aperture scanner. All indications point to more accurate identification of previsual signatures with the newer MSS.

d. Poor for identifying widely separated individual pine trees affected by air oxidants.

e. The seven wavebands found most efficient to identify forest targets are summarized as follows by waveband and forest use class:

MICROMETER WAVEBANDS	TREE VIGOR w/snags	TREE VIGOR no snags	FOREST LAND USE	TREE SPECIES	RANGE	WATER*
0.40 - 0.44	X	--	--	--	--	X
0.55 - 0.58	X	X	--	X	X	--
0.66 - 0.70	--	X	X	--	--	X
0.70 - 0.74	X	X	--	X	X	X
1.5 - 1.8	X	X	X	X	--	X
2.0 - 2.6	--	--	X	X	X	--
9.3 - 11.0	X	X	X	--	X	X

*Includes water turbidity and thermal pollution.

10. Poria weirii (root rot) signatures on Douglas-fir trees in the Cascade Mountains of Oregon have a distinctive ringworm appearance and can be detected on small-scale aerial photographs (on black-and-white as well as on NC or CIR films) -- scale 1:200,000. They might also be detectable on satellite imagery.

C. CALIBRATION AND STANDARDIZATION OF AERIAL FILMS

1. The instrumentation for precise calibration of color aerial film (both NC and CIR) has been developed. Daylight spectral distributions were investigated, and a lamp-filter combination was found to match the typical daylight curve within 0.06 on the $\log_{10}$ scale.

2. A practical field test of color aerial films (NC and CIR) was performed with sensitometric calibration. The general cyan cast of

Eastman Kodak SO-397 film was noted while a slight strength in red and orange colors was attributed to Anscochrome D/200 for spiral reel processing. For overall vegetation, Kodak Aerochrome Infrared (2443) with the Wratten 12 filter was considered better than Kodak Ektachrome Infrared (8443 and 2443) plus Wratten 12 filter, plus CC30 Blue. The latter combination gave the best results for a Colorado range area.

3. A mathematical model of the form $D = A\, e^{-(\beta_o + \beta_1 x + \beta_2 x^2 + \beta_3 x^3)} - C$ was found to fit the characteristic curves of type 2443 CIR film--D being integral density and x equaling log exposure. The model fit the data within 0.03 density units in some cases.

SECTION SUMMARIES

SECTION I - FOREST INVENTORY

Forest and Nonforest Land Classification Using Aircraft and Space Imagery

A test was made to determine the accuracy of interpretation for 13 forest and nonforest land classes on 1:120,000 scale high-altitude color infrared (CIR) photographs. These photographs covered the same eight 41-square-kilometer (16-square-mile) study areas near Atlanta, Georgia, used to test 1:420,000 scale photography in 1971. The photographs were taken during a period of 20 months to represent four seasons -- winter, early summer, late summer, and late fall. Over 97 percent of forest points were interpreted correctly regardless of season. Approximately 80 percent of the combined forest types were correctly identified on winter photography -- 80 percent of the pine and pine/hardwood types combined, 76 percent of the bottomland hardwood, and 85 percent of the upland hardwood. Only 33 percent of the pine/hardwood type was correctly identified and should not be classified on microscale photography. The major difference between the results of this test and the test made on 1:420,000 scale CIR lies in the improved accuracy of classifying agricultural land uses. By class, the improvements ranged from 7 to 40 percent. A summary of the capabilities of large-, medium-, small-scale, and microscale photography is given for forestry. The cost of high-altitude photographic coverage is estimated and compared with the present cost of photos used in the Forest Survey design.

The use of film density for land classification is described in two separate tests. In one, a Philco-Ford film density slicing technique was used to enhance two Apollo 9 CIR photographs. The results showed that color separations will never consistently represent the same land use class unless a technique is devised to equalize density representations within the photo frame. In the second test, red, green, and blue densities were measured on 1:420,000 CIR film for 13 forest and nonforest land use classes. The films were taken during four seasons -- winter, early summer, late summer, and late fall. The densities were normalized and the means and standard deviations computed for each forest and nonforest class. The results show that the combination of red density and winter photography provides the best discrimination between classes. However, variations caused by differences in spectral sensitivity of the film layers to differing light levels and light quality across the film format, as well as those resulting from differences in the position of the density measurement within the film format, cause standard deviations of the class means to overlap. This makes class separation impossible using film density alone.

Classification of Land Use by Automated Procedures

A combination of both supervised and unsupervised pattern recognition techniques was used in the analysis. First, the area was scanned on 1:120,000 color infrared (CIR) film by an automatic scanning microdensitometer with a red, a blue, a green, and a clear filter. Then a clustering algorithm based upon the empirical multivariate distribution of red minus clear, blue minus clear, and green minus clear

densities was used to group picture elements into three-dimensional rectangles formed by defined density intervals -- one from each color. All elements falling into a given rectangle were coded by one of 16 symbols and printed out by computer. The computer map was then colored according to a code. The computer map, the color scheme for clusters, and a map made from interpretation of the aerial photograph are shown for comparison. A first attempt to automatically locate boundaries between areas of dissimilar types is also illustrated.

Land Use Classification in the Southeastern Forest Region by Multispectral Scanning and Computerized Mapping

Airborne multispectral scanner data were collected over two test sites in the southeastern forest region of the United States to test the feasibility of mapping important land use categories. New theoretical techniques were applied to preprocessing compensation for effects of atmosphere and changing solar irradiance. A major contribution of the study is the analysis of signature extension capabilities from one training flight line to three additional lines for both blocks. Qualitative and quantitative analyses of SPARC system processed data are made by comparison to ground truth information as interpreted from 1:35,000 scale color infrared (CIR) photographs and field examination. The effects of time-of-day for MSS data collection versus optimum channel selection are discussed in terms of the impact on classification mapping accuracy.

SECTION II - FOREST STRESS

The Use of Airborne Spectrometers and Multispectral Scanners for Previsual Detection of Ponderosa Pine Trees Under Stress from Insects and Diseases

The installation of ground truth instrumentation and data collection for the May 1972 airborne multispectral scanner (MSS) test flight in the Black Hills is discussed. The final feasibility test for the use of airborne MSS equipment for previsual detection of forest stress employed the University of Michigan M-7 multispectral scanner. This was the first application of a single-line-of-sight scanner for previsual detection of stress in conifer forests. The final test included several innovations in data collection including the addition of a very narrow band, deep-red channel (0.71 to 0.73 micrometers (μm)) apart from the normal spectrometer channels, and flying the scanner in a 45° forward-looking oblique configuration. Primary channels for previsual stress detection were as follows: (1) 0.40 to 0.44 μm, (2) 0.55 to 0.58 μm, (3) 0.66 to 0.70 μm, (4) 0.71 to 0.73 μm, (5) 1.5 to 1.8 μm, and (6) 9.3 to 11.0 μm. Ratio processing of channels 4 to 2 and channels 5 to 2 is expected to make a significant contribution to previsual detection of stress.

Trend and Spread of Bark Beetle Infestations in the Black Hills

A discussion is given of the use of aerial photography for monitoring the trend and the spread of bark beetle infestations in the Black Hills. Analysis of 1:33,500 scale color infrared (CIR) aerial photographs

taken in May 1972 and 1:32,000 CIR photos taken in September 1972 shows an overall 4.3 to 1 increase in beetle infestations within a 93-square-kilometer area of the northern Black Hills. Most significantly, a 3.3 to 1 increase was noted in the infestation size class of 11 to 25 meters. This class is known to contain the greatest volume of merchantable timber over the entire epidemic area. For the past several years, SR&T-supported research has provided new techniques for coordinating entomological information on population dynamics with new techniques developed for assessing beetle impact through the use of aerial photography. Considerable new photo interpretation data (from both large- and small-scale photography) now permit us to optimize photo scale against interpretation errors, given a clear definition of the objectives of the survey.

Detection of Root Disease Impacts on Forest Stands by Sequential Orbital and Suborbital Multispectral Photography

This report summarizes the work done over the past eight years to detect stress caused by a primary forest disease in the Douglas-fir type of the Pacific Northwest and indicates the potentiality of using orbital and suborbital multispectral photography for identifying Poria disease signatures. The initial postulation that a remote sensing technique in the visible or infrared portion of the electromagnetic spectrum might provide previsual discrimination between healthy and diseased trees has not been sufficiently successful to recommend under

normal growing conditions. No tests were conducted in root-rot areas under extreme drought conditions or advanced stages of tree decline; such conditions might permit previsual detection by remote sensing.

A more encouraging approach has been the distinct signature of Poria root-rot centers identified on aerial photographs in the high Cascades of Oregon by the circular bare-ground pattern associated with the progressive spread of the disease. Three test sites have been established in Oregon to determine the extent to which a unique signature can be detected in different forest conditions. Photo interpretation needs to be completed and compared with ground data before we can say how useful remote sensing is to analyze the impact of this root-rot disease on the forest resource.

SECTION III - STANDARDIZATION AND CALIBRATION STUDIES

Development and Field Test of an ERTS-Matched Four-Channel Spectrometer

The design, calibration, and field test of the Forest Service RS-2 field spectrometer are described. The RS-2 is a lightweight and self-contained instrument designed to obtain simultaneous radiometric data in four spectral bandpasses which are identical to those of the ERTS-1 multispectral scanner (MSS). Calibration tests with a precision light source and reflectance standards show the RS-2 is highly accurate in the measurement of target exitance in each of the four ERTS MSS bandpasses. Results are presented of the field test at Atlanta, Georgia (test site 217) in November 1971 which show the relationship between target spectral radiance measured simultaneously on the ground with the RS-2

spectrometer and the University of Michigan airborne M-7 multispectral scanner. The application of the Forest Service RS-2 spectrometer for the measurement of spectral radiance on the ERTS-1 experiment 226A (Black Hills) is discussed.

Calibration of Focal Plane Shutters

A technique is described for measuring the exposure times of focal plane shutters with special emphasis on aerial cameras. The components are a small He-Ne laser, silicon phototransistor detector with amplifier, and an oscilloscope or electronic counter. A sample and hold circuit is described which seeks out the approximate half amplitude points of the light pulse through the shutter for measurement of half width on the time base.

Mathematical Modeling of Film Characteristic Curves

A mathematical model for the D versus LogE characteristic curves of color reversal films has been empirically derived. The equation for density takes the form of an exponential function in log exposure and has been tested for color response curves of Eastman Kodak 2443 color infrared (CIR) film. Results for one sample of film yield least square fits with standard error less than 0.033 density units of three color response curves (red, green, clear). The standard error for the blue response is 0.079. Suggestions are presented for the improvement of the latter.

FOREST AND NONFOREST LAND CLASSIFICATION USING AIRCRAFT AND SPACE IMAGERY

by

Robert C. Aldrich and Wallace J. Greentree

INTRODUCTION

Three applications of remote sensing that will have a great impact on extensive forest inventories in the future are: (1) determining the area of commercial forest land, (2) measuring changes in the area of commercial forest land, and (3) detecting disturbances on commercial forest land from both natural and man-made causes. These and other factors were a strong influence in selecting the objectives of the research study reported here.

Determining the feasibility of using high-altitude and space imagery for defining forest and nonforest land use and for detecting disturbances in the forest environment was the long-range research objective of this study. There were a number of intermediate objectives as well. One was to resolve the question of season -- what is the best season for discriminating between forest and nonforest classes? What are the limits of accuracy for land use classification on high-altitude and space photography (1:120,000 to 1:2,400,000)? We were also concerned with both the conventional and the more unconventional remote sensing tools that are available. Thus, our program focused on three approaches: (1) an analysis of photographic imagery using conventional interpretation techniques with trained interpreters, (2) an analysis of photographic imagery by automated techniques using film densities as variables with computer

discriminant analysis techniques, and (3) a test of a single-aperture 12-channel multispectral scanner and of computer processing to optimize channels for forest and nonforest classification and to create recognition maps of forest and nonforest land use classes.

This report covers progress made during the last year using photo interpretation techniques for classifying forest and nonforest land use in the Atlanta, Georgia, test site (217) (Figure 1). Significant results of work completed during the first two years are given in the summary preceding this section as well as in previous annual reports (Aldrich et al, 1970; Aldrich and Greentree, 1971; Greentree and Aldrich, 1971; Norick and Wilkes, 1971). In the report that follows this, Norick and Wilkes address the problem of computer analysis techniques using film density for land use classification. A third report (Weber et al) describes a first-time test of a 12-channel multispectral scanner for forest and nonforest land use classification. These three reports together make up the final report for the Forest Inventory studies conducted under NASA contract R-09-038-002.

LAND CLASSIFICATION ON HIGH-ALTITUDE AERIAL PHOTOGRAPHY

An accuracy test of photo interpretation using four seasons of 1:120,000 scale color infrared (CIR) photography was made this year to supplement the results of our 1971 test on 1:420,000 CIR photography. The results from these two years of data complete our evaluation of high-altitude photography for forest and nonforest land classification. At the end of the report we will show in summary the kinds of information that foresters can gain from high-, medium-, and low-altitude photography for forest resource surveys.

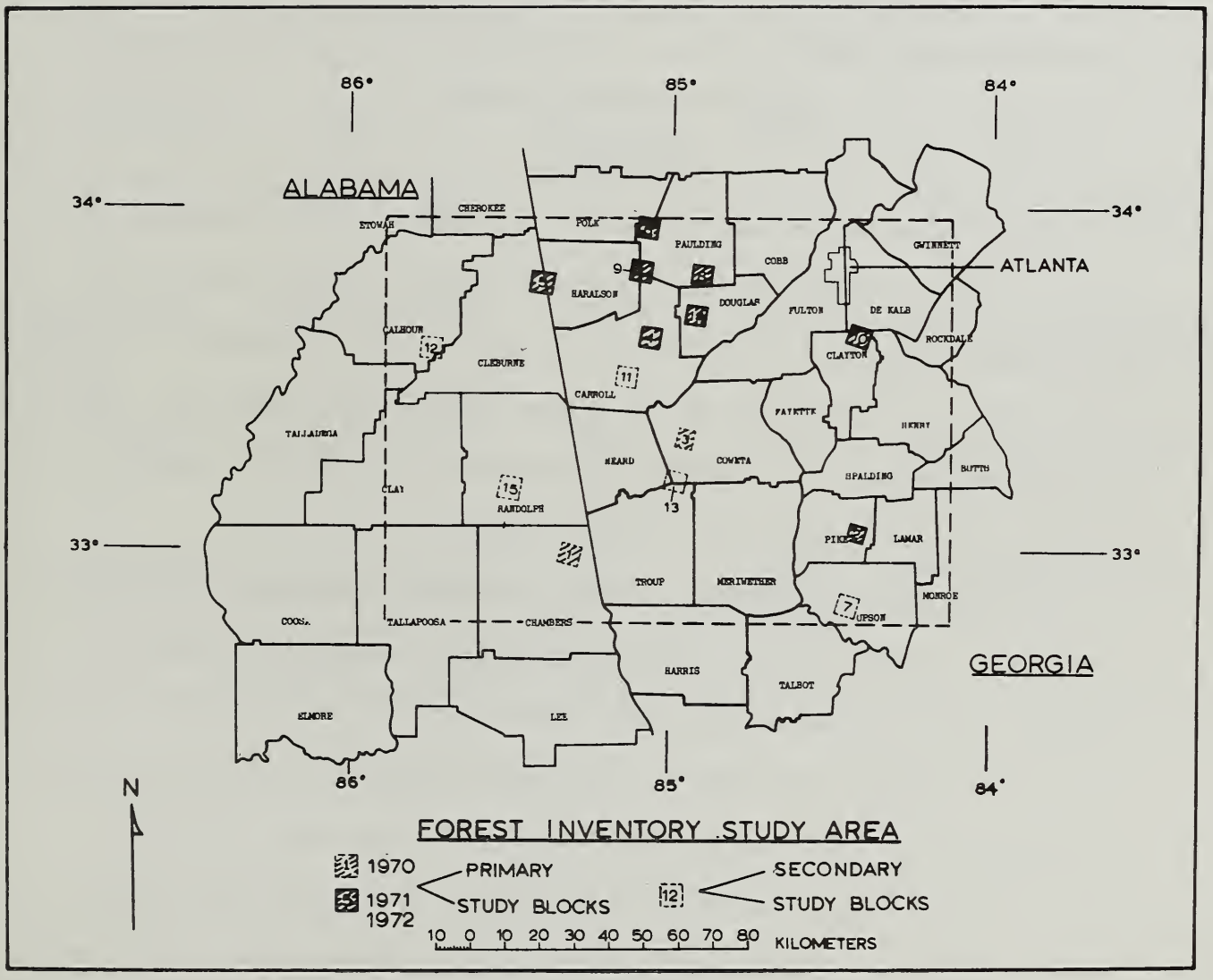

Figure 1. The Atlanta test site includes all or portions of 27 counties in Alabama and Georgia. Eight intensive study areas referred to in this report are shown with heavy hatch marks and solid boundaries. The remaining study blocks (secondary) were not used in this phase of the study.

Although we have found that film density slicing and the direct use of film density in supervised computer classification procedures is not yet feasible, we are including a short evaluation to show the status of this technique. Some new and very promising approaches to multispectral film density stratification are given by Norick and Wilkes in the following report.

PHOTO INTERPRETATION TEST

Procedures

Color infrared photography acquired by NASA's Earth Resources Aircraft Program, Manned Spacecraft Center, Houston, Texas, was used for this study. The films were exposed in a Wild RC-8 (6-inch FL) mapping camera from an altitude of 16,750 meters (55,000 feet) above sea level in an RB-57 aircraft.[1] The aircraft missions, dates, film types, filters, and film quality are given in Table 1.

The forest and nonforest ground classifications used in assessing the accuracy of the photo interpretation were derived from various sources. Basic land use maps made for each of 16 test strips in eight 41-square-kilometer (16-square-mile) study blocks in 1970 were used as a foundation for the ground truth. These map data were updated by ground examinations made at the time of each RB-57 overflight and by careful checks of 1:60,000 CIR film taken at the same time. At least 80 established observation points were re-examined on the ground and numerous roadside observations were made at the time of each overflight.

---

[1] A four-jet engine aircraft capable of an operational ceiling of 60,000 feet.

Table 1. High-altitude photography by RB-57 mission.

RB-57 Mission	Date	Film Type	Filter	Quality
158	March 5, 1971	2443	W15	Slightly overexposed; color quality excellent
191	Nov. 11, 1971	2443	W15	Slightly underexposed; color quality excellent
205	June 1, 1972	2443	W12	Good exposure; color quality excellent
214	Oct. 2, 1972	2443	510 NM (cut-off filter)	Good exposure; color quality excellent

Reductions in financial support this year made it necessary to complete the test with only one interpreter; at least two, but preferably three, interpreters are needed to compute and analyze variations between interpreters and seasons of photography. However, since our analysis in 1971 showed no significant difference between interpreters or season of photography, it is highly unlikely that there would be a difference this year. The one interpreter completing the test was experienced and was one of three interpreters to complete the interpretation of 1:420,000 CIR in 1971. Possible bias was reduced as much as possible by his interpreting this smallest scale first. It is also important to note that a period of one year had elapsed since the original interpretation (thereby reducing the likelihood that his previous knowledge of the area would introduce bias), and the order of interpretation by missions and by study blocks was randomized to reduce bias.

With the exception of Mission 158 (March 1971), the interpreter examined 343 points on each photo mission. On Mission 158, one block was not covered by the photography. This reduced the number of points to 311. The distribution of points by forest and nonforest class is shown in Table 2.

Interpretation was done monocularly using a projection-viewer (Figure 2). This is essentially the same device that was used to interpret 1:420,000 scale photography in 1971 with one major exception -- the projection function is now performed by a Beseler Slide King[2]

[2]Trade names and commercial enterprises or products are mentioned solely for necessary information. No endorsement by the U.S. Department of Agriculture is implied.

Table 2. Distribution of photo observation points by forest and non-forest class.

Season	Land Use[1]													
	1	2	3	4	5	6	7	8	9	10	11	12	13	Total
Winter (March)	54	12	33	60	16	15	38	14	25	5	27	12	0	311
Late fall Early summer Early fall	57	20	33	75	16	15	38	15	25	5	28	15	1	343

[1] FOREST

1 - Pine
2 - Mixed pine/hardwood
3 - Bottomland hardwood
4 - Upland hardwood

NONFOREST

5 - Crop
6 - Plowed field
7 - Pasture
8 - Idle
9 - Abandoned
10 - Orchard
11 - Urban
12 - Turbid water
13 - Clear water

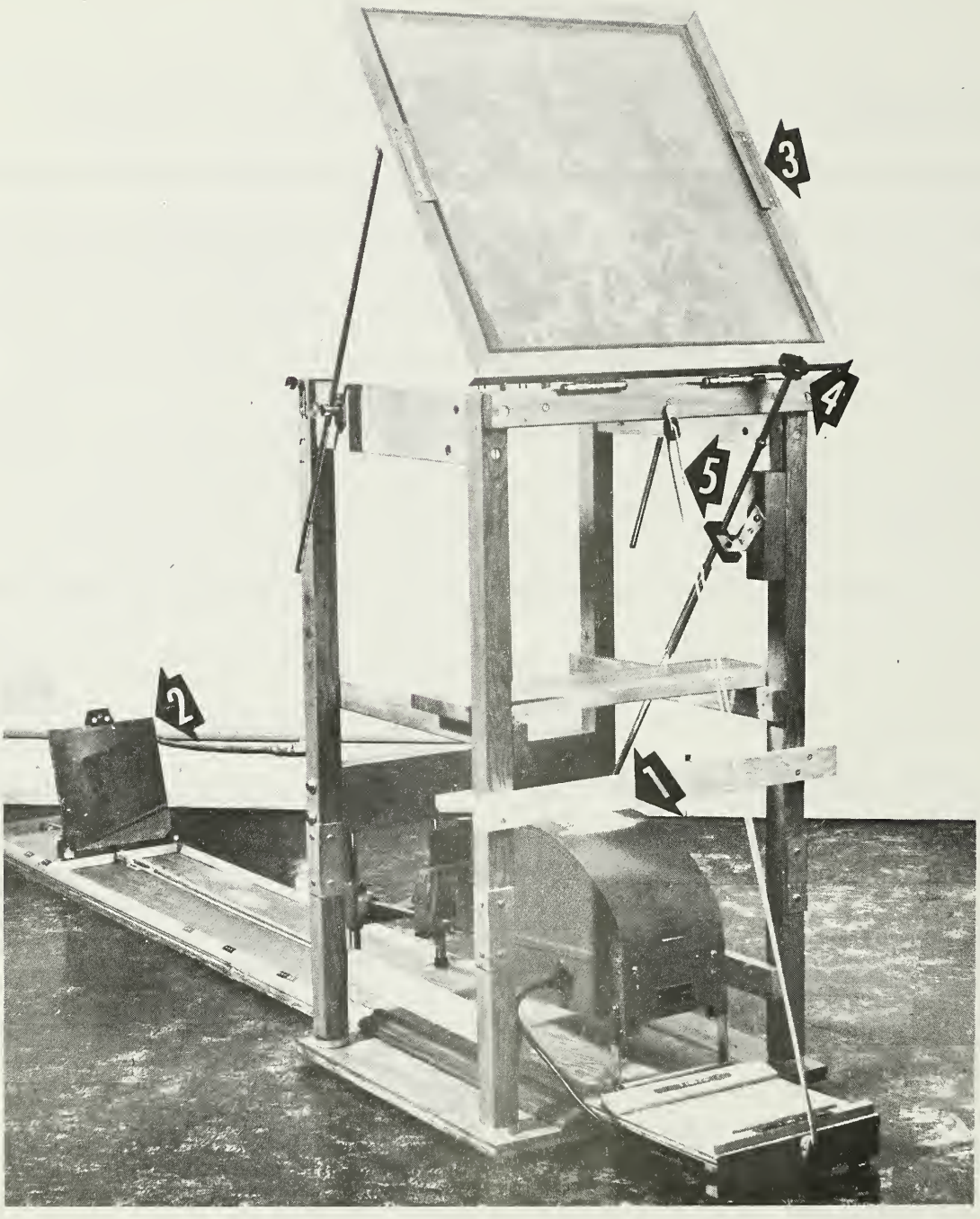

Figure 2. This projection-viewer was used to enlarge 1:120,000 scale photographs to coincide with 1:32,000 ground truth strip maps. (1) Beseler Slide King projector, (2) adjustable mirror, (3) adjustable viewing surface, (4) focusing adjustment, and (5) pulley for adjusting mirror distance for scaling purposes.

projector. The construction of this device has been reported in the literature (Aldrich et al, In press).

Imagery of each study area was cut from the original film and mounted in an 8.25- x 10.16-cm (3-1/4- x 4-inch) lantern slide. Using a random number selector for photo missions and study blocks, each was placed in the projection viewer in turn and enlarged approximately 3.5 times to coincide with 1:32,000 scale templates showing the numbered point locations. Interpretation then proceeded point by point with the forest or land use class being recorded for each point.

Data from the four photo missions were punched for summation and computer analysis.

RESULTS

The results of this photo interpretation test and the test in 1971 (Aldrich and Greentree, 1971) indicate that forest land can be separated from nonforest land on microscale aerial photography with a high level of accuracy. Both 1:120,000 and 1:420,000 scale (CIR) photography resulted in over 96 percent accuracy of classification. The biggest difference between the two scales for interpretation lies in the improvement in discriminating between agricultural land uses. For instance, the accuracy of crops and plowed fields was increased 7 percent on early summer photography. Table 3 shows the best season for interpreting agricultural uses and the accuracy expected for both scales.

The accuracy of interpreting idle and abandoned land improved on 1:120,000 scale photography approximately 40 percent. Orchards that

Table 3. Comparison of the best interpretation accuracy for agricultural classes by season and by photo scale.

Land Use Class	1:120,000 Accuracy (percent)	1:120,000 Season	1:420,000 Accuracy (percent)	1:420,000 Season
Cropland	58	early summer	51	early summer
Pasture	100	winter	90	winter
Idle & Abandoned	70	late summer	30	winter
Orchards	75	early summer	8	early summer

were barely perceptible on 1:420,000 scale photography were correctly identified 75 percent of the time on 1:120,000. The best time of year for interpretation of idle and abandoned land appears to be in late summer and fall. Orchards, like cropland, are best interpreted on early summer photography.

Forest land and improved pastures are interpreted with greatest accuracy on winter photography (Figure 3). Both were 100 percent correctly identified. This confirms our conclusions of 1971 -- namely that even though there was a slightly (insignificant) better accuracy on late summer photography in 1971, the winter season was best for both forest use and forest type classifications. The variation in accuracy is attributed to differences in photo quality.

Winter photography was also best for interpreting both urban land and water. This was a somewhat different result from what we had obtained on 1:420,000 scale photography in 1971. Apparently the improvement was a result of the better resolution and superior quality of the Wilde RC-8 1:120,000 scale photography. Despite the slight improvement of winter photography over the other three seasons tested, all results are very similar -- from 95 to 100 percent of urban classifications and 80 to 90 percent of the water classifications were correct.

Of the few forest points that were misclassified, the greatest number were called either idle and abandoned or urban (Figure 4). Some of these were chance misclassifications caused by a slight misalignment of the template point locator. Others were abandoned land that was reverting to forest with a minimum stocking of forest trees. There were

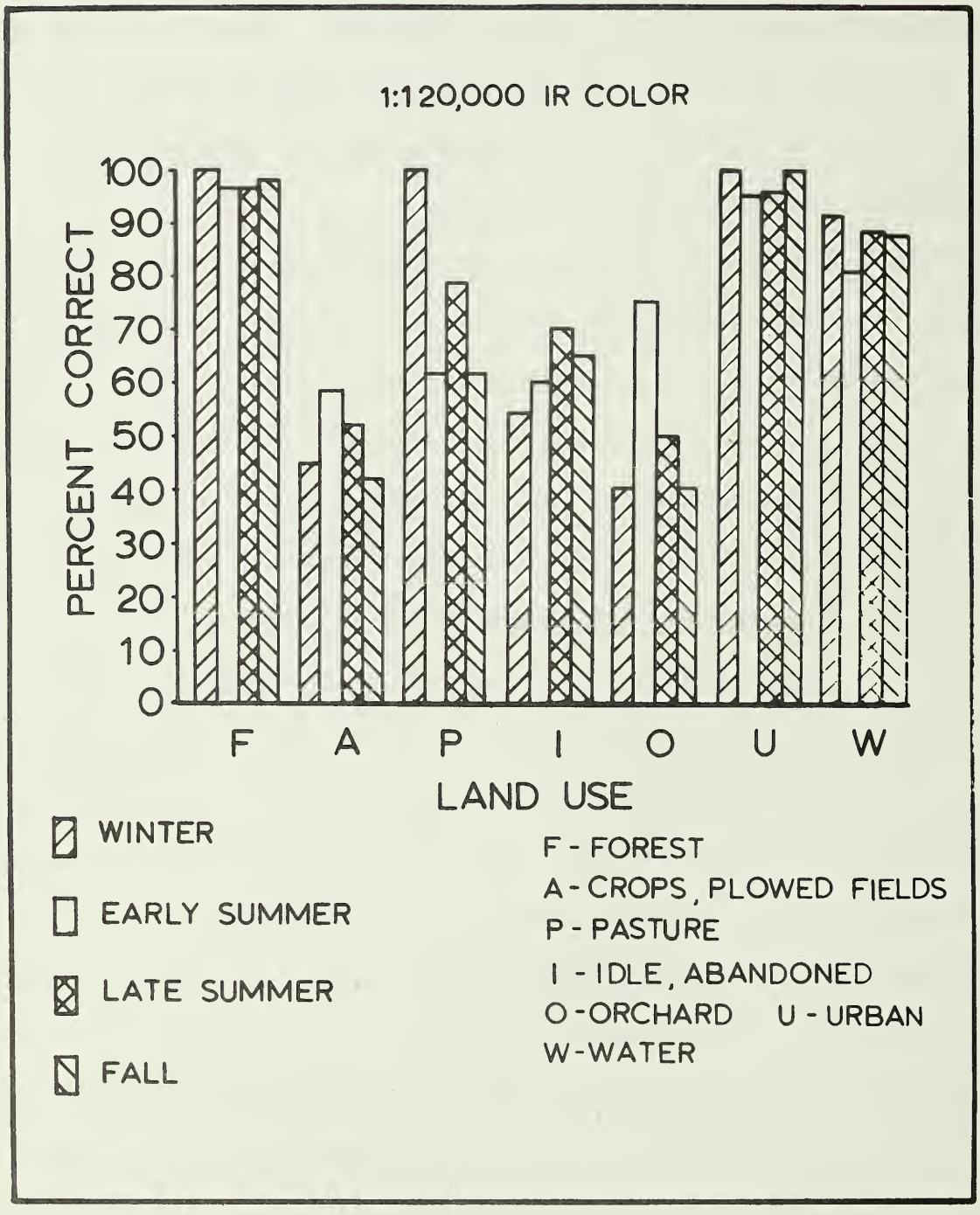

Figure 3. Diagrammatic summary showing the interpretation accuracy for one interpreter classifying land use on 1:120,000 scale CIR photographs taken during four seasons.

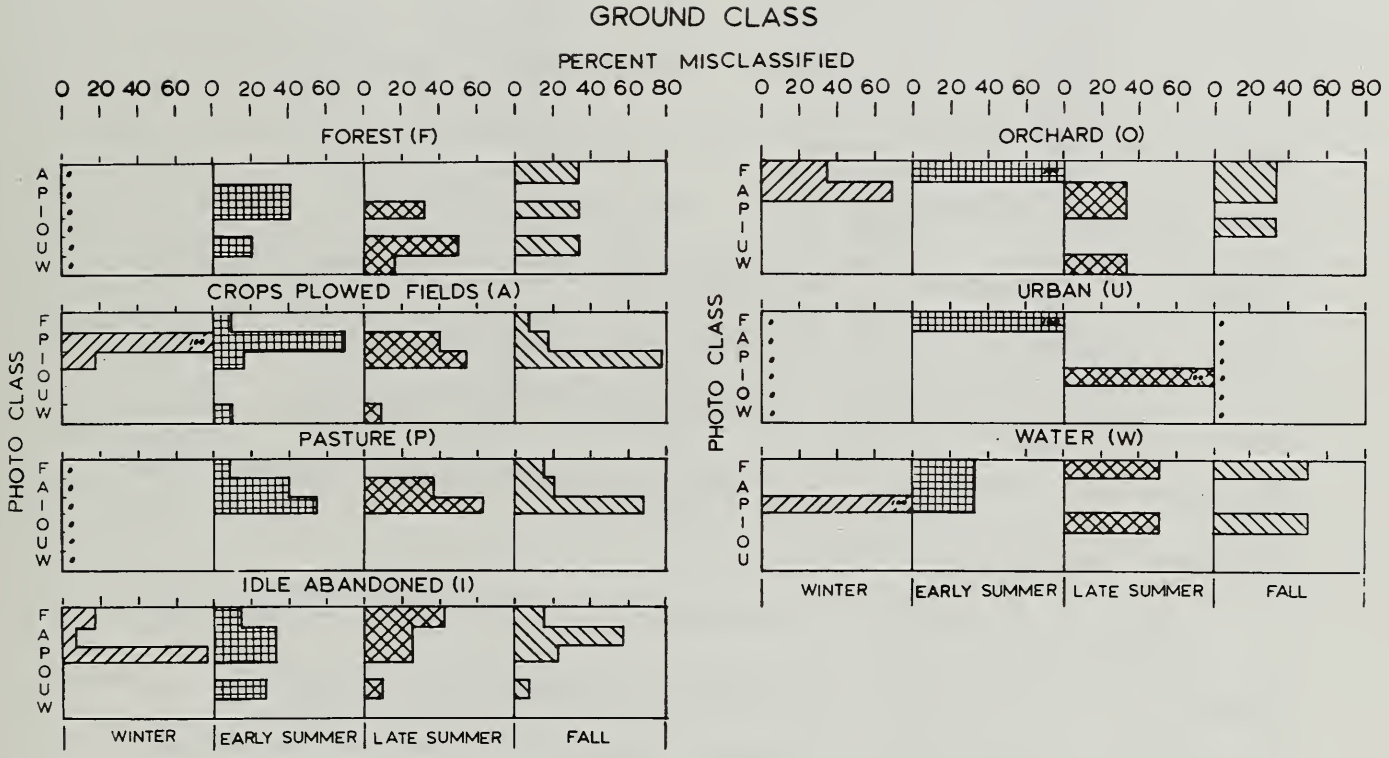

Figure 4. This chart indicates the percentage of all nonforest points that were misclassified by land use and season of photography.

no errors of classification on winter photography which once again pointed out the superiority of winter photography for forest classification.

Ninety percent of the errors in classification of cropland, idle land, and pasture result from misinterpretations between improved grazing land, hay fields, recently idle agriculture, and grain crops such as wheat, barley, and rye.

The accuracy of classifying pine type on 1:120,000 scale CIR photography was slightly lower than on 1:420,000. This was true for all seasons of photography. The best classification was on fall imagery with a score of 75 percent (Figure 5). Winter was second best with 70 percent. It is difficult to explain the reduced accuracy on the larger scale except to theorize that the interpreter tended to throw more plots which were near the borderline into mixed pine/hardwood and hardwood types.

Mixed pine/hardwood is difficult to interpret at any time of year but is usually best identified on wintertime photography. This was true on both scales. Errors in classification are caused by misinterpreting the amount of pine in a stand -- more than 25 percent but less than 50 percent stocking of pine is required by this classification.

Bottomland hardwood interpretation is similar to that achieved and reported in 1971. This type is best identified on winter and late fall photography when deciduous tree leaves have fallen -- 76 percent of these classifications were correct in winter, and 73 percent were

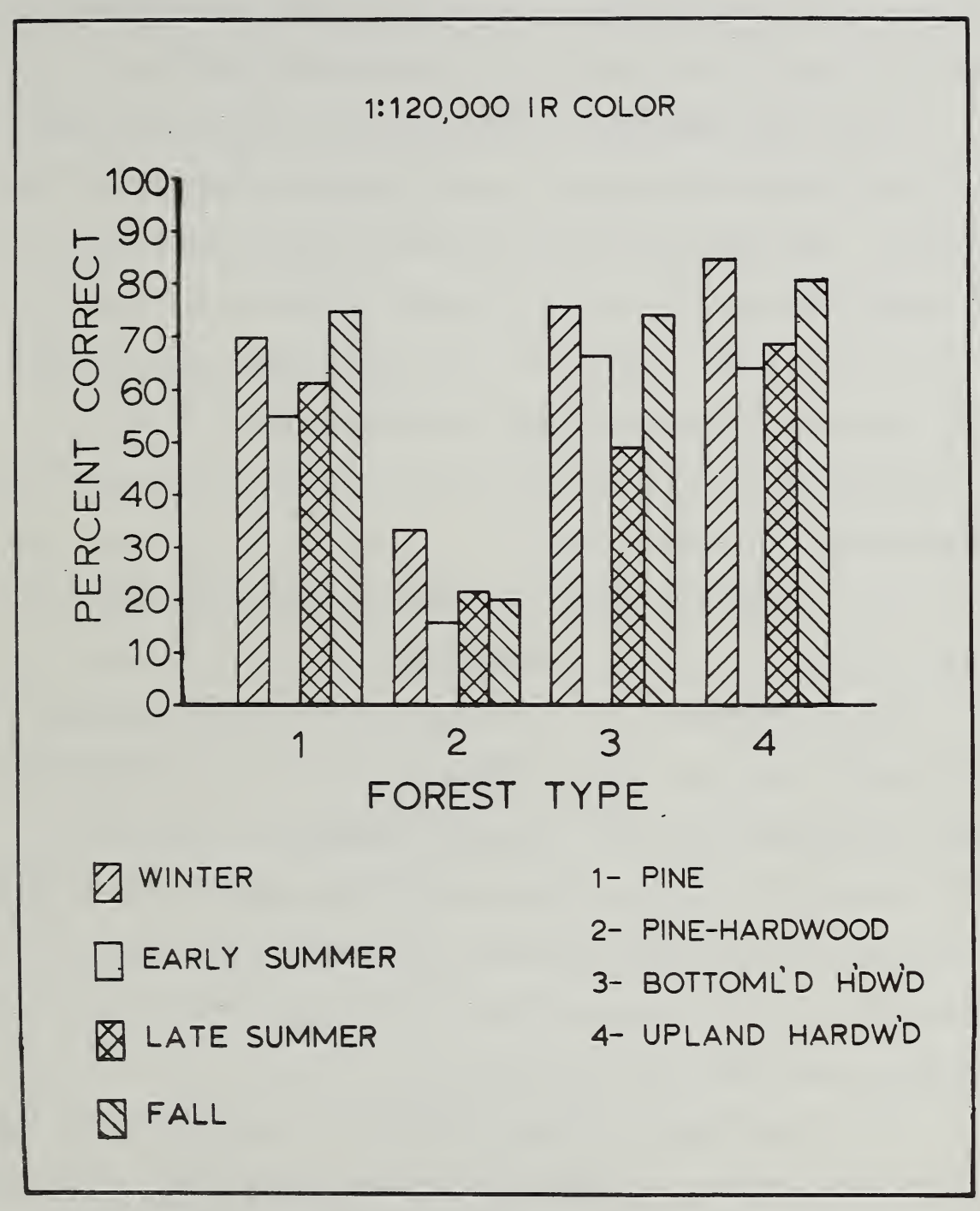

Figure 5. This chart shows the accuracy for one interpreter classifying forest types on 1:120,000 CIR photographs taken during four seasons.

correct in late fall. This is much improved over the 60 percent accuracy reported for 1:420,000 scale photography in 1971.

In 1971 we showed that on 1:420,000 scale CIR film there was little difference in accuracy of upland hardwood interpretation by seasons. The range was 66 to 71 percent. Figure 5 shows that on 1:120,000 scale CIR, 85 percent of upland hardwood was correctly classified on winter photography; fall was next best with 80 percent accuracy. When the hardwoods (deciduous) are foliated, it is possible to correctly classify only 65 percent of this type regardless of the scale.

PHOTOGRAPHIC DENSITY SLICING OF APOLLO 9 PHOTOS

Procedures

Two CIR transparencies from the Apollo 9 (S-065) multiband photography experiment (March 1969) were enhanced using photographic density slicing techniques. These two photographs covered the Atlanta, Georgia, forest inventory test site. The work was performed by the Western Development Laboratories Division of Philco-Ford Corporation under contract to the Geological Survey, U.S. Department of Interior, between August 1970 and April 1971.

In their enhancement system, Philco-Ford first made multispectral separations for the red, green, and blue sensitive layers of CIR photography in negative form. A positive transparency was then made from each negative. Using the three negatives and the three positives, it was possible to recombine the spectral data in nine different ways to better enhance image differences between forest land and nonforested

areas. The final and best possible combination combined the green negative with the red positive for one density slice. This slice was used as a mask on the green negative to enhance the nonforest land. Five additional density slices were made of the film density in the forest land. By increasing density, these resulted in yellow, red, light blue, dark blue, and green in the final enhanced photo. Nonforest areas appeared white.

To check the accuracy of land classification, the enhanced Apollo 9 photo was compared with data on 1:32,000 scale CIR photos taken in March 1970. Five of the 41-square-kilometer (16-square-mile) study blocks used in our previous experiments were used for this check. The resultant density slices when color coded should represent the same nonforest or forest class.

Results

The results of comparing 1:32,000 scale aerial photographic data with two density enhanced Apollo 9 images are shown in Table 4.

Although these enhancements were much improved over an earlier enhancement produced by Philco-Ford, differences in density caused by sun angle, photo exposure, and photo processing reduced the effectiveness of the photographic density slicing technique. Because of differences in density within photographs, it is necessary to evaluate enhancements in terms of nonforest and forest classes in one small area of the photo at a time. Color separations will never consistently represent the same land use class unless a technique is devised for equalizing density representations within the photo frames. Unless this is accomplished,

the advantages of synoptic photos from space would be seriously reduced. For example, it is obvious from Table 4 that there is no consistency in the color assignments for forest and nonforest classes on this Apollo 9 CIR photograph.

Density slicing as a photo enhancement tool should be most useful with photographs produced from electronic signals. Here signals can be adjusted for differences caused by differences in sun angle and atmospheric attenuation. The resulting density slices when color coded will represent essentially the same nonforest or forest classes, wherever they are imaged.

EVALUATION OF MULTISEASONAL FILM DENSITIES

Procedures

During this reporting year, we completed our multiseasonal film density comparison. This was made possible by the flight of NASA's RB-57 Mission 191 on November 11, 1971. Unfortunately, both of the 70 mm CIR films were poor in color quality. Both were exposed in Hasselblad cameras with 40 mm focal length lenses and with the same film and filter combination. One resulted in an overall blue film; the other was an overall green. Since the bluish film showed some evidence of infrared response, we decided to use this film in our study. Sample strips in eight study blocks were scanned with a microdensitometer. A description of the sample strips and the methods and equipment used to measure film density in this study was reported previously (Greentree and Aldrich, 1971) and will not be reported here.

Table 4. Comparison of enhanced Apollo 9 CIR photos (3791, 3792) and forest and nonforest classes from 1:32,000 CIR photos.

1:32,000 CIR LAND USE	TEST BLOCK				
	1	2	3	4	5
	enhancement color				
Pine	orange	orange	red	red-green	red
Pine/hardwood	*	*	green	blue	blue
Upland hardwood	red	red	blue	*	blue
Bottomland hardwood	*	red	dark blue	dark blue	orange
Nonforest	green blue white	green blue white	white	white	white

* None detected

Results

The normalized[3] red, green, and blue densities of 1:420,000 CIR film have been plotted for 13 land use classes for four seasons in Figure 6. Three seasons of data were taken from the 1971 annual report. Only data for RB-57 Mission 191 (November 1971) have been added to complete the seasonal comparison.

As in the past, the red density signatures seem to indicate that a separation can be made between forest and nonforest classes. This again is most evident on the winter film (Mission 158).

Variation in normalized red density, expressed by the standard deviations in Table 5, is very likely to be from two sources: (1) differences in spectral sensitivity of the film layers to differing light levels and light quality across the photo format and (2) the position of the density measurement within the format, i.e., distance from the nadir. Because of these uncontrolled variations, the standard deviations of individual classes overlap and make it very difficult to separate the classes from one another.

The green and blue densities were also normalized and the means plotted (Figure 6). It was again evident that blue and green densities show little difference between classes. However, both the normalized blue and green, and the normalized red density, are being used in both supervised and unsupervised computer classification procedures. Here minor differences may play an important role even though they are not easy to perceive by eye.

---

[3]Normalization was partially achieved by subtracting the density value through the clear density filter from the densities after projection through the red, green, and blue filters, respectively.

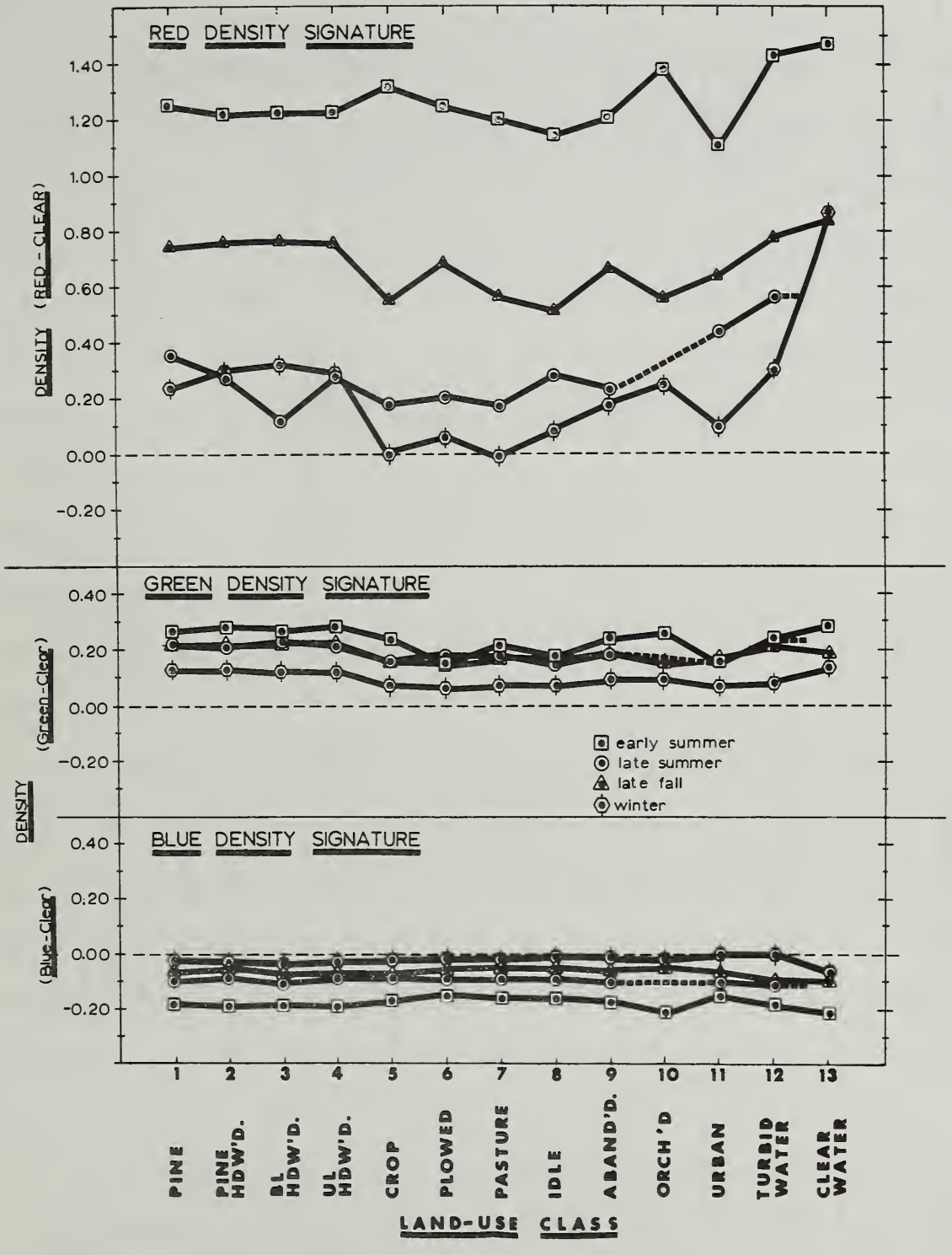

Figure 6. This graph shows a four-season comparison of the mean normalized red, green, and blue film densities for 13 land use classes. Density measurements were made on 1:420,000 scale CIR transparencies. Normalizing consisted of subtracting the red, green, and blue densities from the film density to white light (no filter).

Table 5. Number of density data points, the mean red density, and the standard deviations by land use by season of photography. Combined study blocks.[1]

Land Use Class[2]	EARLY SUMMER			LATE SUMMER			LATE FALL			WINTER		
	No. of Data Points	Mean Density	Std. Dev.	No. of Data Points	Mean Density	Std. Dev.	No. of Data Points	Mean Density	Std. Dev.	No. of Data Points	Mean Density	Std. Dev.
1	2312	1.253	±.172	1602	0.350	±.202	1734	0.744	±.108	1554	0.234	±.226
2	355	1.221	±.144	283	0.273	±.206	309	0.762	±.091	229	0.291	±.256
3	536	1.219	±.220	193	0.108	±.174	380	0.760	±.112	372	0.324	±.276
4	855	1.221	±.172	681	0.270	±.198	815	0.748	±.102	703	0.286	±.220
5	97	1.312	±.150	35	0.184	±.183	78	0.554	±.191	77	0.001	±.100
6	139	1.238	±.209	36	0.202	±.120	129	0.678	±.158	127	0.056	±.133
7	1046	1.185	±.213	665	0.174	±.167	893	0.562	±.183	883	-0.012	±.129
8	52	1.132	±.230	39	0.283	±.272	52	0.506	±.181	53	0.084	±.191
9	350	1.202	±.185	210	0.234	±.174	294	0.657	±.223	289	0.165	±.212
10	32	1.374	±.073				23	0.555	±.219	25	0.244	±.170
11	553	1.110	±.189	493	0.430	±.291	306	0.626	±.189	531	0.090	±.156
12	43	1.421	±.219	18	0.561	±.422	3	0.766	±.066	35	0.287	±.175
13	3	1.460	±.020				38	0.831	±.247	3	0.850	±.289
Total	6373			4255			5054			4881		

[1]Normalized data. Red density minus clear density (white light).

[2]Pine - 1
Mixed - 2
Bottomland hardwood - 3
Upland hardwood - 4
Crops - 5
Plowed field - 6
Pasture - 7
Idle - 8
Abandoned - 9
Orchard - 10
Urban - 11
Turbid water - 12
Clear water - 13

Some interesting trends can be seen when one compares film density by season (Figure 6). For instance, forest classes have the highest normalized densities in early summer and the lowest in the winter. This occurs in both the red and green densities, but the trend is reversed in the blue density. Note that clear water shows the highest density on all four seasons. These and other interesting reversal patterns may be useful for discriminating among the land use classes by season. However, the trends shown in the graph should be viewed only as relative differences because the density signatures have not been corrected for film sensitivity and position variations. Moreover, the film/filter combinations used on all missions were not always the same.

Before automated systems for scanning aerial or space photographs can be of benefit to forest resource managers, algorithms must be developed to correct film densities for unwanted system variations. Research must continue toward this goal while we continue to test and develop computer classification techniques. The latter must be done on carefully selected areas near the photograph nadir where variations will be minimal.

RECOMMENDED USES OF PHOTOGRAPHIC IMAGERY IN FORESTRY

Although automation of photo interpretation and the use of electronic multispectral scanners show promise for the future, it will be several years before they are perfected for forestry use. Even then, a skilled photo interpreter will be required as an interface with the machine.

What can foresters do while these bigger and better instruments are being perfected? One of the greatest challenges facing the forest inventory specialist today is to perfect and exploit the concept of multistage sampling. This concept usually entails the use of one or more levels of photography to provide increasingly more refined information to satisfy the requirements of the inventory. Even one level of up-to-date photographic information can improve sampling efficiency over that of out-of-date poor photography, or no photography at all.

Selecting the best scale or scales and the best film or films to provide the required information will be extremely important. There are a number of photo image characteristics that are either interpreted or measured which should be considered. These are grouped for convenience into four categories: (1) land use, (2) stand volume, (3) cover type, and (4) forest disturbance. Each of these categories is important in extensive forest inventories. An ability to determine land use leads to accurate forest area estimates and forest area changes; stand volume is used to stratify the forest to reduce sampling variability; cover types are important for management decisions; locating forest disturbances will make it possible to update forest statistics between inventories. These categories and the image characteristics that we feel will lead to their interpretation are tabulated below:

CLASSIFICATION CATEGORY	PHOTO CHARACTERISTIC
1. Land use	a. ground cover
	b. physiography
	c. surface characteristics
	d. roads and man-made features
	e. streams and lakes
2. Stand volume	a. stand height
	b. mean crown diameter
	c. crown closure
	d. crown area
	e. number of trees
	f. stand area
3. Cover type	a. tree species
	b. understory
	c. ground cover
	d. soil moisture
4. Forest disturbance	a. roads and man-made features
	b. crown closure
	c. mortality
	d. ground cover
	e. surface characteristics

Certainly all of these characteristics can be identified or measured to some degree on aerial photographs. However, not all of them can be resolved on 1:20,000 scale panchromatic photographs currently used in the Southeastern United States for forest and land use

classification. For instance, except for extensive homogeneous stands, tree species cannot be identified on 1:20,000 scale panchromatic photographs. However, large-scale color photography will enable the trained interpreter to identify 80 to 90 percent of the trees by species even in mixed stands. Panchromatic photography cannot be relied on to detect soil moisture. But because water absorbs infrared radiation and results in dark images, CIR film enables the interpreter to detect soil moisture differences and follow stream courses through forested areas by both vegetation and soil color differences. Soils with a high moisture level appear blue-gray on CIR film. This characteristic holds true from almost any altitude including from space orbit. This meritorious quality of CIR film can be extended even into stand classification on scales smaller than 1:20,000 because this film is superior for atmospheric haze penetration.

Let's look a little closer at the general effectiveness of three commonly used film types by four arbitrary scale classifications (Table 6). This comparison is made by using the four categories and 12 photo characteristics that were discussed previously. Although this is admittedly a subjective demonstration, it nevertheless indicates what one might expect to map from different types and scales of imagery.

There is little doubt that tree species and other measures of cover type can be interpreted best on large-scale color photographs. Subtle shades of green and yellow-green, and crown margins and branching

Table 6. The predicted relative accuracy by forest classification category, photo characteristic, scale, and film type.

Classification Category or Characteristic	Large Scale 1:1,000-1:4,000 Resolution: > 1m			Medium Scale 1:8,000-1:24,000 Resolution: 1m-3m			Small Scale 1:30,000-1:90,000 Resolution: 3m-10m			Microscale 1:100,000-1:500,000 Resolution: 10m-30m		
	Pan	Color[1]	CIR[2]	Pan	Color	CIR	Pan	Color	CIR	Pan	Color	CIR
	Relative Accuracy[3]											
LAND USE	X	X	X	✓	X	X	✓	✓	X	*	*	X
Ground cover	✓	X	✓	*	✓	✓	*	✓	✓	--	*	✓
Physiography	✓	✓	✓	X	X	X	X	X	X	✓	✓	✓
Roads	✓	✓	✓	X	X	X	✓	✓	X	✓	*	✓
Streams and lakes	✓	✓	✓	X	X	X	✓	✓	X	--	--	X
STAND VOLUME	X	X	X	✓	✓	✓	*	*	*	--	--	--
Stand height	X	X	X	✓	✓	✓	*	*	*	--	--	--
Crown closure	X	X	X	✓	✓	✓	*	*	✓	*	--	✓
No. of trees	X	X	X	✓	✓	✓	*	*	✓	--	--	--
Stand area	X	X	X	✓	✓	✓	*	*	✓	--	--	*
COVER TYPE	X	X	X	✓	X	X	*	*	✓	*	*	✓
Understory	--	X	--	--	✓	--	--	--	--	--	--	--
Tree species	✓	X	✓	--	*	--	--	--	--	--	--	--
Soil moisture	✓	✓	X	*	*	X	--	--	X	--	--	✓
FOREST DISTURBANCE	X	X	X	✓	✓	X	*	*	X	--	--	✓
Mortality	*	X	X	--	✓	X	--	*	✓	--	--	*
Surface characteristics	X	X	X	✓	✓	✓	*	*	✓	--	--	*

[1] Ektachrome SO-397

[2] Ektachrome Infrared (2443)

[3] X - excellent; ✓ - good; * - fair; -- - inadequate

characteristics are quite visible at this scale. Although panchromatic and CIR can be useful at large scales, a healthy human eye is better able to discriminate between shades of true color than between shades of gray or false color.

Stand, or tree volumes, can be estimated best on large-scale photographs. It has been said that interpreters who are very familiar with the timber in their area can estimate stand heights on large-scale photos within reasonable limits. Certainly parallax measurements for stand and tree heights, as well as measurements of crown diameter, crown closure, and number of trees can be made most precisely. Moreover, these large-scale photographs are usually taken on a 70 mm format (2-1/4 x 2-1/4 inches) and require foresters to use only the simplest of interpretation devices -- pocket stereoscopes, parallax wedges, dot grids, and crown diameter scales.

Medium-scale photographs are still the most useful from the standpoint of versatility in resource surveys. They are good for stand volume and cover types, but they are probably best for land use classification, stream and lake surveys, soils and soil moisture, and tree mortality. Normal color (NC) and CIR films are far superior to panchromatic film as far as informational content is concerned.

Small-scale photography by our standards has a rather wide range -- 1:30,000 to 1:90,000. Despite the small size of the images, it has been our experience that scales within this range provide almost the same amount of information on CIR film (Figure 7). However, this should be qualified by adding that magnifying stereoscopes (1.5X to 9X magnification)

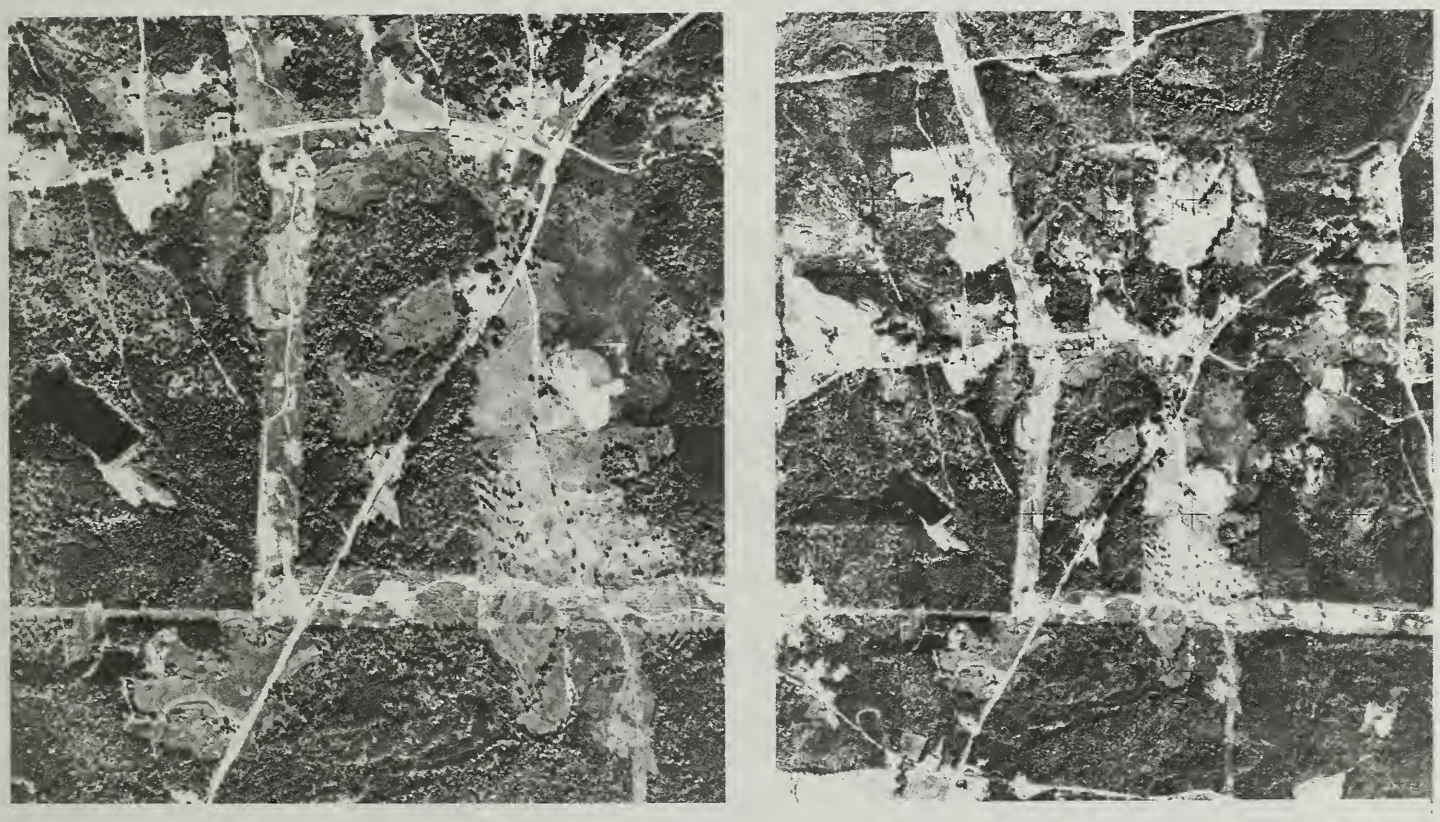

A B

Figure 7. Most information on 1:15,840 scale panchromatic photographs is also found on small-scale CIR photographs: (A) 1:32,000 and (B) 1:60,000. These black-and-white photos were enlarged 2 times from the original CIR transparencies.

must be used to bring out this information. For the Southeastern United States, we have been able to map broad timber stand-size classes, forest types, ground cover, ground condition, soil moisture, roads, streams and lakes, land use, and physiography using these photographic scales.

Now let's look at microscale photography. We define microscale photography as having images so small that they must be interpreted using a magnifying viewer or a stereo microscope. A magnifying viewer would be the preferred instrument if stand delineation is one of the inventory goals. Furthermore, at these scales there is little advantage in using stereo coverage. For this reason, simpler devices such as the projection viewer shown in Figure 2 can be used.

In the Southeastern United States, CIR is the most effective film for land use and forest classification at microscales. Again, the improvement in discrimination is because CIR film penetrates atmospheric haze better than other films. Figure 8 indicates the extent to which broad forest type, land use, roads, streams and lakes can be identified on 1:120,000 and 1:420,000 scale high-altitude photography taken in November 1971.

Selecting the best season for photography will usually be a compromise between what is available and the type of information being sought. Weather conditions will often be a controlling factor when one is faced with obtaining photography during the preferred season.

Certainly the type of information required is the most important factor in selecting season. Hunter and Bird (1971) claim that vegetation in the northern temperate zone is interpreted best on early

Figure 8. Imagery such as this example of 1:120,000 (left) and 1:420,000 scale (right) CIR will provide almost all of the information found on small and medium scales. These photographs were enlarged 2 times from the original CIR.

spring infrared photography before deciduous foliage covers the ground. They also claim that fall, when deciduous tree foliage increases in reflectance and coniferous tree foliage decreases in reflectance, is another good time for vegetation interpretation. We won't deny this; however, in the Southeastern United States we found that on high-altitude CIR photography, the best period for differentiating broad forest types was from late November to early April. This was because the background (ground cover) was important for differentiating between upland deciduous and bottomland deciduous types. Soil moisture, organic matter, and surface water were the influencing factors here. During the period of full leaf development, it was almost impossible to differentiate these two types except by association with physiography. Table 7 shows by seasons, land use, and broad vegetation types some general impressions from interpreting high-altitude 1:420,000, 1:120,000, and 1:60,000 scale CIR photography.

If the resource inventory specialist is concerned with detecting man-made disturbances in the forest, the best season is probably when deciduous foliage is nearly mature. Of the three seasons in Table 7, late spring to early summer and late summer are probably the best. Late fall to early spring, after foliage has dropped, can only be rated as fair. Cuttings, fires, hardwood conversion areas, and defoliation by natural causes will not be apparent during this period. Figure 9 shows how two 1:420,000 scale CIR photographs taken two years apart might be used to detect disturbances in a forest environment.

In summary, high-altitude photography can be extremely useful for gathering forest resource information. It can be used for accurate

Table 7. Comparison of relative accuracies expected in classifying forest and nonforest categories by season of photography on small-scale and microscale imagery.

CATEGORY	Late summer-early fall Sept. 1-Oct. 15	Late fall-early spring Nov. 15-Apr. 15	Late spring-early summer May 15-June 15
Pine	X	X	X
Mixed pine/ Hardwood	√	X	√
Upland hardwood	*	X	*
Bottomland hardwood	*	X	*
Agriculture	*	√	X
Pasture	*	√	X
Urban	X	X	X
Water	√	X	√

X - excellent
√ - good
* - fair

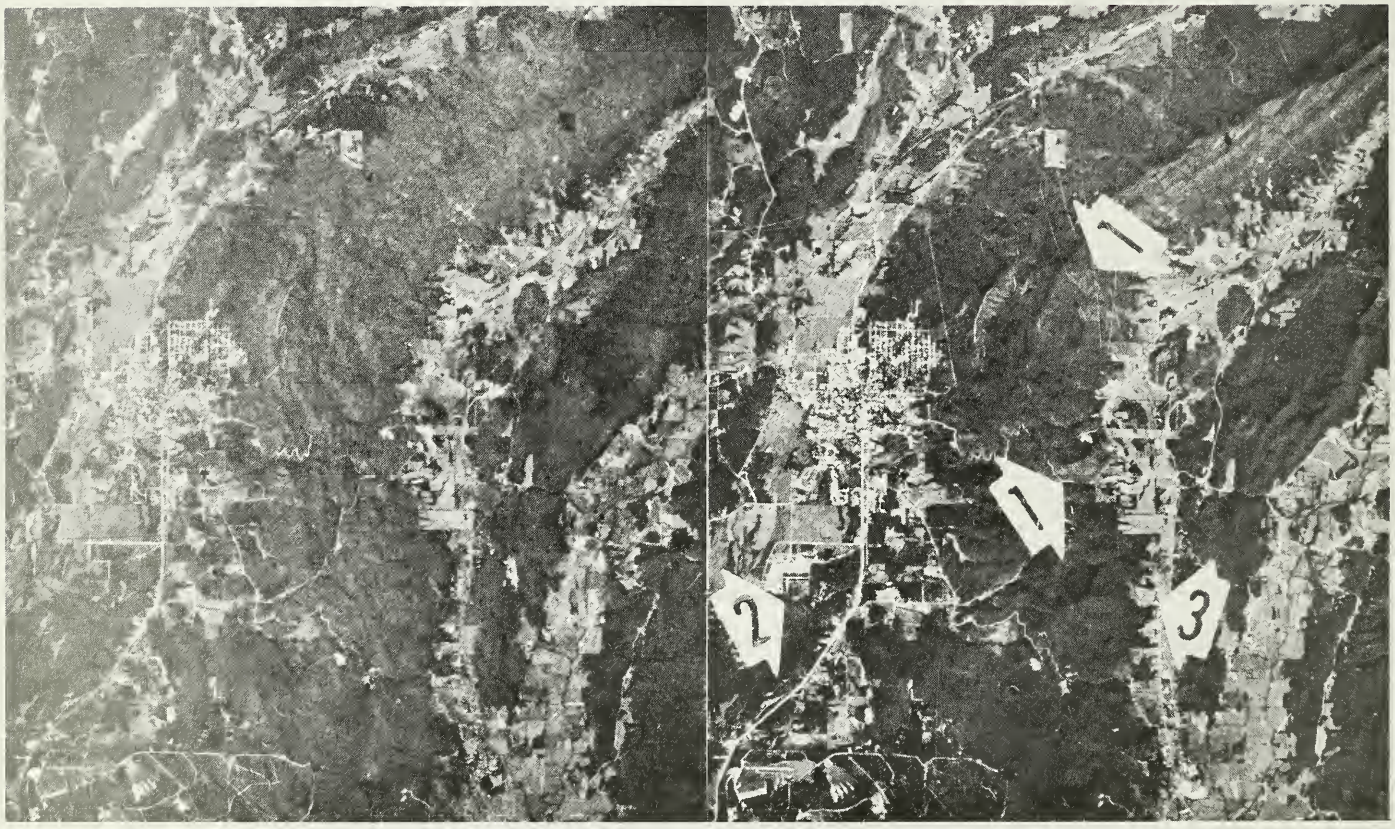

Figure 9. These two 1:420,000 scale CIR photographs show the effects of elapsed time and season of photography for detecting disturbances in the forest. (A) late summer, September 1970; (B) fall, October 1972. The disturbances shown are (1) new hardwood conversion sites on Talladega National Forest, (2) urban encroachment, (3) clearing for agriculture.

forest area estimates, to stratify forest cover types, to monitor changes in the forest area, and to detect disturbances in the forest that may affect timber volume and growth. However, the cost advantages of high-altitude photography are not easy to derive because the operational costs of a resource survey aircraft program would have to be determined by the number of potential users. One cost-benefit analysis was described by Katz (1969). Using conservative figures for the use of a fleet of 10 Boeing 707 jets, Katz showed a cost of $0.43 per square mile ($0.17 per square kilometer). This figure was based upon the coverage of a 48.3-kilometer (30-mile) swath with a high-resolution panoramic camera and several other sensors. When these figures are used to estimate cost based on a 24.1-kilometer (15-mile) swath with a 23- x 23-cm (9- x 9-inch) format mapping camera, the cost is increased to $1.12 per square mile ($0.44 per square kilometer). This figure is compared below with the estimated cost of 1:20,000 scale U.S. Department of Agriculture panchromatic prints for one Forest Survey unit in north-central Georgia of 2.5 million hectares (6.3 million acres).[4]

Type of Photography	Mission	No. of Photos	Cost per Sq. Mile	Cost per Sq. Km.	Total Cost
1:20,000 pan prints	U.S.D.A. Contract	2500[5]	$0.30	$0.12	$ 3,125
1:120,000 CIR film	Boeing 707 Earth Resources	80	$1.12	$0.44	$11,021

[4]The Forest Survey purchases photographic prints from the Agriculture Stabilization and Conservation Service, U.S. Department of Agriculture. Thus, cost estimates do not include aircraft costs and costs that are involved in a contract photo operation.

[5]$1.25 per photo. Alternate photos in all flight lines.

The reduced number of photographs and the increased amount of information should be given serious consideration when comparing these costs. However, only a comparative test will show whether there are enough gains to justify the additional cost. Eventually, we may be required to pay this added cost to provide the information required for all levels of management decisions.

LITERATURE CITED

1. Aldrich, R. C., W. J. Greentree, R. C. Heller, and N. X. Norick. 1970. The use of space and high-altitude aerial photography to classify forest land and to detect forest disturbances. Annual Progress Report for Earth Resources Survey Program, OSSA/NASA, by the Pacific Southwest Forest and Range Experiment Station, 36 p., illus.
2. Aldrich, R. C., and W. J. Greentree. 1971. Microscale photo interpretation of forest and nonforest land classes. In Monitoring Forest Land from High Altitude and from Space. Annual Progress Report for Earth Resources Survey Program, OSSA/NASA, by the Pacific Southwest Forest and Range Experiment Station, 25 p., illus.
3. Greentree, W. J., and R. C. Aldrich. 1971. Multiseasonal film densities for automated forest and nonforest land classification. In Monitoring Forest Land from High Altitude and from Space. Annual Progress Report for Earth Resources Survey Program, OSSA/NASA, by the Pacific Southwest Forest and Range Experiment Station, 15 p., illus.

4. Norick, N. X., and M. Wilkes. 1971. Classification of land use by automated procedures. In Monitoring Forest Land from High Altitude and from Space. Annual Progress Report for Earth Resources Survey Program, OSSA/NASA, by the Pacific Southwest Forest and Range Experiment Station, 24 p., illus.

5. Aldrich, R. C., J. von Mosch, and W. Greentree. Projection-viewer for microscale aerial photography. U.S. Forest Service Res. Note PSW, Berkeley, Calif. In press.

6. Hunter, G. T., and S. J. G. Bird. 1970. Critical terrain analysis Technical Papers. 36th Annual American Society of Photogrammetry, March 1-6, 1970.

7. Katz, A. H. 1969. Let aircraft make earth resource surveys. Astronautics and Aeronautics, p. 60-68.

CLASSIFICATION OF LAND USE BY AUTOMATED PROCEDURES

by

Nancy X. Norick and Marilyn Wilkes

Efforts continued during 1972 to develop and test automated techniques for classifying forest and nonforest land uses in the Atlanta, Georgia, test site (217). This year our efforts have taken a new direction. Instead of using data from one-dimensional microdensitometer scans along a line as reported in 1971 (Norick and Wilkes, 1971), we are now using two-dimensional scans of an extensive area. Also, instead of using only supervised pattern recognition techniques, i.e., taking half of a random sample for a training set to develop discriminant functions and using the other half for a test set, we are now using a combination of both supervised and unsupervised methods. The unsupervised algorithms find ways of clustering picture elements or sets of picture elements into spectrally and/or spacially similar groups independent of land classes. The clusters, or strata, are then classified according to land class attributes. The object is to find clustering algorithms that consistently separate the land and forest types of interest.

An area representing approximately 732 meters (2400 feet) by 1.6 kilometers (one mile) on the ground was located on a color infrared (CIR) photograph and analyzed extensively. The data were from 1:120,000 scale CIR (2443) film taken during Earth Resources Aircraft Program RB-57 Mission 191. Figure 1A shows a color-coded map made from this

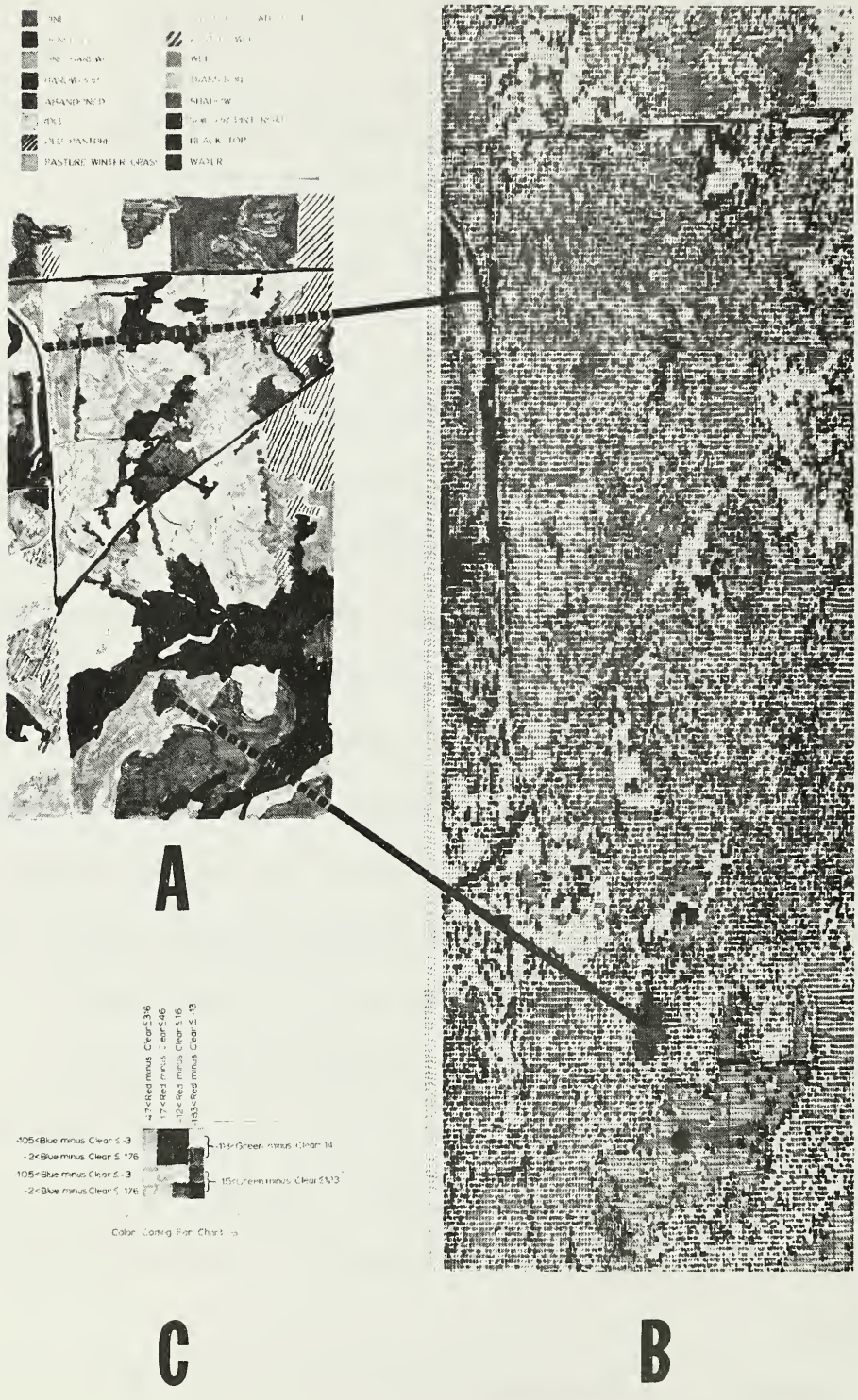

Figure 1. These map representations for a small area near Carrollton, Georgia, illustrate how unsupervised pattern recognition techniques can stratify forest and nonforest land use classes: (A) a map of ground conditions drawn from an enlarged 1:120,000 scale CIR photograph (photo date - Nov. 11, 1971), (B) a computer map using 16 three-dimensional rectangles formed using a clustering algorithm based upon the empirical multivariate distribution of red minus clear, blue minus clear, and green minus clear densities, and (C) a color-coded legend for (B) showing the 16 three-dimensional rectangles. The overlay on (A) is a first attempt to automatically locate boundaries between areas of dissimilar types. Identical points on the photo map (A) and the computer map (B) are connected by lines for orientation. Note that the computer map is exaggerated by a factor of two in the vertical direction.

film by a photo interpreter. The same piece of film was then scanned by an automatic scanning microdensitometer with red, blue, green, and clear filters (white light). The Photometric Data Systems microdensitometer was set to an aperture diameter of 56 micrometers and was programmed to collect data at 54-micrometer intervals in both the x and y directions. A matrix of 131 x 236 of these picture elements was used in the area analysis.

The first clustering algorithm used in our analysis was based upon the empirical multivariate distribution of red minus clear, blue minus clear, and green minus clear densities. An explanation of this distribution was reported last year (Norick and Wilkes, 1971). The range of red minus clear was divided into 4 intervals. The intervals were determined so that each had approximately one-fourth of the observations in it. The ranges of the other two densities were divided into 2 intervals each at the approximate medians of their marginal distributions. Each triad of intervals -- one from each color -- forms a three-dimensional rectangle. For example, $-183 < R-C \leq -13$; $-105 < B-C \leq -3$; and $-113 < G-C \leq 14$ forms one rectangle (densities are measured here on a scale from 0 to 1023). There are 16 possible rectangles for this configuration (4 intervals x 2 intervals x 2 intervals = 16). All picture elements falling into a given rectangle were given one of 16 symbols. These symbols were printed out by computer (Figure 1B) and color coded according to the color scheme in Figure 1C.

A comparison of Figure 1A and Figure 1B indicates that different forest and nonforest classes delineated by the photo interpreter do have

unique representations in the color-coded computer printout. This led to the problem of automatically locating boundaries between areas of dissimilar types. The overlay on Figure 1B demonstrates our first attempt at this. First, the multivariate means and covariances were computed for cells of 4 x 4 picture (density) elements. The Bhattacharyya distance (Fukunaga, 1972) between cells was then calculated. A threshold distance was set and all adjacent cells in rows (across) and in columns (down) that were closer than this threshold distance were grouped together. The resulting clusters are indicated on the template (Figure 1B) by black lines. Areas where no clustering occurred are masked out with solid black. This method holds promise as a way of separating forest and nonforest and some forest types. Setting a lower threshold distance would make finer distinctions (more clusters). A higher threshold would tend to group more units together (fewer clusters).

We are just beginning to search for the optimum value for separating various types of land and vegetative classes. Once we have found the optimum threshold distance for separating classes, our next step will be to compare clusters with the Bhattacharyya distance to clusters of known types. A type map will result based on the k-nearest neighbor rule. Computer programs are now being written to do this. This research will be continued and reported as part of our Forest Service ERTS and Skylab proposals.

LITERATURE CITED

1. Fukunaga, Keinosuke. 1972. Introduction to Statistical Pattern Recognition. Academic Press, New York and London.

2. Norick, N. X., and M. Wilkes. 1971. Classification of land use by automated procedures. In Monitoring Forest Land from High Altitude and from Space. Annual Progress Report for Earth Resources Survey Program, OSSA/NASA, by the Pacific Southwest Forest and Range Experiment Station. 24 p., illus.

LAND USE CLASSIFICATION IN THE SOUTHEASTERN FOREST REGION BY MULTISPECTRAL SCANNING AND COMPUTERIZED MAPPING[1]

by

F. P. Weber, R. C. Aldrich, F. G. Sadowski, and F. J. Thomson

INTRODUCTION

A twofold challenge faces natural resource inventory specialists in the 1970's: (1) to develop a rapid classification system for following the dynamic changes affecting our Nation's resources and (2) to make that system accurate and efficient enough to be cost-effective. Some scientists believe, as we do, that such a system may well be an airborne multispectral scanner (MSS) for collecting data coupled with a hybrid analog/digital computer for analyzing and displaying the information gathered.

Past studies have shown that air photo interpretation used in combination with ground examinations can result in land use and forest classification accuracies of well over 80 percent -- even at photographic scales as small as 1:420,000 (Aldrich, 1953; Aldrich and Greentree, 1972). But current national standards require an accuracy of better than 95 percent in the estimation of forest area on extensive forest inventories. Interpretation of aerial photographs can provide inventory estimates of this accuracy, but not without expending large amounts of time in photo preparations,

---

[1]The results reported herein were presented by F. J. Thomson at the 8th International Symposium on Remote Sensing of Environment, University of Michigan, on October 6, 1972. This paper will appear in the Proceedings of that Symposium.

tedious photo interpretation, and data handling.

Since the early 1960's there has been extensive research on the development of spectral signatures and pattern recognition theory in processing multispectral data. Some of this work focused on forest resource problems and has been conducted cooperatively by the U.S. Forest Service, U.S. National Aeronautics and Space Administration (NASA), and the Willow Run Laboratories (WRL) of the University of Michigan (Weber, 1971). The goal of this research has been to analyze, more quickly and accurately than a human photo interpreter can, the large volume of airborne data generated by a multispectral scanner.

Several investigators have studied the feasibility of mapping classes of terrain objects by using the spectral signature as representative of the object (Burge and Brown, 1970; Erickson and Thomson, 1971; Kolipinski et al., 1969). Further studies in pattern recognition using maximum likelihood ratio processing have been accomplished on both analog and digital computers (Marshall et al., 1969; Nalepka et al., 1971). Weber and Polcyn (1972) report application of these methods in a forest stress classification study.

Our study is similar to previous multispectral processing feasibility studies, with one important exception: Attention was centered on the ability to process economically data sets of a useful size (i.e., 42 square km) by using the same procedure used on smaller data sets (i.e., 10 square km). When we began to study large data sets, some of the variables which were ignored in the smaller sets used for feasibility studies could no longer be ignored. Most important of these variables are solar irradiance

and atmospheric path radiance and transmission. Furthermore, we considered whether the signature from a single training set was truly representative of all of that material in a large block of data. Solutions to these and other problems were crucial to the success of pattern recognition techniques applied to multispectral data. If the performance obtained in feasibility studies cannot be extended to large data sets, the technique is not practical.

The University of Michigan's Willow Run Laboratories have done a large amount of theoretical work to determine the nature of, and to attempt to compensate for, changes in solar irradiance and atmospheric conditions. Because such changes directly affect the data, techniques have been devised to correct raw MSS data before processing (Nalepka et al., 1971; Malila et al., 1971). Theoretical study of these effects is being pursued with models (Suits et al., 1972; Turner et al., 1971).

In this study we applied preprocessing theory to compensate for effects of atmosphere and changing solar irradiance. We used signatures from one of four parallel, overlapping flight lines to classify data on all four lines. Compensation for solar irradiance changes in the morning data was made by dividing all data by the sun sensor signal level. Thus, this study was not only a feasibility study of mapping important land use categories but also tested the ability to extend the utility of spectral signatures collected from one run to three additional runs made shortly before or after the first.

This paper reports a test of multispectral scanning of two 42-square-km sites near Atlanta, Georgia. The purposes of the test were: (1) to

prepare land use (forest and nonforest) maps with estimates of use, by terrain classes, and (2) to determine the accuracy of class signatures developed on a single training flight for classifying data on four adjacent flight lines (signature extension).

DATA COLLECTION

Within each test block a small area with features representative of the block was selected for ground instrumentation. Two sets of data were to be collected within each block -- one in the early morning and one at midday.

Data collection began at about 1330 hours (local sun time) November 3, 1971, at Block 2 (Figure 1). The University of Michigan's multispectral C-47 aircraft flew four parallel flight lines at an altitude of 3,450 meters (m).

A second flight was made over Block 2 the next morning, starting at about 0900 hours. After successfully completing the work in Block 2, we moved to Block 4. The first data set in Block 4 was completed on the afternoon of November 4. The next morning, commencing at about 0930 hours, we collected the last of the four ground and aircraft multispectral data sets. On November 7, the U.S. Forest Service's Aero Commander photographed Blocks 2 and 4 with color infrared (CIR) film at a photo scale of 1:35,000.

While the Michigan aircraft was collecting data, men on the ground, who had two-way radio contact with the plane, were also collecting data. Solar radiation was measured by a portable pyrheliograph at the ground site. Two men in a "cherry picker" (Figure 2) collected data on spectral irradiance of several landscape targets, such as conifers, hardwoods, pastures, transitional fields, and water. They also measured target net

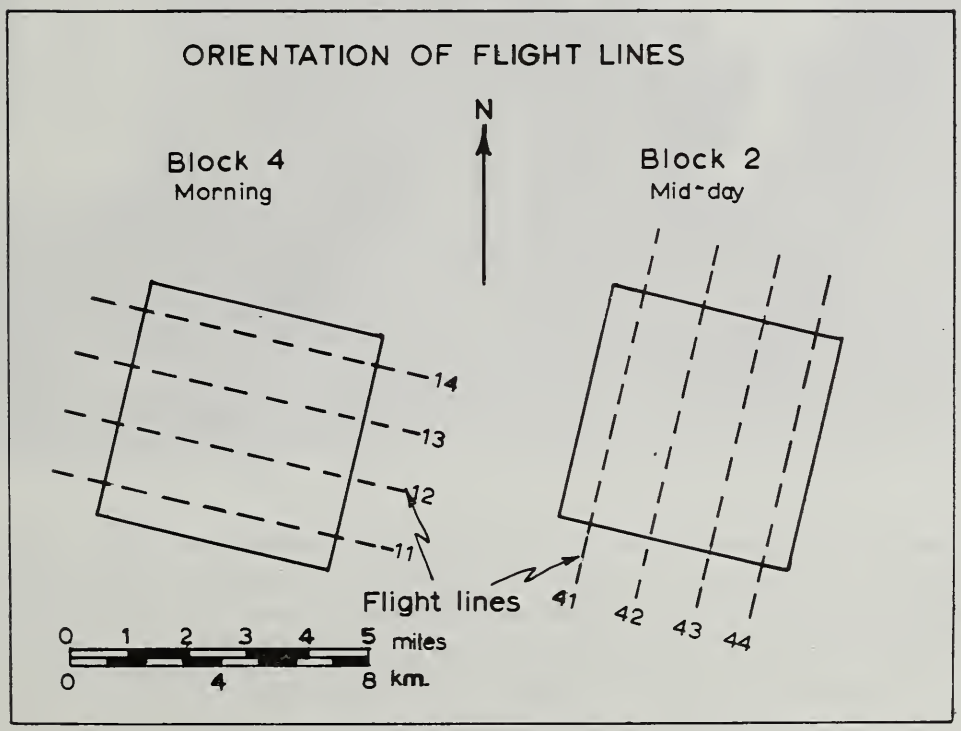

Figure 1. UPPER PHOTO: These two 42-square-km test sites were used in the study. Block 2 is 96 km south of Atlanta, and Block 4 is 73 km west of Atlanta. LOWER PHOTO: Flight lines were oriented as shown for early morning, 0900 hours (Block 4), and midday, 1200 hours (Block 2), flights.

Figure 2. Researcher is shown in a cherry picker above the test site measuring the spectral radiance of vegetation with a 4-channel spectrometer. Ground data were collected as a coordinated effort with the airborne MSS flights to provide baseline calibration data used during multispectral processing.

radiation and reflected solar radiation. During the period November 3 to 5, a two-man ground crew inspected about 50 percent of both blocks and recorded ground classification data.

MICHIGAN MULTISPECTRAL SCANNER SYSTEM

Hasell (1972) has described the construction details of the Michigan M-7 scanner used in this study. In the past we had used earlier versions of it which were double-ended and multipathed to achieve multispectral sensing in forest resource problems. Analysis of the data had strongly indicated the requirement for a multispectral scanner to produce simultaneously registered data covering the bandwidth 0.4 to 13.5 micrometers (μm) in select narrowband increments (Weber and Polcyn, 1972). Our study in the Southeastern United States provided the first opportunity to test the merits of multispectral data collected with a truly single-line-of-sight scanner.

DATA PROCESSING

In this study we used both the digital and analog computing facilities. To produce the land use maps, a pattern classification technique known as the maximum likelihood ratio was applied to the spectral signature data we obtained. And to insure the fairest test of signature extension, careful preparation of the raw MSS taped data was required (Nalepka and Thomson, 1972). In particular, we had to compensate for variations in spectral signatures that depended on observed scan angle. The four optimum channels for classifying land use classes were identified by digital computer

analysis. This analysis was done before preparation of recognition maps on a hybrid digital/analog computer. Additional digital analysis was conducted after the recognition maps were prepared to identify causes of some misclassifications in data collected in early morning.

DATA PROCESSING HARDWARE

The digital computer we used was a CDC 1604B with 16k-48bit words of storage. Associated with the computer are eight 7-track, 200 bpi digital tape drives and a special-purpose analog/digital and digital/analog interface. A multispectral analysis computer program was developed to convert analog scanner data to digital, display them, quantify variation in spectral signatures, compensate for these variations, and prepare recognition maps using the supervised-learning, maximum-likelihood-ratio classifier (Erickson and Thomson, 1971).

The SPectral Analysis Recognition Computer (SPARC) system is a parallel-organized system designed to implement likelihood ratio classification of multispectral data at real-time rates. The system consists of an analog tape recorder, suitable interface gear, a preprocessor, the computer itself, 70 mm film printing, and CRT display equipment. It can classify data at about 80,000 decisions per second and prepare 70 mm filmstrip recognition maps at the same time.

Because of its parallel organization, SPARC can use only a limited number of channels and training sets. Any combination of channels and land use classes whose product is 48 or less can be used. In this study we used four channels and 12 training sets.

SPARC operates in two modes -- training and operational. The machine is programmed to recognize land use classes in the training mode. An

operator enters samples of data from training sets and a statistical description of each training set. Thus, each class to be recognized must be represented by at least one training set within SPARC. Once training has been completed, the operational phase begins. Unknown data are classified by using the likelihood ratio as a measure of similarity of scene-point spectral signatures to those of the training sets. Recognition maps of each class are printed on 70 mm film. To depict an entire scene, the number of filmstrips must equal the number of training sets.

The 70 mm recognition maps may be individually analyzed by overlaying each map with conventional video filmstrips. The individual maps can also be color coded and combined into a mosaic by means of the color ozalid process. The color ozalid approach was used for this study.

PROCESSING EFFORT

Experimental Plan

Two data sets were defined by the principal investigator for processing -- the 1200 hours flight of Block 2 on November 3 and the 0900 hours flight of Block 4 on November 4.

Each of the two 42-square-km blocks was processed separately. One of the four parallel flight lines from each block was digitized initially. The lines selected were line 43 from Block 2 and line 14 from Block 4. These lines provided the best selection of training areas for the land use recognition classes desired. The objective of the digital work was to identify angle correction functions and determine optimum spectral channels for use in the analog processing. Once determined, the results were applied to the remaining three flight lines in each respective block.

Signatures of representative areas for each land use category were programmed into the SPARC and recognition obtained. Signatures trained on flight lines 43 and 14, respectively, then were played on the three remaining flight lines of the corresponding block as a test of signature extension capabilities. We hypothesized that uniform color coding of results and the mosaicking of adjacent flight lines for each block would result in reliable area-recognition maps of good geometric fidelity.

Processing Effort - Block 2

Digital Work

Data from flight line 43 were digitized by using a computer program called A2F3 that reads analog data in an analog/digital converter and "smooths" the data by averaging from 3 to 15 consecutive scan lines into a single composite scan line. Program A2F3 also repacks the data into the standard digital tape format and writes the resulting scan lines as records on digital tape. Thus, it produces finished ready-to-process digital data from analog data in a single step.

The data were digitized using 2.5 milliradians per resolution element, and eight consecutive scan lines were "smoothed." Each resultant digital element, therefore, represented an effective ground resolution patch size of 7.6 m x 7.6 m which closely approximates the minimum scanner resolution capability at an altitude of 3,048 m.

All 12 MSS channels were digitized simultaneously, except for the near infrared channel of 2.0 to 2.6 μm which was rendered unusable owing to cross-coupling of signals from the adjacent thermal channel.

A program called GRAYMAP produced a digital printout of a red channel

(0.62 to 0.70 μm). It divides the signal range of a selected channel into seven intervals and assigns a unique typewriter symbol of decreasing density to six of the intervals, with the seventh left blank. The digital elements on the tape are then scanned consecutively, point by point and line by line. The value of each element is classified into the appropriate interval, and the corresponding symbol is assigned. A printout of the results yields a maplike presentation in which tone gradations are represented by symbols of varying density so that light-toned areas appear white and dark-toned areas appear black. Numbers printed along the top and down one side allow for a coordinate reference system useful for locating specific points. Such a map provides a visual display with which to check the merits of the digitization process and to locate training areas for signature extraction.

Before processing can continue, the digitized data must be calibrated to some reference, all channels brought into registration, and the dynamic range scaled. These three steps are taken by using the programs AUTOCAL and CSD which: (1) clamp the voltage levels from inside the scanner housing to zero. (This enables all radiation inputs from the scene and calibration sources to be referenced to a uniform minimum voltage level.); (2) deskew signals from adjacent wavelength intervals. (Owing to slight misalignments of tape recorder and playback heads, signals from adjacent channels may not be properly registered. Consequently, signals in two widely separated channels on the tape may appear to come from the same data point although actually arising from two different data points. Such misregistration is termed "skew" and must be corrected.); and (3) scale

the voltage levels in each channel to make optimum use of the dynamic range available and prevent loss of signal due to overshoot.

Once the data were corrected, the variations in observed radiance were identified by the program ACORN4. These variations occur because the angle of observation changes as each scan line is traced across the scene. The result is varying magnitudes of path radiance due to varying path lengths or variations, or both, in bidirectional reflectance of the scene components. Compensations for such variations are made by averaging the variation of scene radiance with scan angle over the length of the flight line and by generating second-degree functions which define the variation with scan angle for each channel.

The program NUDATA then normalizes the digital data by subtracting or multiplying the data by the coefficients of the functions calculated in ACORN4. The coefficients were also later used on the preprocessor of the SPARC system.

After the data were normalized, the analysis to determine the performance of the spectral channels in separating the land uses of interest was begun. Training areas, originally designated on 1:35,000 scale CIR photography, were located on the digital graymap. Rectangles were drawn within the bounds of each training area, and the line and point numbers of the four corners then identified the area for signature extraction by the program IMPROVE. IMPROVE was used to average the voltage levels within a training area for each channel and print out the resulting mean and standard deviation for each MSS channel along with a covariance matrix for all channels. The training signatures were computed from either individual area or from a combination of several separate areas.

Eight land use classes -- four forest and four nonforest -- had originally been designated for recognition and classification. These classes are as follows:

Forest	Nonforest
Conifers	Agriculture
Upland hardwood	Pasture
Bottomland hardwood	Water
Undecided	Transitional

Analysis of the resulting spectral signatures indicated significant variability within two of the nonforest categories -- agriculture and pasture. Therefore, we decided that additional land use categories would have to be designated to obtain significant recognition results. Agriculture and pasture were each divided into three subcategories, and the resulting classification scheme became:

Forest	Nonforest
Conifers	Row crops
Upland hardwood	Bare soil
Bottomland hardwood	Orchard
Undecided	Improved pasture
	Old pasture
	Pasture
	Water
	Transitional

The signatures computed by IMPROVE were used to determine the optimum channels for use on the SPARC system. Optimum channels are those spectral

regions which are most useful in discriminating the training areas. Since 12 land use classes were now selected for recognition on the SPARC, only the four best channels, instead of the original eight, could be used (the product of land use classes and channels cannot exceed 48).

The program STEPLIN computes the Average Pairwise Probability of Misclassification (APPM) for each channel for all possible pairs of signatures. The channel having the lowest APPM is selected as the best one. Next, the program computes the APPM for all possible pairs of channels given the best channel. Again, the channel with the lowest APPM is selected and becomes the second best channel. Then the program computes the APPM for all triples of channels given the best pair. This process is repeated until all channels are classified.

The first four channels selected were 1.5 to 1.8 μm, 9.3 to 11.5 μm, 1.0 to 1.4 μm, and 0.41 to 0.49 μm. The fifth channel selected -- the red region of 0.62 to 0.70 μm -- had an average probability of misclassification for all 12 categories that was only 0.3 percent higher than that of the fourth channel selected, given the previous selection of the three best channels (Table 1). However, the red spectral region enhanced discrimination between varying pasture conditions (which constitute a significant portion of the scene) and was ultimately used in place of the blue channel.

It seemed useful at this point to create a digital recognition map to determine the adequacy of the 12-category/4-channel setup in recognizing the scene. The program EXPLIN performed a linear approximation to the maximum likelihood ratio decision rule in classifying the digital data

Table 1. Optimum Channel Selection Sequence for All 12 Categories of Block 2

Spectral Channel	ITERATION NUMBER										
	1	2	3	4	5	6	7	8	9	10	11
0.41-0.48 μm	0.1130	0.0297	0.0151	0.0093*							
0.46-0.49 μm	0.1324	0.0398	0.0185	0.0118	0.0086	0.0065	0.0056	0.0051	0.0049	0.0045	0.0042*
0.50-0.54 μm	0.1198	0.0389	0.0179	0.0109	0.0083	0.0063	0.0055	0.0050*			
0.52-0.57 μm	0.1165	0.0340	0.0167	0.0105	0.0080	0.0059*					
0.55-0.60 μm	0.0987	0.0331	0.0189	0.0122	0.0087	0.0067	0.0056	0.0052	0.0046*		
0.58-0.64 μm	0.0959	0.0329	0.0197	0.0127	0.0081	0.0068	0.0055	0.0051	0.0047	0.0044*	
0.62-0.70 μm	0.1004	0.0324	0.0197	0.0126	0.0073*						
0.67-0.94 μm	0.2026	0.0323	0.0178	0.0129	0.0089	0.0067	0.0054*				
1.0 -1.4 μm	0.1575	0.0325	0.0140*								
1.5 -1.8 μm	0.0514*										
9.3 -11.5 μm	0.1389	0.0226*									

*indicates the lowest average pairwise probability of misclassification for each iteration. Thus, the 1.5 to 1.8 was first, 9.3 to 11.5 second, 1.0 to 1.4 third, etc.

points. The resultant signal levels on the output tape represented the recognition of various categories with an additional level for an unrecognized category to avoid numerous false classifications. Typewriter symbols were assigned to each signal level with a blank designated for the unrecognized category. A computer printout of signal levels resulted in the digital recognition map. Color coding of various groups of categories was achieved by printing only a subset of signal levels for a particular color of printer ribbon. Each time the data were processed the computer/printer ribbons were changed, and another subset of levels was printed. The resulting land classification map consisted of four colors and three tones.

Analog Work

For analog processing the preprocessor unit was programmed with the ACORN4-derived angle-correction coefficients. A single representative area for each land use class was identified on flight line 43 of Block 2. In the digital program, it was possible to lump several training areas together and obtain a composite signature for a land use class. But the analog program does not have this capability. Each area must be "trained" separately; therefore, it was important to pick areas which were most representative of the category.

SPARC training required that a duplicate analog tape (which had been deskewed) be cut into sections, each section containing all of the data from a flight line. Each tape section was made into a continuous loop, and the loops then played on a conventional tape recorder with a loop adaptor. The SPARC operator viewed the loop on a real-time, C-scan

display. Each time the loop recycled, the scene was repeated on the C-scan. This repetitive display of the tape data containing the training areas permitted bracketing each training set with horizontal and vertical electronic gating mechanisms so that only signals from the training area were sent to the SPARC. The mean, standard deviation, and covariance for each of the digitally selected optimum channels were entered into SPARC. When all channels had been trained on the first set, the next training set was gated in and the channels trained in like manner. When all training sets had been programmed, the training phase of SPARC recognition was completed.

In an effort to guarantee that all 12 land use classes were programmed accurately, a Euclidean distance decision rule (Nalepka et al., 1971) was used to recognize training sets. The criterion for acceptable training of each set involved recognition of at least 90 percent of the area within the set. In applying the Euclidean distance rule, we specified a threshold and identified all points whose probability density function (pdf) values exceeded it. All points whose pdf values fell below the threshold were not identified. Recognition results were quantified with a high-speed digital counter which tallied the number of points (resolution elements) identified as the target of interest. Percent recognition was the number of points counted as recognition for the target compared to the total number of points in the gated training set.

The operational phase of the SPARC recognition process involved playing another copy of the original analog tape through the tape recorder in standard fashion. Each time the tape was played, one of the land use

classes was recognized. As each scene point on the tape was reached, a likelihood ratio was computed, and a decision was made as to whether the point resembled the target. If so, SPARC put out a recognition signal, and the high-speed counter recorded the tally. The recognition signal was printed on 70 mm film moving past a rapid line-scanning cathode ray tube. This process continued on a real-time basis until all scene points were classified.

When all 12 recognition strips for flight line 43 were complete, the operational phase of the SPARC work was repeated for each of the three remaining flight lines in Block 2 as a test of "signature extension." Preprocessing coefficients and signature settings remained unchanged from flight line 43. Geometric corrections were made to all flight lines to insure as uniform an aspect ratio as possible. Scanner angular distortion was corrected with the use of a tangent function, and forward scale was standardized for all lines within each block.

Each set of recognition strips for a particular flight line was color coded by using an ozalid process. The individual color separations were then overlaid and registered to form an ozalid "sandwich." Each sandwich was photographed to create a color-coded recognition map of each flight line. The resulting four photographs were finally mosaicked to create a color-coded recognition map for the entire block (Figure 3) which was compared in the analysis with the ground truth map for Block 2 (Figure 4).

Processing Effort - Block 4

Digital Work

Data from Block 4 were processed in much the same way as those from

Figure 3. The final SPARC color-coded recognition map for Block 2 is shown with the 12 land use classes indicated.

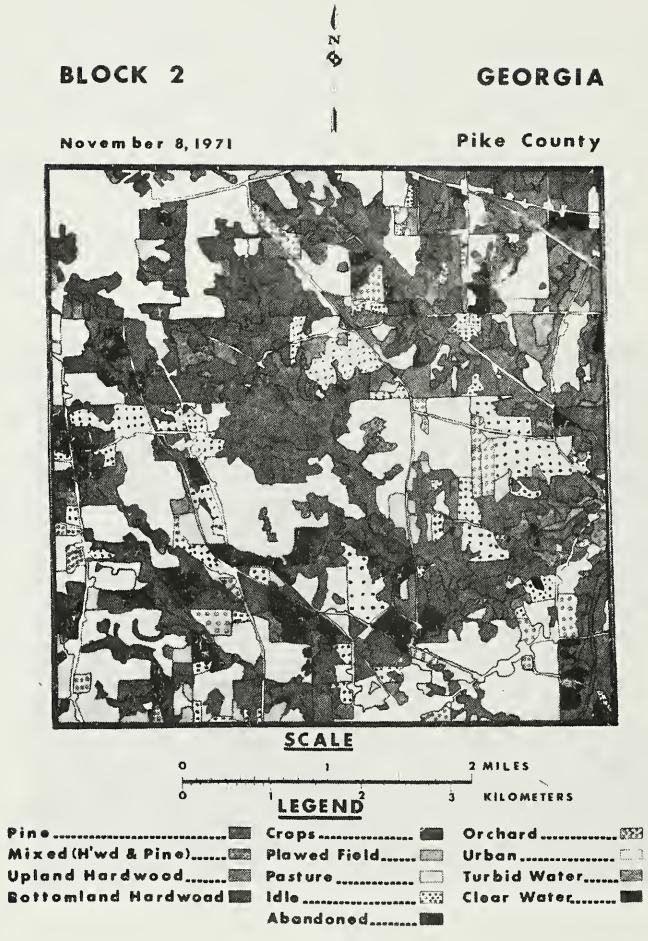

Figure 4. The ground truth map for Block 2 is shown. A comparison of this map with the SPARC-produced map of Figure 3 will give the reader a feeling for the accuracy of the SPARC classification.

Block 2. Line 14 was processed digitally to obtain optimum channels and preprocessing coefficients for use on the SPARC. The reflective infrared channel of 1.5 to 1.8 μm was not available for this data set since it had been assigned to the same malfunctioning preamplifier that rendered the 2.0 to 2.6 μm channel unusable for Block 2. This was unfortunate since it was the 1.5 to 1.8 μm channel which had been the best channel for discriminating the various categories in Block 2.

Angle correction functions were again identified and used to normalize both the digitized data and the analog data of all four flight lines. Eleven signatures were derived from the digitized data to correspond with like land use categories recognized in Block 2. (An "orchards" category does not appear in Block 4.)

For this data set, optimum channels were determined for each of three postulated classification problems in an attempt to identify channels most useful in discriminating the more dominant scene components from each other (i.e., forests and pastures). The cases considered were: (1) all 11 land use categories, (2) the four forest categories, and (3) the four forest and three pasture categories (Table 2). The thermal channel (9.3 to 11.5 μm) was not used in the selection process. We judged that the use of thermal data collected in the morning would result in poor signature extension because of the rapid change in terrain feature temperature. Channel selection for the SPARC work was based on an ability to discriminate well in all three classification problems. The four channels selected were 0.52 to 0.57 μm, 0.58 to 0.64 μm, 0.62 to 0.70 μm, and 2.0 to 2.6 μm. Although the channel 0.41 to 0.48 μm performed well in discriminating the

Table 2. Optimum Channel Selection Sequence for Each of Three Postulated Classification Problems for Block 4

	ITERATION NUMBER									
	1	2	3	4	5	6	7	8	9	10
ALL 11 LAND USE CATEGORIES										
Spectral Channel (μm)	0.58-0.64	2.0-2.6	0.67-0.94	0.62-0.70	0.41-0.48	1.0-1.4	0.52-0.57	0.55-0.60	0.46-0.49	0.50-0.54
APPM*	0.1238	0.0711	0.0444	0.0326	0.0251	0.0210	0.0185	0.0179	0.0172	0.0166
FOUR FOREST CATEGORIES										
Spectral Channel (μm)	0.41-0.48	0.58-0.64	1.0-1.4	2.0-2.6	0.62-0.70	0.67-0.94	0.52-0.57	0.46-0.49	0.55-0.60	0.50-0.54
APPM*	0.2056	0.1620	0.1383	0.1277	0.1081	0.1007	0.0955	0.0921	0.0896	0.0877
FOUR FOREST AND THREE PASTURE CATEGORIES										
Spectral Channel (μm)	0.52-0.57	0.41-0.48	0.58-0.64	2.0-2.6	0.62-0.70	1.0-1.4	0.67-0.94	0.46-0.49	0.50-0.54	0.55-0.60
APPM*	0.1408	0.0919	0.0710	0.0574	0.0463	0.0390	0.0355	0.0343	0.0332	0.0323

*APPM is average pairwise probability of misclassification

various forest and pasture categories, it was rejected on the basis of inordinate noise on duplicated tape for SPARC. The 1.0 to 1.4 μm channel also had to be rejected due to excessive signal overshoot caused by a malfunctioning preamplifier during the flight.

Analog Work

The use of a different set of channels and data collected at a different time of day necessitated some changes in the classification scheme developed for Block 2 during the training phase of the SPARC work. For example, differentiating between upland and bottomland hardwoods was not possible in Block 2 although it was attempted. Areas typed on the 1:35,000 scale CIR photography as mixed conifer/hardwood had a multispectral signature so similar to that of pure conifers that the two had to be combined for effective recognition. Areas designated as row crops on the photography were indistinguishable from pastures. We decided that two signatures were required for acceptable water recognition -- one for clear deep water and a second for the muddier, shallow ponds. An additional signature was used for each of the transitional and improved pasture categories to minimize the variability within these categories.

Thus, in all, eight categories were programmed into the SPARC computer representing these land uses in Block 4:

Forest	Nonforest
Conifers	Improved pasture
Hardwoods	Old pasture
	Pasture
	Bare soil

Forest	Nonforest
	Water
	Transitional

Recognition strips were then printed for each of the eight categories in line 14. Signature extension, color coding of recognition strips, and mosaicking of the flight lines were done similarly to Block 2.

Further Digital Analysis - Block 4

Additional processing of Block 4 was necessary to investigate the reasons for variable recognition results obtained during the signature extension work. As initially processed, angle correction functions derived during the digital processing of line 14 (the last line flown) were applied to all the flight lines for the SPARC recognition procedure. Although the application of uniform correction functions to successive lines of data may be acceptable for midday periods, whether such corrections are reliable in early morning situations, when illumination level and sun angle are changing rapidly, was not certain. (Block 4 was flown at 0912 hours local time, with the time interval between the start of line 11 and the end of line 14 being 31 minutes.)

Flight lines 11, 12, and 13 were digitized, clamped, scaled, and deskewed for the optimum channels used to process line 14. Average scan lines for each flight line in each channel were then plotted. Examination of the curves suggested two possible causes for the slight change in recognition that was shown from line 14 to each of the earlier lines -- change in illumination level and change in angle effects.

Owing to limited time and funding, additional SPARC processing was

restricted to line 12. Illumination change was assessed by noting the signal level at the peak of the aircraft sun sensor pulse in each channel in lines 12 and 14. Such a pulse appears in every reflective channel on every scan line of the data. It is the result of incident illumination on the top of the aircraft being transmitted through a flat opal glass port about 8 inches in diameter. The radiation is directed into the scanner housing where it is recorded on each successive revolution of the scanner collecting optics. The resultant signal pulse is available for use as some measure of incident illumination level during the flight. Signal levels for line 12 were lower than for line 14 as follows:

	0.52 to 0.57 μm	0.58 to 0.64 μm	0.62 to 0.70 μm	2.0 to 2.6 μm
$\frac{SS_{(line\ 12)}}{SS_{(line\ 14)}}$	$\frac{1.3}{1.4} = 92.8\%$	$\frac{1.3}{1.5} = 86.6\%$	$\frac{0.8}{0.9} = 88.8\%$	$\frac{1.5}{1.6} = 93.7\%$

in which SS is the peak voltage of the sun sensor for the line indicated. We decided to increase the gain in each of the channels for line 12 as a means of compensating for the lower illumination level present at the time the data were recorded. Gains were increased by elevating the peaks of the sun sensor by these amounts:

Spectral Channel	% Increase
0.52 to 0.57 μm	7.2
0.58 to 0.64 μm	13.4
0.62 to 0.70 μm	11.2
2.0 to 2.6 μm	6.3

Recognition strips of line 12 were then printed and area counts obtained for each of the signatures as trained on line 14.

A change in angle effects was also deemed important as a potential

source of error. The nonuniformity of signal on either side of nadir seemed to increase as zenith angle increased (i.e., with decreasing line number). The calculation of zenith angle for each of the two lines can account for some variations in angle effects across the scene, considering the magnitude of the zenith angles (65.62° for line 14 and 68.80° for line 12).

Coefficients for use in normalizing the average scan lines were derived digitally with the program ACORN4 for line 12 as had been done for line 14. The preprocessor of the SPARC was then configured with the coefficients, and recognition strips for line 12 were again printed.

Finally, a set of recognition strips was printed and area counts obtained employing both of the corrections. The resulting SPARC mosaic composite (Figure 5) was compared to the color-coded ground truth map (Figure 6).

COMPARISON OF SPARC MOSAIC WITH CIR PHOTOS AND GROUND TRUTH

A technique was developed to compare SPARC-produced color-coded mosaics made from multispectral scanner data with maps made by interpretation of 1:35,000 scale CIR photographs and ground checks of over 50 percent of the classifications. A systematic dot grid (10 dots per square inch) was placed over the land use map of each of the two blocks drawn to a scale of 1:35,000 and the numbered points listed by the classification within which they fell. There were 490 of these points that fell within the boundaries of Block 2 and 458 points that fell within the boundaries of Block 4 (Tables 3 and 4). Each photographic sample point in Block 2 represents about 7 hectares (17.5 acres), whereas in Block 4

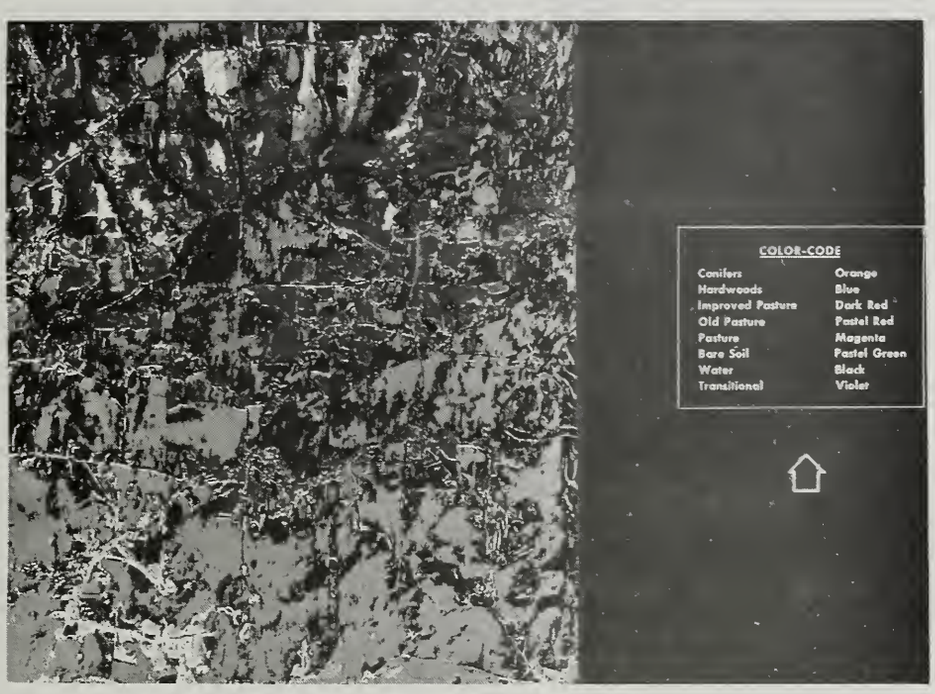

Figure 5. The final SPARC color-coded recognition map for Block 4 is shown here with the 8 land use classes indicated.

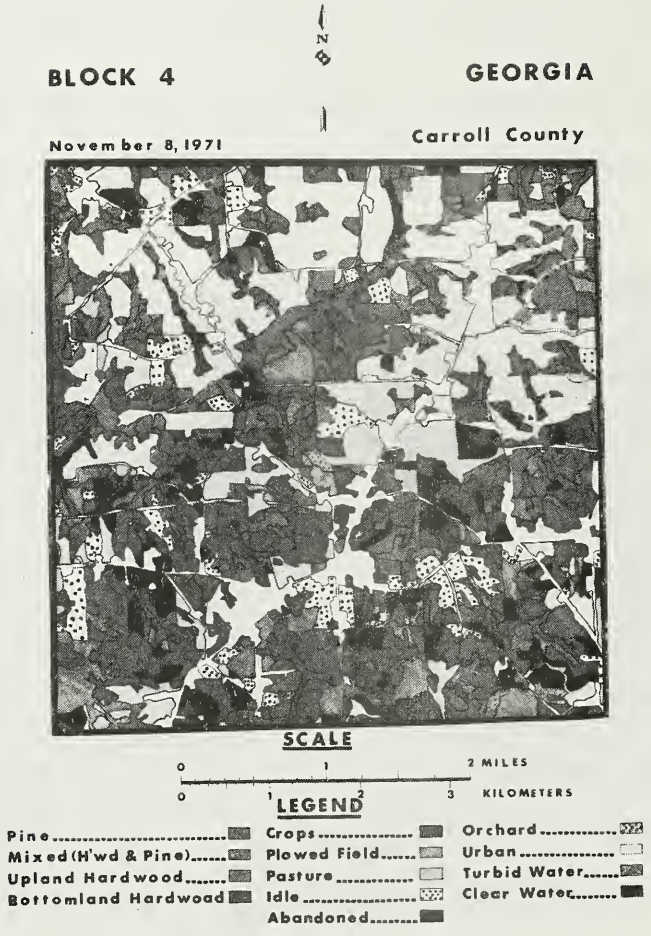

Figure 6. The ground truth map for Block 4 is shown here. A comparison of this map with the SPARC-produced map in Figure 5 will give the reader a feeling for the accuracy of the Block 2 SPARC classification.

Table 3. Scene Composition in Block 2 By Photo Interpretation/Ground Survey and SPARC

Land Classification	Number of Photo Points	Area, by Land Use	
		CIR/Photo/Ground Survey	SPARC
		--------- Percent --------	
Pine	100	20.4	3.7
Pine/hardwood mixture	--	--	15.4
Upland hardwood	20	4.1	27.8
Bottomland hardwood	89	18.2	6.0
Agriculture	70	14.3	7.8
Pasture	118	24.1	28.0
Transitional	20	4.0	3.5
Orchard	16	3.3	1.6
Urban	50	10.2	5.3
Water	7	1.4	0.9
TOTAL	490	100.0	100.0

Table 4. Scene Composition in Block 4
by Photo Interpretation/Ground Survey and SPARC

Land Classification	Number of Photo Points	Area, by Land Use	
		CIR/Photo/Ground Survey	SPARC
		--------- Percent ---------	
Pine	135	29.5	37.8
Hardwood	96	21.0	28.5
Agriculture	36	7.9	2.2
Pasture	106	23.1	19.7
Transitional	28	6.1	5.9
Urban	45	9.8	4.3
Water	12	2.6	1.6
TOTAL	458	100.0	100.0

each point represents 8 hectares (20.5 acres).

Next, we selected 20 points at random from each land class (except orchards and water) recorded in each test block -- a total of 171 points. These sample points were used to check the MSS imagery as displayed on the SPARC mosaics. In Block 2 we could identify only 16 orchard samples on the photo points, and only seven points fell in water. We found an additional eight points to represent water and finished with a total of 15 samples. Block 4 had no orchards; thus, this class was not a factor in this block. Only 12 points were in the water class, but eight additional samples were found to supplement these.

Templates were made to show the location of 171 points in Block 2 and 160 points in Block 4. The color-coded film transparency of each multispectral scanner mosaic was placed in an enlarging projector-viewer and scaled to the 1:35,000 scale of the photo/ground survey map. Since there was geometric distortion throughout the MSS mosaics, the scale was adjusted for best fit while we checked sections of the mosaic. The template of point locations was placed over the projected image and keyed to the 1:35,000 photo/ground survey map. With the images coinciding as nearly as possible each point was examined and the MSS classification recorded.

RESULTS

BLOCK 2 - MIDDAY FLIGHT

Twelve-Category Recognition of Flight Line 43

As originally designed, the eight-category recognition scheme for Block 2 would have allowed for the use of six waveband channels on the

SPARC. However, the great amount of variability noted in the signatures of two of the categories (pasture and agriculture) necessitated the creation of six categories to replace the intended two. The effect was to reduce the number of channels for use in the recognition effort. This limitation was not considered to be significant because of some previous experiences in multispectral recognition studies. The APPM decreased rapidly as the first few channels were selected for use (Table 1). The APPM associated with the use of a fifth channel after the four most optimum have been selected was already less than 1 percent for all cases. The reduction in classification error from the four- to the six-channel case was not more than 0.35 percent. Thus, the increase in APPM is minimal especially when more training sets are used on SPARC with fewer channels.

A qualitative comparison of the SPARC color-coded recognition for flight line 43 with the type-mapped CIR photograph revealed generally good recognition. Areas typed on the photo as being row crops, bare soil, and water seemed to be accurately identified. Forested areas are well differentiated from nonforested areas. Within forested areas, large dense conifer plantations are solidly recognized. Some confusion exists around edges of plantations and with small clumps of conifers in that bottomland hardwoods and mixed conifer/hardwood forest categories seem to mask the conifer's signature. Within hardwood areas, the predominant recognition seems to be of upland hardwoods, with bottomland hardwoods and mixed conifer/hardwood categories being somewhat more selective. Whether this situation portrays the actual site conditions or is the result of slightly different signature settings on the SPARC is difficult to say.

Pastures show the extreme variability that necessitated the creation of three subcategories during the digital processing. With few exceptions, pasture recognition is characterized by all three of the pasture signatures within the same field boundary. Several sizable fields in the center of the southern half of the flight line have little or no recognition. Although no significant difference between these fields and others in the area can be detected on the photography, they seem to be unique spectrally. During the training phase of SPARC work, training was attempted in this area, but the resulting signature was very poor in recognizing other areas in the scene, so the training area was moved. A few smaller pastures are recognized as row crops. This is not surprising, considering the time of year and the similarity between mowed hay fields and "browned-out" pastures.

Orchards vary widely in appearance on the photography, ranging from peach and pecan seedlings with bare soil backgrounds to mature trees with pasture-like backgrounds. The training area for the orchards category was placed in a young orchard (not the seedling stage) with a predominantly bare soil background. Other similar orchards were recognized, but mature orchards were understandably classified as upland hardwoods and very young orchards as bare soil.

Transitional areas are spotty in recognition, with much competition between them and upland hardwoods. Water areas were recognized accurately except for one unrecognizable small pond in the center of the line. The very light tone of this pond on the photograph is probably indicative of heavy sediment content to the extent that the spectral signature is significantly different from the "water" signature trained on the SPARC.

In several areas on the SPARC map, low-lying regions of pastures, row crops, and orchards illustrate changes in recognition from the immediate surrounding regions. Many of the same areas show tone changes in recognition from the immediate surrounding regions. Many of the same areas show tone changes on the photography but no changes in texture or pattern, indicating spectral variation as a possible consequence of soil moisture conditions. Thus, in the case of automated classification of many land use categories, some of which are only slightly different from each other, it appears that soil moisture conditions adversely affect the accuracy of correct identification.

Signature Extension of Block 2

Recognition for signatures trained on flight line 43 was extended to line 44 flown after line 43 and the two lines, 42 and 41, flown before 43. From a qualitative viewpoint, recognition of land use categories showed only slight change in comparison to line 43. Transitional areas seemed to be more solidly recognized -- both east and west of line 43 -- although we do not know why. Recognition within hardwood areas appears to decline somewhat on the two earlier flight lines, with bottomland hardwood recognition noticeably lacking on line 41. On the signature extension, pastures seemed to be classified into only the "improved" or "old" categories on lines 42 and 41. Very little "pasture" appears on these two lines.

In comparing results from SPARC and from the photo/ground survey for Block 2, we found that 75 of the sample points or 44 percent were correctly classified (Table 5). The class with the greatest accuracy was pasture -- 85 percent of the points in pasture were correctly classified, but 18 points

Table 5. Accuracy of SPARC Classification
As Determined by Photographic Sample Point Analysis

Land Classification	Classification Accuracy		Commission Errors
	Number of Points	Percent	Number of Points
	BLOCK 2		
Pine[1]	4	20	1
Bottomland hardwood	10	50	20
Upland hardwood	11	55	35
Agriculture	10	50	3
Pasture[2]	17	85	18
Transitional	0	0	1
Orchard[3]	2	14	0
Urban[4]	12	60	14
Water[5]	9	60	4
ALL CLASSES	75	44	96
	BLOCK 4		
Pine	16	80	20
Hardwood	24	60	19
Agriculture	3	15	2
Pasture[6]	18	90	18
Transitional	9	45	2
Urban	15	75	1
Water	12	60	1
ALL CLASSES	97	61	63

[1]Fourth forest category, "mixed pine/hardwood" was not considered in analysis

[2]Includes all three categories of pastures

[3]Insufficient number of points to obtain 20 samples; 16 used

[4]Unclassified areas considered urban

[5]Insufficient number of points to obtain 20 samples; 15 used

[6]Includes both categories of pasture

were called pasture when they were actually something else (i.e., the misclassifications were commission errors). The class that showed the poorest result was transitional agriculture -- abandoned agriculture returning to forest. In this case only one point was correct. There were no commission errors. Of the forest classes, pine (conifer) was correctly classified on 29 percent of the point samples, with one commission error. Bottomland and upland hardwoods were classified correctly 50 and 55 percent of the time, respectively, but with a high number of commission errors.

These results suggest the need to reconcile the additional SPARC classification of mixed conifer/hardwood. SPARC was trained to classify only the pure pine plantations as conifer, whereas pines growing in association with hardwoods were recognized as a mixed conifer/hardwood category. If we combined the conifer category with the conifer/hardwood category, we would total 19.1 percent (SPARC) as compared to 20.4 percent (photo point analysis).

As indicated previously, SPARC area counts for each category were tabulated with the high-speed digital counter as recognition strips were printed. Recognition was therefore expressed on a quantitative basis as well as illustrated graphically. Table 3 indicates the scene composition of Block 2 on a percent basis, comparing SPARC classification with photographic point classification. Due to the extensive overlap between MSS flight lines, most of the scene was included more than once when totaling recognition for each category over all four flight lines. However, since total area was also included more than once, percentages for the entire block would not be far off if it is assumed that recognition in any one flight line is uniform over that line and objects recognized are uniformly distributed.

Digital and SPARC Map Comparisons

A brief comparison of the digital recognition results for flight line 43 was made with the SPARC results. Their differences were:

Program EXPLIN	SPARC
WATER: Excellent recognition	Good recognition -- 1 pond missed. Some perimeters of smaller ponds missed.
CONIFERS, BOTTOMLAND HARDWOODS, MIXED: Good separation of conifers from hardwoods.	Some conifer areas classified as bottomland hardwoods or undecided forest.
UPLAND HARDWOODS, TRANSITION: Proper classification of transitional areas.	Too much classification of transitional areas as upland hardwoods.
ORCHARDS: Seem to span a broad signature. Young orchards are well recognized and portions of bare soil, row crops, and sparse pasture areas are also classified as orchards. Old orchards classified as hardwoods.	Seem to be a more stringent signature. Young orchards are spotty in recognition while not many other areas are classified as orchards. Old orchards classified as hardwoods.
ROW CROPS: Most row crop areas have some indication of proper recognition, but entire areas are not solidly recognized. Rather much row crop area is classified as orchards, transition, bare soil, and unrecognized categories.	Good recognition
BARE SOIL: Many bare soil areas classified as orchards.	Good recognition
PASTURES: Much less improved pasture recognition. "Pasture"	Considerably improved pasture recognition

PASTURES (cont'd):
category increases. Some portions of fields which were recognized by SPARC are not recognized by EXPLIN.

Overall it appears that EXPLIN was best at classifying the water, transition, and four forest categories. SPARC did better with the orchards, row crops, and bare soil categories. A judgment concerning pasture recognition must be withheld because subcategories of pastures were not typed on the 1:35,000 scale CIR photograph used for ground truth information.

BLOCK 4 - MORNING FLIGHT

Eight-Category Recognition of Flight Line 14

The absence of the 1.5 to 1.8 μm waveband channel made it difficult to differentiate between upland and bottomland forest or between mixed conifer/hardwood forest and conifers during the SPARC training phase of Block 4. Not only had this channel been the best for discriminating all land use categories in Block 2, but it had been particularly effective in separating the four forest categories from each other. The fact that the channels 0.41 to 0.48 μm and 1.0 to 1.4 μm were unavailable for use also contributed to the recognition difficulties and the resultant decrease in number of categories.

A qualitative comparison of the SPARC color-coded recognition for flight line 14 was again made with the type-mapped CIR photograph. Areas of conifers, hardwoods, bare soil, water, and transition seemed to be accurately recognized. Shadows along tree lines were prominent due to the low sun angle. Many of them were recognized as water. Such recognition

may be related to the existence of early morning frost which was known to have been present.

Many pasture areas in flight line 14 are not well recognized, again pointing out the extreme variability of these areas. Increased pasture recognition could probably have been obtained in both blocks with the addition of more training areas.

A different type of quantitative assessment of recognition reliability on flight line 14 was made as an additional experiment to test an objective method for reporting recognition results. Line 14 provided a good opportunity to make such a test since the various categories of land use were fairly well distributed throughout the scene. Moreover, the frequency of each category permitted the selection of several test areas.

Using the typed CIR photograph, we selected areas which appeared similar to the eight land use classes for which SPARC was trained. Three areas per class were defined, approximately 2,500 m^2 in size. Areas used for training signatures were not selected. A gate was placed in each of the selected areas, and the appropriate signature was played on the SPARC. Recognition of the area within the gate was recorded in terms of the area count registered on the high-speed digital counter. Percent recognition was obtained by dividing the number of correctly recognized points by the total area count of the training area (Table 6).

Good performance in this test requires that the test areas be accurately typed on the photograph. And areas selected within each category should be spectrally representative of the class. Areas of conifers and bare soil show high recognition because they satisfy both of these requirements.

Table 6. Quantitative Analysis of SPARC Recognition Accuracy for Test Areas in Line 14, Block 4, by Comparison to Photographic Inspection

Test Area	Percent Recognition
Conifers (1)	98.0
Conifers (2)	98.7
Conifers (3)	87.4
Mean	94.7
Hardwoods (1)	86.3
Hardwoods (2)	78.3
Hardwoods (3)	68.9
Mean	77.8
Improved pasture (1)	77.6
Improved pasture (2)	59.8
Improved pasture (3)	95.6
Mean	77.7
Old pasture (1)	72.3
Old pasture (2)	88.5
Old pasture (3)	35.4
Mean	65.4
Pasture (1)	87.1
Pasture (2)	90.6
Pasture (3)	8.9
Mean	62.2
Bare soil (1)	97.4
Bare soil (2)	85.3
Bare soil (3)	87.9
Mean	90.2
Water (1)	79.7
Water (2)	74.2
Water (3)	93.7
Mean	82.5
Transition (1)	56.4
Transition (2)	0.6
Transition (3)	14.1
Mean	23.7

Hardwoods and water show slightly less recognition because of some inherent spectral variability between test areas and the trained areas. Ponds have obvious tone differences on the photograph owing to depth and sediment content. And deciduous forest areas do not manifest the smooth, continuous canopy that conifers do.

The mediocre accuracy achieved in attempting to classify the three pasture categories can be attributed to the spectral variability inherent in pasture areas in November and the failure of the photographic type map to recognize three separate categories of pasture. Test areas were selected from the photo solely on the basis of tone similarity to the trained areas.

Low performance for "transitional" areas is mostly due to the great spectral variability from one area to the next. A difficulty encountered in testing transitional areas was finding areas large enough in which to place a gate. Aside from the two large training areas used during initial recognition work, other transitional areas are spotty in appearance. This difference made it difficult to get a high percentage of recognition in any gated area.

Signature Extension for Block 4 - Morning Flight

Table 1 indicates the scene composition of Block 4 on a percent basis. Several noticeable deviations from proper recognition were manifested on each of the three earlier flight lines in Block 4. The water, transitional, and pasture categories showed changes, with the others showing little or no change.

Water recognition faded slightly on each earlier line; that is, ponds

began to display less solid recognition. Small ponds on the earliest flight line were identified, but on the remaining lines only 50 percent were recognized at best. There was a significant increase in the recognition of shadows as water on each earlier flight line -- a development which dramatizes the rapidly changing sun angle.

Transitional areas actually became more and more misclassified as hardwoods on each earlier flight line. Most of these areas were small fringe areas. However, large areas of transition continued to be correctly identified -- even on the earliest flight line.

The recognition of pastures appeared to improve greatly on the three earlier flight lines.

A comparison of the SPARC results with the ground survey showed that there were fewer errors in Block 4 than in Block 2 (Table 5). For instance, pasture again was classified with the greatest accuracy but with a high number of commission errors -- 90 percent were correct, and there were 18 commission errors. The transitional class was correct 45 percent of the time, with two commission errors. Of the forest types, pine was correct 80 percent of the time but with a high number of commission errors. Combined hardwood types were correct at 60 percent of the point samples, with moderately high commission errors.

The accuracies for water and urban areas seem to be rather consistent between the two test blocks according to the point sample analysis. For instance, water was correct in 60 percent of the cases on both blocks. For the purpose of the point sample analysis, the urban class (towns, highways, and other manmade features) was considered the same as the SPARC

unclassified area. Using this criterion, we found 60 and 75 percent agreement on the urban classification for the two blocks. A large number of commission errors were found in Block 2 but only a few in Block 4.

Additional Processing of Line 12, Block 4

Our attempts to correct for changes in illumination and angle effects on line 12 were inconclusive. In general, water recognition increased for each successive correction. However, the variation in recognition was not uniform; that is, some ponds increased while others decreased in recognition for each correction applied. The variation seemed to be independent of pond location in the flight line.

A slight increase in the proper recognition of transitional areas was noted with the correction for illumination level. However, the improvement did not account sufficiently for all the transitional areas typed on the photograph.

For most categories, the correction for illumination level (both by itself and in combination with the correction for angle effects) resulted in large, inordinate changes in recognition. However, the application of new preprocessing coefficients as a correction for varying angle effects yielded relatively small changes. In some cases the changes were barely detectable; in others they seemed to increase recognition accuracy slightly. Exceptions included the water and transition categories; water recognition increased greatly to an acceptable level of accuracy, and transition recognition declined instead of increasing.

These results suggest that the correction for angle effects owing to sun angle change is a more important consideration than the correction for

illumination level, but some cautions must be borne in mind.

First, the adjustment for angle effects on line 12 was done correctly in that new coefficients were computed from the data. However, the observation that prompted the correction was based on a comparison of data collected over two flight lines of nonidentical terrain. The change in angle effect suggested by the average scan lines may have been a consequence of the terrain itself -- the slight change in sun angle may have had little or no effect.

Second, the assessment of, and adjustment for, change in illumination level may not have been correct. That the sun sensor accounted for illumination change in the low sun angles is doubtful for two reasons:

1. The projected area of the flat opal glass surface exposed to the sun varies as the cosine of the illumination angle. At low sun angles, slight attitude changes caused by aircraft roll will have considerable effects on the exposed surface area of the sun sensor.

2. The transmission of opal glass varies with angles of incidence (Wiseman, 1969).

A more accurate method of assessing illumination change would have involved the use of a pyrheliograph and other ground-based data collected at the time of the flight.

MOSAIC QUALITY

Each block mosaic was assembled by standard photo-mosaicking procedures. Sufficient sidelap between flight lines was insured during the planning phase of data collection. All flight lines were flown in the same direction so that crab angles, if any, would be constant for all

runs. A standard processing function involved correcting the data for roll to prevent displacement of features along the scan line.

The length of recognition strips for successive flight lines was adjusted by using the first flight line processed for that block as a standard. This effort to insure uniform aspect ratio was corrected for slight changes in aircraft speed (averaged over the run) that occur from one run to the next. Any residual mismatch of terrain features must be attributed to random pitch and crab motions or speed variations of the aircraft during the flight. The effect of these slight changes in aircraft attitude on data collected from 10,000 ft is considerable. Witness the mismatch of terrain features at the northern end of lines 42 and 41 in Block 2. SPARC mosaics show obvious geometric distortions when compared to the 1:35,000 scale CIR photography. This fact makes point comparisons difficult at best. However, errors introduced from mosaic distortions are clearly the type which can be improved on in future missions.

CONCLUSIONS AND RECOMMENDATIONS

At first glance the results of this feasibility test may appear to be discouraging, but they do afford some promising leads. This study marked the first time multispectral scanner data were used to classify forest type and land use on an area basis. And we did not expect to solve all problems in one test. On the whole, the study demonstrated an advancement in making terrain class maps by automatic data processing methods. Signature extension from one flight line to the remaining three was deemed reasonably successful. But it was not as successful for the morning data as for the noon data.

On the basis of the results, we concluded that:

1. Recognition of 12 categories (four forest, three pasture, bare soil, water, row crop, orchard, and transition) was possible by using data collected near noon from Block 2. On Block-4 data collected in early morning, eight-category recognition seemed reasonable (two forest, three pasture, water, bare soil, and transition). The drop in the number of discriminable classes can be attributed in part to the nonavailability of the 1.5 to 1.8 μm channel. This channel was found best for discrimination of hardwood forest categories.

2. Some deficiency in signature extension existed even after attempts to correct data for changes in irradiance (using sun sensor) and for effects of scan angle for each line. This deficiency may be caused by imperfect estimates of scan angle variations, which in turn are caused by scene non-homogeneity and by the poor diffusion provided by the sun sensor at the low sun angles encountered in the morning data. More work is required to extend adequately signatures in morning data. Specific areas for study would include: (a) a better algorithm for applying sun sensor corrections and other ancillary information, (b) an improved sun sensor design, and (c) the use of atmospheric model results to correct preprocessing data.

3. The quality of the mosaic of recognition maps is compromised by uncertainties of aircraft altitude and velocity change. Uncertainty in these parameters directly affects both map quality and accuracy of point location. Better geometric fidelity is required before forest managers can accept classification data, by location. Improvements in knowledge of aircraft parameters is required and should be immediately studied.

4. Optimum channels for the noon data include a visible red, two near infrared, and a thermal channel. This combination demonstrates the utility of the single-aperture M-7 scanner which brought these bands together for the first time in an operational airbonre multispectral scanner.

5. Electronic classification using multispectral scanner data is new to forestry classification, and we recognize that the forest and non-forest classes used in the processing may not be the best for multispectral recognition. For this reason, our classifications should be reexamined and redefined, if necessary, to improve recognition accuracy.

Additional research is needed at all seasons to test and improve techniques and classifications. The potential for automatic processing of airborne data by the means described in this report is more promising, however, than that of other means tried to date.

LITERATURE CITED

1. Aldrich, Robert C. 1953. Accuracy of land-use classification and area estimates using aerial photographs. Journal of Forestry 51(1): 12-15.
2. Aldrich, R. C., and W. J. Greentree. 1972. Microscale photo interpretation of forest and nonforest land classes. Fourth Annual Earth Resources Program Review, Manned Spacecraft Center, Houston, Texas. 1972: 121-1 through 121-21.
3. Burge, W. G., and W. L. Brown. 1970. A study of waterfowl habitat in North Dakota using remote sensing techniques. Report No. 2771-7-F, Willow Run Laboratories, Institute of Science and Technology, University of Michigan.

4. Erickson, J. D., and F. J. Thomson. 1971. Investigations related to multispectral imaging systems for earth resources surveys. Report No. 31650-17-P, Willow Run Laboratories, Institute of Science and Technology, University of Michigan.

5. Hasell, Philip G., Jr. 1972. Michigan experimental multispectral scanner system. Fourth Annual Earth Resources Program Review, Manned Spacecraft Center, Houston, Texas. 1972: 34-1 through 34-13.

6. Kolipinski, M. C., A. L. Higer, N. S. Thomson, and F. J. Thomson. 1969. Inventory of hydrobiological features using automatically processed multispectral data. Proceedings of the Sixth International Symposium on Remote Sensing of Environment, Institute of Science and Technology, University of Michigan. 1969: 79-95.

7. Malila, W. A., R. B. Crane, C. A. Omarzu, and R. E. Turner. 1971. Studies of spectral discrimination. Report No. 31650-22-T, Willow Run Laboratories, Institute of Science and Technology, University of Michigan.

8. Marshall, R. E., N. S. Thomson, F. J. Thomson, and F. J. Kriegler. 1969. Use of multispectral recognition techniques for conducting rapid, wide wheat surveys. Proceedings of the Sixth International Symposium on Remote Sensing of Environment, Institute of Science and Technology, University of Michigan. 1969: 3-20.

9. Nalepka, R. F., H. M. Horwitz, and N. S. Thomson. 1971. Investigations of multispectral sensing of crops. Report No. 31650-30-T, Willow Run Laboratories, Institute of Science and Technology, University of Michigan.

10. Nalepka, R. F., and F. J. Thomson. 1972. Contribution to the corn blight watch final report. Report No. 31650-104-L, Willow Run Laboratories, Institute of Science and Technology, University of Michigan.

11. Suits, G. H., G. Safir, and A. Ellingboe. 1972. Prediction of directional reflectance of a corn field under stress. Fourth Annual Earth Resources Program Review, Manned Spacecraft Center, Houston, Texas. 1972: 31-1 through 31-11.

12. Turner, R. E., W. A. Malila, and R. F. Nalepka. 1971. Importance of atmospheric scattering in remote sensing or everything you've always wanted to know about atmospheric scattering but were afraid to ask. Proceedings of the Seventh International Symposium on Remote Sensing of Environment, Institute of Science and Technology, University of Michigan. 1971: 1651-1698.

13. Weber, F. P. 1971. The use of airborne spectrometers and multispectral scanners for previsual detection of ponderosa pine trees under stress from insects and disease. In: Monitoring Forest Land from High Altitude and from Space. Annual Progress Report for Earth Resources Survey Program, OSSA/NASA, by the Pacific Southwest Forest and Range Experiment Station. 24 p.

14. Weber, F. P., and F. C. Polcyn. 1972. Remote sensing to detect stress in forests. Photogrammetric Engineering 38(2): 163-175.

THE USE OF AIRBORNE SPECTROMETERS AND MULTISPECTRAL SCANNERS FOR PREVISUAL DETECTION OF PONDEROSA PINE TREES UNDER STRESS FROM INSECTS AND DISEASES

by

F. P. Weber

The culmination of seven years of research on the use of multispectral scanners (MSS) for previsual detection of stress in conifer trees was embodied in the May 1972 flight of the University of Michigan's M-7 scanner over the Black Hills test site (149). A summary of prior years' events leading to this final mission is given in last year's annual progress report (Weber, 1971).

In preparation for the final NASA SR&T-supported multispectral flight mission over the Black Hills, a suitable test site was located and established in September 1971. Our criterion for site selection was to find an area where the bark beetle population was building up, but an area which was not yet complicated by the presence of many old infestations. We found such an area eight kilometers south of Lead, South Dakota, (Figure 1) which served the dual purpose of providing ground truth information for the conclusion of the SR&T program and also for the transition into the ERTS-1 research program.

To prepare the test site for the multispectral flight, instruments were installed to monitor biophysical and environmental phenomena which were to provide baseline and calibration data for the interpretation of the aircraft data. A double tramway system was built to place

Figure 1. The Black Hills multispectral scanner test site, which was flown on May 24, 1972, by the University of Michigan's M-7 scanner is located 8 kilometers south of Lead, South Dakota. The 3.2-square-kilometer island of timber indicated by the arrow was the focal point for the previsual stress detection study.

instruments above both healthy and bark beetle-attacked ponderosa pine. The tramway instruments included an inverted pyranometer, net allwave radiometer, radiant exitance flux plate, and a 4-channel spectrometer. Other instruments were deployed throughout the test site to measure leaf temperatures, soil moisture, soil temperature, wind speed, and vapor pressure deficit. All instrumentation data were collected on a Vidar 5403 digital data acquisition system for computer analysis.

Several important innovations were made for this MSS mission in the Black Hills. Most important, this was the first application of the new M-7 scanner for stress detection in conifer forests. From our previous research, it was concluded that previsual detection of stress in forests could not be a reality until a single-line-of-sight scanner was available which combined narrow wavelength bands spread over a broad portion of the spectrum (Weber and Polcyn, 1972). The M-7 scanner is such a device. Analysis of land use mapping data collected in the southeastern forest region (reported in Section I herein) supports our belief that we finally have at our disposal the prototype scanner for future operational forest applications.

A second important innovation was the added capability of looking at a narrow, deep-red spectral band (0.71 to 0.73 micrometers (μm) separately from the spectrometer portion of the scanner. This narrow band of energy was recorded by sampling a part of the line-of-sight energy directed to the thermal detector with a photomultiplier detector which received the energy from the normal path by reflection from a dichroic mirror. This new detector position in the M-7 scanner was

created at our request for the Black Hills test and permitted recording the data of an essential narrow band without affecting the wavelength sensitivity of the spectrometer bands.

A third innovation for the Black Hills mission was to position the scanner into a 45° forward-looking oblique position on one flight line flown at each time of day. This different view of the side of tree crowns with respect to the angle of solar illumination might provide a different possibility for previsual detection of stress. If this proves true, it would be in spite of the fact that the geometry of the scanner imagery is severely distorted by having the scanner operate without benefit of roll compensation.

The May 1972 mission in the Black Hills was to be the finale of the feasibility study to determine the value of multispectral scanners for previsual detection of stress in conifer trees with existing equipment technology. Because of the importance of this data, the experiment was designed to measure the effects of aircraft altitude and time of day on the quality of the resulting data. Four parallel flight lines were established running east to west for the morning test and, similarly, three south to north lines were established for the midday flights (Figure 2). The morning midday missions were flown at two altitudes -- 458 meters (m) and 2,288 m. Alternate flight lines were flown at the higher altitudes whereas all flight lines were covered at the lower altitudes.

Although a five-man field crew had worked for two weeks in early May preparing the test site instrumentation, snow and general inclement

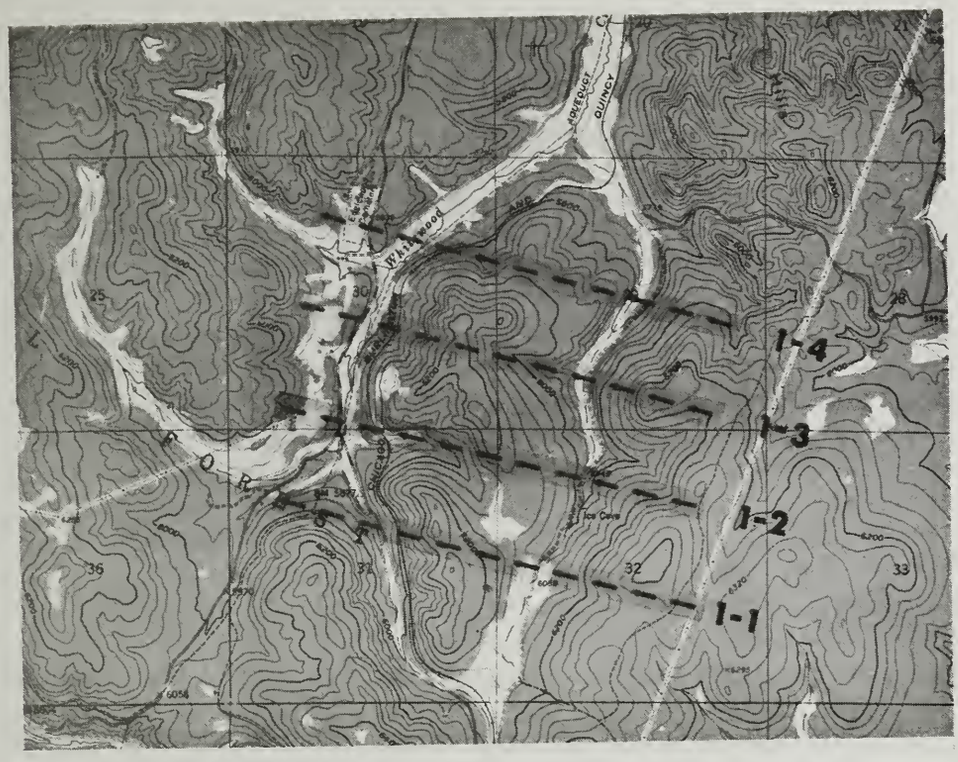

Figure 2a. Flight lines 1-1 through 1-4 were flown (approximately) from east to west on the morning mission at a flight altitude of 458 m above the ground. Flight lines 1-2 and 1-4 were reflown east to west at an altitude of 2,288 m.

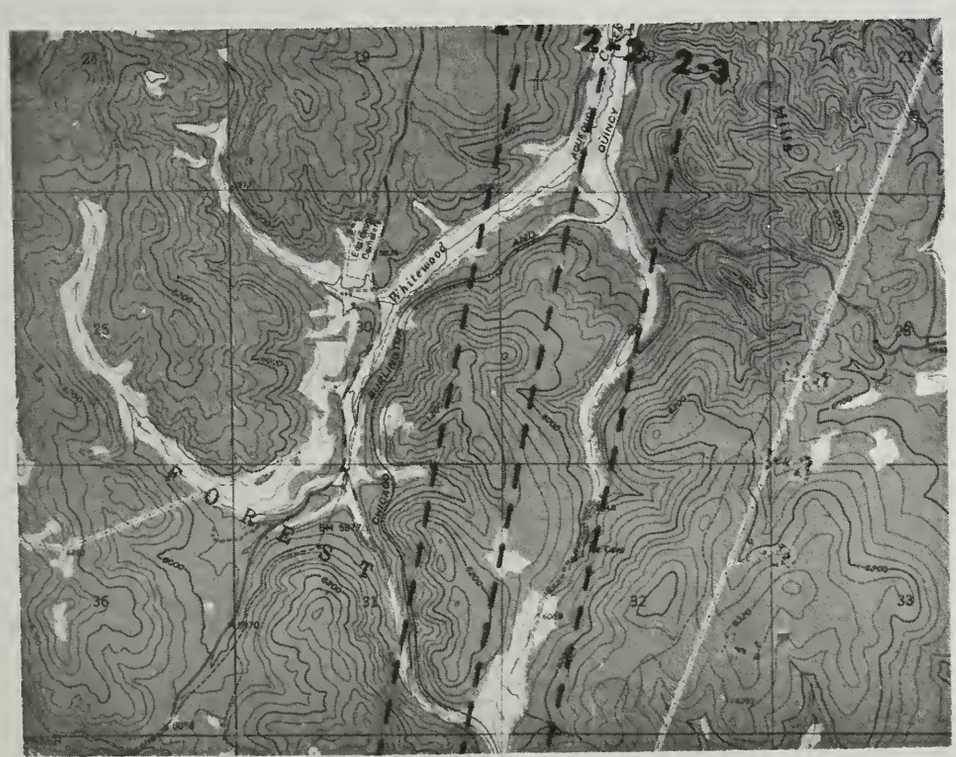

Figure 2b. Flight lines 2-1 through 2-3 were flown (approximately) from south to north on the midday mission at a flight altitude of 458 m. Flight line 2-2 was reflown south to north at an altitude of 2,288 m above the ground.

conditions delayed the airborne mission for two days. However, weather conditions during the test period followed a consistent pattern. Skies were clear in early morning, with cumulus buildups beginning by mid-morning. Rain, with occasional hail, was common by midday. Because of the consistency of this weather pattern, it was decided to advance the mission times by one hour for each mission. On Thursday, May 25, both the morning and midday missions were accomplished in spite of several delays for the passage of clouds from the test site. Because of the importance of the mission to attaining successful completion of the research program, several flight lines were reflown to insure the adequacy of the data.

During the first week of June, four wavelength bands of MSS imagery were previewed at the Willow Run Laboratories (WRL) in Ann Arbor, Michigan. Although no analyses were performed on the data, it was determined that all 12 MSS channels were functioning properly and as a result several good data sets were recorded, including at least one each from the morning and midday missions. It was further determined that the hybrid band of 0.71 to 0.73 μm contained excellent data which should contribute substantially to the detection and recognition analysis. Data sets resulting from the scanner flown in the 45^{o} forward-looking oblique showed definite promise for information extraction, and although there is as yet no experience in processing this kind of information, that data set should be analyzed.

Although our data have not been processed or analyzed to date, we had a brief opportunity to ground check some ratio processing results of

Black Hills data in August. These data were collected in May on the same mission to the Black Hills and were a part of two long flight lines flown over the northern Hills. Data processing was a joint venture of WRL and the Bureau of Mines, Denver. Enough data from those two flight lines were ground checked so as to (1) verify the quality of the May scanner data and (2) establish the possibility that ratio processing may be a big factor in previsual detection of stress in ponderosa pine forests.

It is unfortunate that the conclusion to the SR&T-supported multispectral scanner research cannot be written at this time. However, this effort came at the close of the program in a transition period of fiscal austerity affecting both NASA and the Forest Service. As a result, there has been no financial support for processing the multispectral data. In the past, it has been the practice to follow MSS data collection contracts with MSS data processing contracts with the University of Michigan. This has not been the case, and the point has been stalemated since May, with our final data sitting in the can. We hope that this unfortunate situation can soon be resolved.

LITERATURE CITED

1. Weber, F. P. 1971. The use of airborne spectrometers and multispectral scanners for previsual detection of ponderosa pine trees under stress from insects and disease. In: Monitoring Forest Land from High Altitude and from Space. Annual Progress Report for Earth Resources Survey Program OSSA/NASA, by the Pacific Southwest Forest and Range Experiment Station. 24 p.

2. Weber, F. P., and F. C. Polcyn. 1972. Remote sensing to detect stress in forests. Photogramm. Eng. 38(2):163-175.

TREND AND SPREAD OF BARK BEETLE INFESTATIONS IN THE BLACK HILLS

by

F. P. Weber, T. H. Waite, and R. C. Heller

An aerial photographic study of the trend and spread of the mountain pine beetle (Dendroctonus ponderosae Hopk.) in the Black Hills of South Dakota has been conducted during the past several years under the NASA SR&T program. Photo interpretation data from this study have provided valuable background information for our current ERTS-1 research program on forest stress. For example, from studying aerial photographs taken at different times of the year we now know that late August or early September is the best time of year for maximum discrimination of faded (discolored) bark beetle-attacked pine. This applies to medium- and small-scale imagery whether obtained by high-flight aircraft or spacecraft. Perhaps more important is the information gained on the accuracy of infestation spot detection on different scales of photography. This accuracy is directly related to infestation size. For example, we have been able to consistently identify all of the infestations larger than 30 meters (m) in diameter on August photography at a scale of 1:8,000. However, on photography at a scale of 1:174,000 we could identify only about 30 percent of the infestations 30 m in size. Of course, on the larger scale photos (1:8,000), some infestations as small as 5 m in diameter were detected, but the accuracy was only 70 percent.

The knowledge of how scale and time of year affect photo interpretation accuracy has been valuable in designing our ERTS-1 stress detection

experiment in the Black Hills. From our study of ERTS-1 imagery we primarily wish to answer two questions with regard to stress detection: (1) can the largest bark beetle infestations be mapped on ERTS-scale imagery? and (2) what is the minimum size infestation spot which can be detected on ERTS imagery? We felt the answers to these questions must be forthcoming before we could expand to a broad-area application of earth observation satellite imagery for stress detection in forests.

Throughout the SR&T program we were unable to obtain good quality RB-57 high-altitude photographic coverage of the Black Hills. This type of small-scale, large-area coverage was essential to the planning and conduct of the ERTS-1 experiment. As a substitute, we used the Forest Service Aero Commander and our Zeiss camera system to photograph 4,662 square km of the northern Black Hills in May 1972. Photo coverage was obtained with color infrared (CIR) film at a scale of 1:33,500. As resource and planning photography, it served well for locating ERTS training sites and test sets within the Black Hills ecosystem. In addition, the May photography is being used in comparison with fall 1972 photography to calculate the current spread factor for the mountain pine beetle epidemic.

On September 8, 1972, eleven townships (1,026 square km) of the northern Hills were rephotographed with CIR at a scale of 1:32,000. The 11-township area defines the extent of the current bark beetle epidemic. The fall photography is being used to pinpoint the location of all the current bark beetle infestations (in terms of current faders)

and list them by size class and number of trees.[1] This information is required as ground truth for the multispectral scanner flights of May and September 1972 and also for the interpretation of any usable 1972 ERTS imagery.

As an example of the buildup and spread of the current bark beetle epidemic within the 11-township area, it is revealing to compare the aerial photographs (Figure 1A and 1B) of the multispectral scanner test site. This is the same 3.2-square-km MSS test site discussed in the first part of Section II of this report. The area was selected a year ago for the MSS previsual detection investigation because there were few infestations in the area to complicate image interpretation. From photo interpretation of the May 1972 photography, it was discovered that there were 21 infestations which included a total of 139 trees (Table 1). The largest spot was less than 50 m in diameter. It should be kept in mind that the damage evaluation on the May photography resulted from attacks by the 1970 generation of bark beetles. Looking at the same test area on the aerial photography taken in September 1972, we discovered 61 new infestations with a total of more than 300 trees. This is about a twofold increase in infestations and trees. The largest infestation (resulting from damage done by the 1971 generation of the beetle) was 100 m in diameter and included 47 trees.

---

[1] In the Black Hills, only one generation of bark beetles develops in a 12-month period. For example, the 1970 generation began in August 1970 and matured in August 1971; however, the host trees did not discolor until early summer 1971 and are called "current faders."

Figure 1A. This CIR aerial photograph was taken on May 14, 1972, over the Black Hills test site 149 (ERTS 226A) at a scale of 1:33,500. The locations of the 1970 infestations are indicated by arrows on the photograph.

Figure 1B. This CIR aerial photograph was taken on September 8, 1972, at a scale of 1:32,000 over the Black Hills test site. The locations of the 1971 infestations are indicated by arrows on the photograph and should be compared with Figure 1A to judge the spread of the bark beetle epidemic.

Table 1. The spread of the mountain pine beetle epidemic from the 1970 to the 1971 beetle generation is illustrated by a comparison of the photo interpretation results for the 3.2-square-km MSS study area from May and September 1972 photography.

CIR PHOTOGRAPHY TAKEN IN 1972

	MAY		SEPTEMBER	
Infestation Size	Number of Infestations	Total Number of Infested Trees	Number of Infestations	Total Number of Infested Trees
Less than 10 meters	10	27	46	114
10 to 25 meters	9	78	8	60
26 to 50 meters	2	34	5	105
51 to 100 meters	--	--	2	72
	21	139	61	351

This is the same infestation which has been instrumented for our ERTS-1 DCP/biophysical investigation. The comparison of photo interpretation results from May and September CIR photography for the 3.2-square-km study area is shown in Table 1.

Although the photo interpretation of the total 11-township area for both the May and September photography is not yet complete, some important trends are apparent now. The trend established with 70 percent of the photo interpretation complete is a 3 to 1 population expansion from 1970 to 1971 in terms of numbers of new infestations. By far the greatest numbers of new infestations from the 1971 population contain less than 10 trees. Our past experience has been that in the second year (1972) of an expanding epidemic there will be considerable aggregation of beetle activity with the result of larger infestations. This means that if the bark beetle epidemic continues as expected in the northern Black Hills, there should be sufficient numbers of large infestations in evidence during the summer of 1973 to provide an excellent detection test on the ERTS-1 and Skylab imagery.

As further evidence of an expanding bark beetle infestation in the northern Black Hills, we can look at some additional results of the interpretation of the May and September 1972 small-scale photography. The data in Table 2 are for one township (93 square km) selected from the 11-township epidemic area. This township (T.51N. R.2E.) is in an area considered by entomologists to be the reservoir of beetles for the expanding population. Perhaps the most significant point revealed in Table 2 is the apparent 3.3 to 1 blowup factor in terms of numbers of

Table 2. Expansion of the bark beetle epidemic in the northern Black Hills is shown in the comparison of photo interpretation data of May and September 1972 for a critical 93-square-kilometer area (T.51N. R.2E.)

Infestation Size	Number of New Infestations		
	1970 Population[1]	1971 Population[2]	Ratio-71/70
< 10 meters	61	262	4.3 to 1
10 to 25 meters	32	106	3.3 to 1
26 to 50 meters	12	60	5.0 to 1
51 to 100 meters	6	46	7.7 to 1
100 to 300 meters	2	17	8.5 to 1
> 300 meters	2	2	1 to 1
Total	115	493	4.3 to 1

[1] Interpreted from the May 1972 1:33,500 scale CIR photography - 1971 fading trees.

[2] Interpreted from the September 1:32,000 scale CIR photography - 1972 fading trees.

infestation spots in the size class 11 to 25 m. This is the infestation size class which has been found to contain most of the dead trees resulting from attacks during an expanding epidemic.

A valuable benefit of the long-term SR&T support of our study on forest stress has been to establish important trend information which is needed to understand what is going to happen to a bark beetle infestation. Entomologists have been able to do this with ground survey data for some time, but the value of this study has been to tie together entomological information on population dynamics with new techniques developed for assessing beetle impact through the use of aerial photography.

Through this continuing research program, we have learned that previsual detection of bark beetle-attacked trees cannot be accomplished with normal color (NC) or CIR aerial photography. If there is to be previsual detection, it must be done with multispectral scanners or other sensors. However, we have considerable photo interpretation data (from both large- and small-scale photography) which will now permit us to optimize photo scale against interpretation errors, given a clear definition of the objectives of the survey. In terms of monitoring beetle activity in the Black Hills, for example, this may require a multistage survey with the need for such a survey established through monitoring of ERTS-type multispectral imagery. The feasibility of monitoring forest stress from an earth observation satellite remains to be demonstrated in our ERTS-1 research program. In any event (either with or without ERTS), forest managers now have at their disposal methods

for evaluating bark beetle activity, and these methods have resulted directly from SR&T-supported research.

DETECTION OF ROOT DISEASE IMPACTS ON FOREST STANDS BY SEQUENTIAL ORBITAL AND SUBORBITAL MULTISPECTRAL PHOTOGRAPHY

by

John F. Wear

INTRODUCTION

Forest diseases create greater adverse impact on the forest resources of the United States than any other catastrophic agent, including fire. Continuing timber losses over extensive forest areas by forest diseases are of great concern to earth resource managers. This study concerns Poria weirii root rot disease that attacks valuable Douglas fir and hemlock trees in the Pacific Northwest (Figure 1). Approximately 170 million board feet of timber in the Pacific Northwest are destroyed or degraded by this root rot each year.(1) With satisfactory aerial survey techniques to locate disease centers (Figure 2), distressed timber may be salvaged and management plans changed to minimize further impact of forest disease on our valuable forest resources.

The following summarizes the past seven years of cooperative effort by NASA's Earth Resources Survey Program and the U.S. Forest Service in remote sensing tests and developments considered important for discriminating root-rot infected Douglas fir trees from healthy trees in the Pacific Northwest. The primary thrust of this remote sensing project was to develop aerial sensing techniques that would previsually identify centers of root-rot infection for eventual use from suborbital aircraft and orbiting satellites.

Figure 1. Merchantable stand of 50 year old Douglas fir "rot thrown" by Poria weirii root rot disease. Note typical decay pattern in pattern in splintered stump. Disease disintegrates tree roots one foot per year until tree falls or is windthrown.

Figure 2. Distressed trees will continue to fall into the opening. Salvage operations require knowledge on location of these centers.

Three portions of the electromagnetic spectrum considered to have the best potential were the visible, reflective infrared, and thermal infrared bands. To determine the best "window" or band of the visible spectrum to define disease distressed trees from healthy trees, aerial techniques were devised to collect branchlets from the tops of many trees in each class (Figure 3). This efficient tree sampling technique was invented which incorporates a special pole pruner that cuts and holds branchlets taken from the top of dominant trees via helicopter.(2) Many foliar samples can be collected from many trees in a short time without causing changes in foliage characteristics that might affect reflectance curves. Spectrometric analysis of foliage was expected to identify specific "windows" that could prove effective as an aerial survey tool.

The SANTAD computer program, developed by N. Norick, analyzed the reflectance curves from the foliage samples in terms of tone values produced. Twenty-three filter types and four black-and-white films(3) were tested, but no consistent film-filter combination was discerned to discriminate healthy and diseased trees at different moisture periods of the year.(4)

Also aerial color Ektachrome Aero (E-3) and color infrared Ektachrome Aero Infrared (8443) photography was taken at 1/5000 and 1/2500 scales in 1966, 1967, and 1968 in an effort to obtain previsual discrimination of affected trees in the visible and near infrared portions of the spectrum (.34 micrometer to .90 micrometer). A few trees in the most advanced stages of decline were detected primarily because of a foliage color change to yellow. Thus, previsual discrimination by

Figure 3. Collecting branchlets from the tops of dominant trees for spectrometric analysis is simple and efficient from a helicopter using a light weight pole pruner to clip and retain samples.

photography in the visible spectrum is not considered a practical survey method at this time.

Thermal infrared tests with a PRT-4 radiometer in 1966 and a PRT-5 radiometer in 1967 operating from a helicopter at 150 feet above individual trees (Figure 4) showed significant to highly significant temperature differences at specific periods of the year and time of day.(2 and 4) In 1968, thermal sensing with a non-imaging PRT-5 radiometer from a helicopter was performed over trees at two different forest sites; 45 trees at each site representing three age classes and three tree conditions (healthy, diseased without visible crown symptoms, and diseased with visible crown symptoms). Significant temperature differences were recorded between the sunlit and shaded sides of trees but not between healthy and diseased trees (optimum moisture and low stress factors in 1968). During the period, an aerial video scanning system with thermal readout was also designed and implemented (Figures 5 and 6) for thermal surveys of large forest areas from a helicopter.(5) It was not possible to conduct tests of this new equipment over study trees at each test site in 1968.

In the absence of reflectance differences between healthy and diseased Douglas fir trees, more intensive and comprehensive "ground truth" was needed to measure the effect of pest organisms on tree growth and tree decline as a means to determine the ideal airborne remote sensor. In 1969, measurements of biophysical and physiological processes in healthy and diseased Douglas fir trees were initiated at the Wind River Test Site in southern Washington. Biophysical research was oriented to measure energy balance of the forest canopy, leaf

Figure 4. Infrared heat emissions from individual trees are recorded with PRT-5 radiometer and chart recorder. Helicopter orbits tree for total reading from 150 feet.

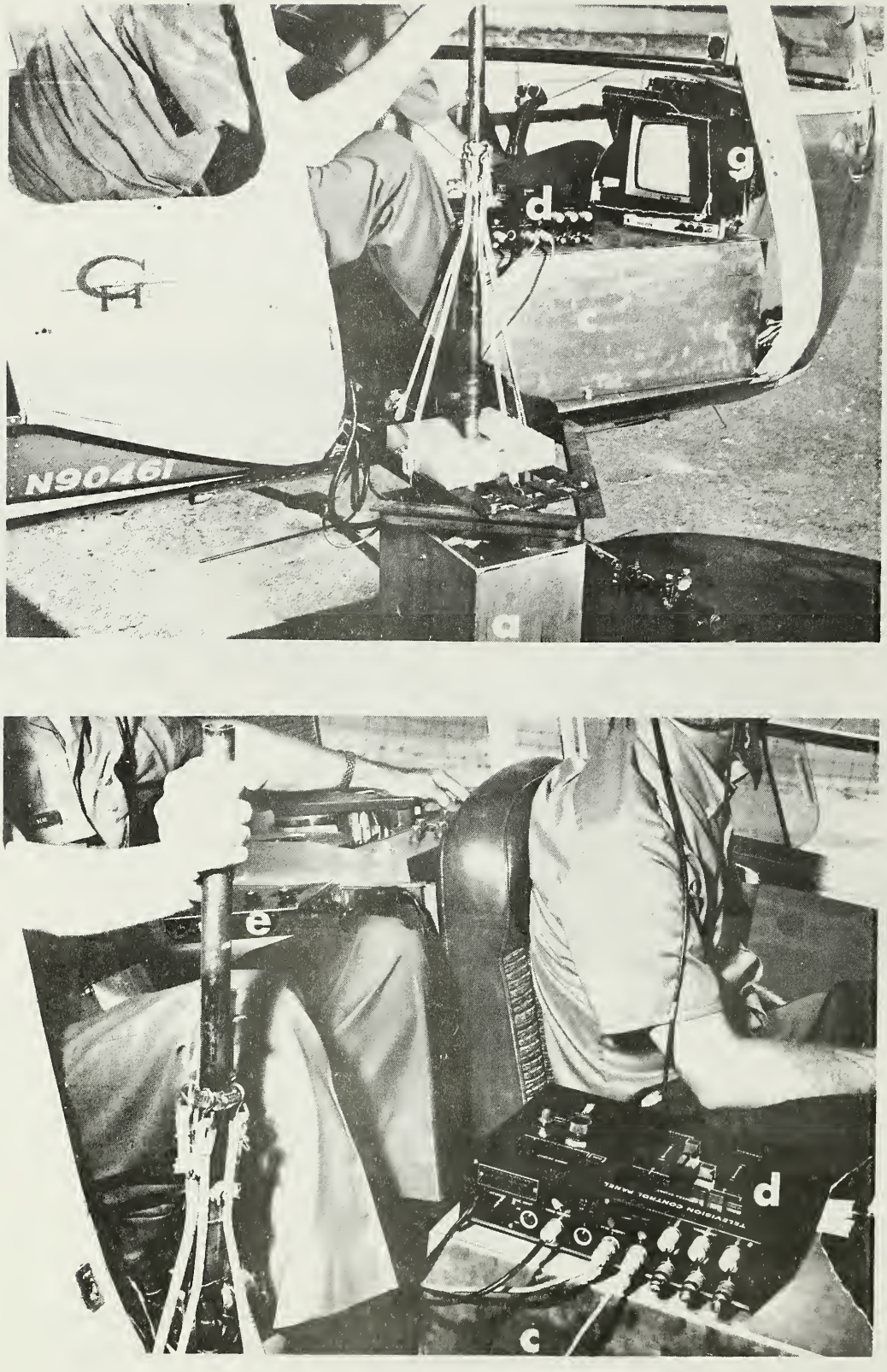

Figure 5. Thermal IR radiometer and video scan recording system provide pictorial and digital readout of thermal emittance from objects below helicopter. Tape recording with instant replay captures temperature differences and sufficient ground detail to pinpoint location. In scanning mode forward speed of helicopter would not affect instantaneous radiometer readings of trees, brush, or terrain features.

Figure 6. Upward view of vertical pod on helicopter that contains boresighted thermal radiometer and vidicon camera. Leveling the pod in flight is manual operation.

moisture tension, foliage temperatures, soil moisture tension, rate of sap flow, and various types of meteorological data (wind speed, relative humidity, ambient air temperature, vapor pressure deficit, and rainfall). An aerial tramway system was established that could collect data continuously from healthy and diseased trees (Figure 7). A tri-tower system evolved with one central common tower for two tramways, one operating over healthy trees and one over diseased trees. A vast array of sophisticated instruments were installed to collect data on the above biophysical and physiological processes. Data from the many sensors were fed over miles of wire into recording instruments located inside a trailer next to the tramway system. A Vidar 5403 digital data logger provided 35 channel per second input in 1970 to greatly improve data collection. Details of the instrumentation, installation procedures, and sample graphed information over the summer periods are described in the 1969 and 1970 Annual Reports.

In 1969, the University of Michigan's multispectral scanner system collected thermal and multispectral data over the instrumented Wind River Test Site on July 14 and 15. Unfavorable environmental conditions existed in late September for an overflight when maximum stress factors would be evident. Optical mechanical scanner data from the Michigan flights were processed and reported in 1970.[7] Results of the multispectral evaluation using likelihood ratio processing of three-channel infrared data on SPARC (1.0 - 5.5 μm), ten-channel spectrometer data on SPARC (.4 - 1.0 μm), and thermal infrared data (8 - 14 μm) on analog and digital processing revealed no discrimination of Poria stressed trees within the general area. Color mosaics and thermal greymap

Figure 7. One of three steel towers supporting a double tramway system. Radiation sensors on tramcart are automatically pulled on cables. Sensor data is transferred electronically to a data logger in a mobile laboratory.

interpretations provided pattern recognition in several broad bands but lacked resolution to delineate just a few trees. High water table and above average environmental conditions (no severe stress) help to account for the uniform thermal radiance characteristics of the Douglas fir forest on the Wind River Test Site.

In 1969, extensive ground instrumentation collected data on biophysical and physiological parameters of forest trees at the Wind River Test Site. Despite good soil water storage in the general area, daytime differences were recorded in leaf water potential and relative rates of evapotranspiration between healthy and diseased trees. Higher leaf stress was consistently recorded around midday by diseased trees. Healthy trees indicated greater leaf stress in the morning and early evening.(6) In 1970, "ground truth" was obtained through a more comprehensive array of instruments integrated into the two tramway systems. Precision measurements of emitted energy of individual trees was provided by a radiometric device incorporated into the net radiometers. It measures longwave thermal infrared emission (radiant exitance) in the 3 - 15 μm band and corresponds to measurements made by an airborne thermal detector. Two inverted Star pyranometers, one travelling on a tramway over healthy trees, and the second over diseased trees collected reflected shortwave radiant energy. Incident shortwave radiation collected by a Kahl Scientific Star pyranometer was collated with the reflected energy to calculate albedo. Albedo indicates contrast ratios on spectrometer imagery. Net allwave radiation collected by a Kahl Scientific net allwave radiometer mounted on each tramway measured directly allwave incident energy (.4 - 15 μm) minus allwave reflected

and emitted energy. From the net allwave radiation data collected during the 1970 season at the Wind River Test Site, a consistent lower value was measured in diseased trees which indicates a higher reflected or emitted energy component.(7) Furthermore, remote sensing of shortwave radiation data as indicated by albedo response shows a consistent two percent higher incident shortwave radiation of diseased trees. It is difficult, however, to ascribe significance to these parameters either singly or together because of the differences in energy balance components. Stress factors between healthy and diseased trees need to be more pronounced than occurred in 1970 (high water table, low stress components) and aerial remote sensing instrumentation of greater resolution and precision are needed to discriminate previously incipient Poria weirii root rot in Douglas fir trees.

In 1970, a new spectral signature indicator for Poria weirii root rot disease was discovered on 1:15,840 scale photography in Douglas fir stands in the Oregon Cascades (Figure 8). The circular pattern resulting from the spread of the disease is the bare ground and disintegrated tree trunks of infected Douglas fir. Remote sensing research since 1970 has been oriented to capitalize on this signature which can be discerned on suborbital imagery and potentially on satellite imagery.(7)

In 1971, a comprehensive remote sensing survey research and development program was designed to meet objectives oriented with the discovery of the new unique spectral signature of root rot disease in the high Cascades. Expectations were that the signature would apply to the Douglas fir-hemlock type throughout the Northwest and perhaps be useful throughout the United States. The 1971 Annual Report(8) describes

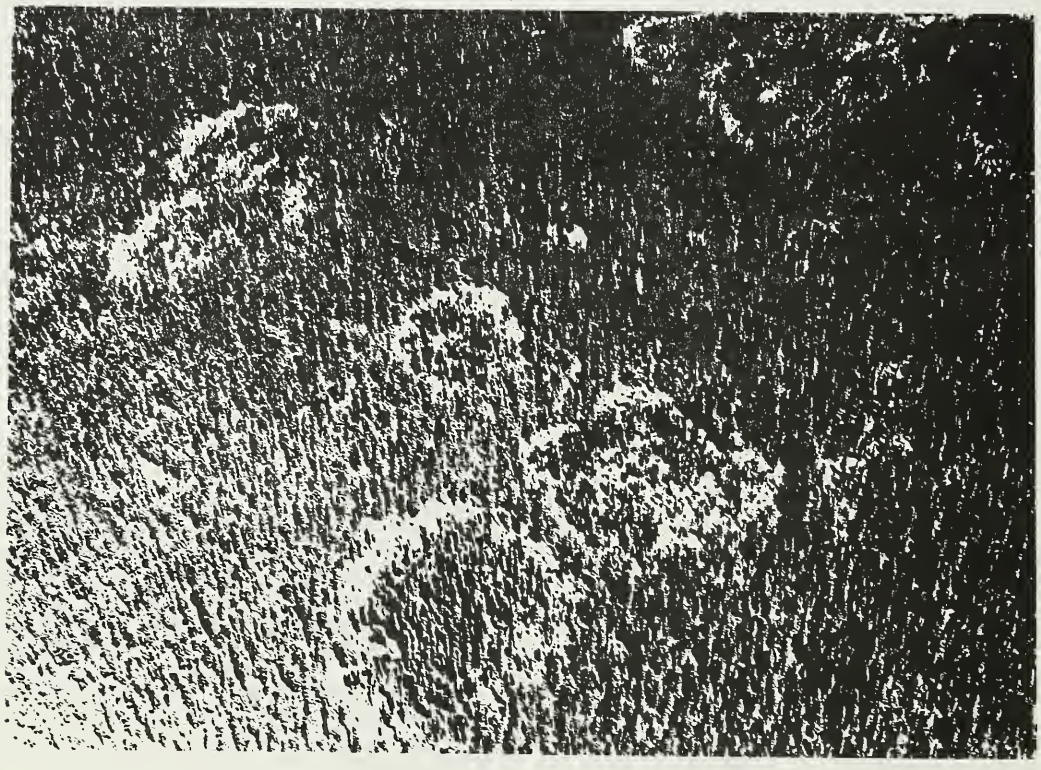

Figure 8. Oblique view of Poria weirii signature in the high Cascades of Oregon. Progressive spread evident as trees on edge fall and disintegrate. Less susceptible trees (white and true firs, red cedar, white, white pine) fill in after Douglas fir and hemlock succomb.

the problem, the selection of three test sites, the four photo interpretation phases of the project, the interagency cooperation, aerial photography, and collection of ground truth. Following the photo interpretation of approximately 8,300 aerial photos in the Douglas fir-hemlock types of Oregon and Washington for this particular spectral signature, three test sites encompassing nine square miles each (three-mile x three-mile block) were selected for detailed study. Each test site included a wide variety of disease, stand and climatic conditions, slope and elevations, and forest types.

1. The Waldo Lake Test Site (Williamette N. F.) is in the high Cascades of Oregon, has some brushy areas, and moderate to easy terrain accessibility.

2. The Olallie Lake Test Site (Mt. Hood N. F.) is in the Oregon Cascades, brushy with areas of dense reproduction, and moderate terrain accessibility.

3. The Divide Lookout Test Site (Siuslaw N. F.) is in the Oregon Cascades, brushy with extensive understory of vine maple, rhododendron, and red alder and has extremely rough terrain with deeply dissected slopes of 80 to 90%.

Aerial photography in 1971 included three scales and three film types for each test site. The Divide Lookout Test Site in the Coast Range was photographed at 1:4,000, 1:8,000, and 1:15,840 scales because of the need for interpretative capabilities at the ground level in the Poria pockets ("holes" in the forest canopy). 1:8,000, 1:15,840, and 1:31,680 scales were taken of the other two test sites. U.S. Forest Service photographic aircraft from R-6 and the PSW Forest and Range

Experiment Station used Aero color negative film (2445) which provides either color or black-and-white prints, and color infrared film (2443) using a Wratten #15 filter to secure the above photo scales. Scheduling constraints for NASA overflights at smaller scales up to 1:250,000 did not materialize because of priority of the extensive corn blight surveillance program.

A new photo interpretation testing technique was devised that would remove almost entirely interpreter bias that is commonly found in multiple and sequential photographic interpretations of the same areas with different films and scales. Eight plots from a total of over 75 plots at each test site were randomly selected for each film-scale combination. Nine combinations are possible at each test site (three films, three scales) so that a total of 72 plots were interpreted only once by each interpreter. Five interpreters had separate random lists of plots to interpret. Each plot was interpreted for presence or absence of Poria root rot disease. The interaction between photo type scale combinations (nine) and interpreters (five) is used as the error term for testing significance.

Only preliminary results of the photo interpretations covering part of the 1971 multispectral imagery were available for the 1971 Annual Report. Results on the Waldo Lake Test Site and Olallie Lake Test Site were most encouraging. Two interpreters with considerable field experience in field checking Poria pockets obtained interpretation accuracies around 90% for Waldo Lake, 80% for Olallie Lake, but only 60% for Divide Lookout on the Coast Range. Neither the type of film nor the scale of photography affected the results significantly

which should indicate potential success-ratio for root rot disease surveys in certain areas from suborbital and orbital altitudes.

CURRENT RESEARCH ACTIVITIES

Two major remote sensing projects were conducted in 1972 on the Poria weirii root rot problem in Douglas-fir type of the Pacific Northwest. First was the photo interpretation carried out by five interpreters of 216 selected plots on the three established test sites (Waldo Lake, Olallie Lake and Divide Lookout) with three films and three scales. These data were analyzed to determine the optimum film-scale combination needed to detect root rot centers up to 1:32,000 photo scale. Second, a follow-on photographic mission was planned to obtain multispectral imagery of the three test sites from 1:64,000 to 1:250,000 photo scales as a means of estimating the potentialities of suborbital and orbital imagery for detecting root rot diseases.

OPTIMUM FILM-SCALE COMBINATION

Results of the five interpretations on the 1971 photography show that larger photo scales do not materially improve interpretation accuracy. This can be discerned in Table 1. Interpretation accuracy actually improved in many cases at smaller photo scales. Tests of significance were made for interpreters, photo scales, film types, and photo scale-film type interaction (Tables 2, 3, and 4) for the 1971 photography. Analysis of variance showed no significant differences between interpreters, photo scales, film types, or photo scale-film type interactions for the Olallie Lake and Divide Lookout Test Sites (Tables 3 and 4). Highly significant differences were noted for photo scale and photo scale-film type interaction for the Waldo Lake Test

Table 1. Photo interpreter accuracy* for photo scale-film type combinations.

Waldo Lake Test Site

Film Type	Photo Scale 1:31680	1:15840	1:8000
Black-and-white	85.0	60.0	77.5
Color	82.5	70.0	40.0
Color IR	77.5	52.5	77.5

Olallie Lake Test Site

Film Type	Photo Scale 1:31680	1:15840	1:8000
Black-and-white	70.0	62.5	62.5
Color	72.5	60.0	52.5
Color IR	62.5	62.5	72.5

Divide Lookout Test Site

Film Type	Photo Scale 1:15840	1:8000	1:4000
Black-and-white	62.5	50.0	62.5
Color	57.5	52.5	45.0
Color IR	60.0	42.5	40.0

*Percent correct.

Table 2. Waldo Lake Test Site analysis of variance.

Source of variation	D.F.	S.S.	M.S.	F.
Interpreters	4	0.04	0.01	1.00 N.S.
Photo scale	2	2.92	1.46	14.60**
Film type	2	0.60	0.30	3.00 N.S.
Scale x type	4	3.88	0.97	9.71**
Error	20	--	--	--
Total	32			

**Significant at 0.05 confidence level.
N.S. -- Non-significant

Table 3. Olallie Lake Test Site analysis of variance.

Source of variation	D.F.	S.S.	M.S.	F.
Interpreters	4	0.96	0.24	1.99 N.S.
Photo scale	2	0.32	0.16	1.32 N.S.
Film type	2	0.12	0.58	0.48 N.S.
Scale x type	4	0.92	0.23	1.91 N.S.
Error	20	--	--	--
Total	32			

N.S. -- Non-significant

Table 4. Divide Lookout Test Site analysis of variance.

Source of variation	D.F.	S.S.	M.S.	F.
Interpreters	4	0.23	0.06	0.35 N.S.
Photo scale	2	1.02	0.51	3.09 N.S.
Film type	2	0.72	0.36	2.17 N.S.
Scale x type	4	0.67	0.17	1.01 N.S.
Error	20	--	--	--
Total	32			

N.S. -- Non-significant

Site. Interpretations on black-and-white prints were generally better than on color or color infrared films.

SUBORBITAL IMAGERY

The success achieved with small scale imagery of 1:32,000 on black-and-white photography to detect Poria root rot centers indicated the need to test additional suborbital imagery. In late June 1972, the USFS Remote Sensing Project's photo equipped Aero Commander photographed the three test sites at three photo scales ranging from 1:46,000 to 1:184,000 on Waldo Lake and Olallie Lake Test Sites and 1:52,000 to 1:208,000 on Divide Lookout Test Site. A pod of 70 mm cameras (six inches, three inches, and 1-1/2 inches focal lengths) was used with Aero color negative film (2445) and color infrared film (2443). Delays in film processing and problems in obtaining satisfactory black-and-white prints from Aero color negative film have delayed considerably the multiple interpretations needed to determine the upper limits of photo interpretation accuracy for root rot disease centers. It is apparent that Aero color negative film requires additional filters for exposures made above 20,000 feet above sea level if black-and-white prints are desired (color compensating filters are available and provide satisfactory color prints or color transparencies). Results of the suborbital imagery interpretations will be published in a later Forest Service publication. Figures 9 through 14 show the differences in the appearance of Poria weirii root rot signatures from small side openings to large openings up to 3,000 feet across on photo scales obtained through 1972.

Figure 9. 1:8,000 scale vertical photo at Waldo Lake Test Site. Note small new centers, older enlarging centers, and large coalescing centers.

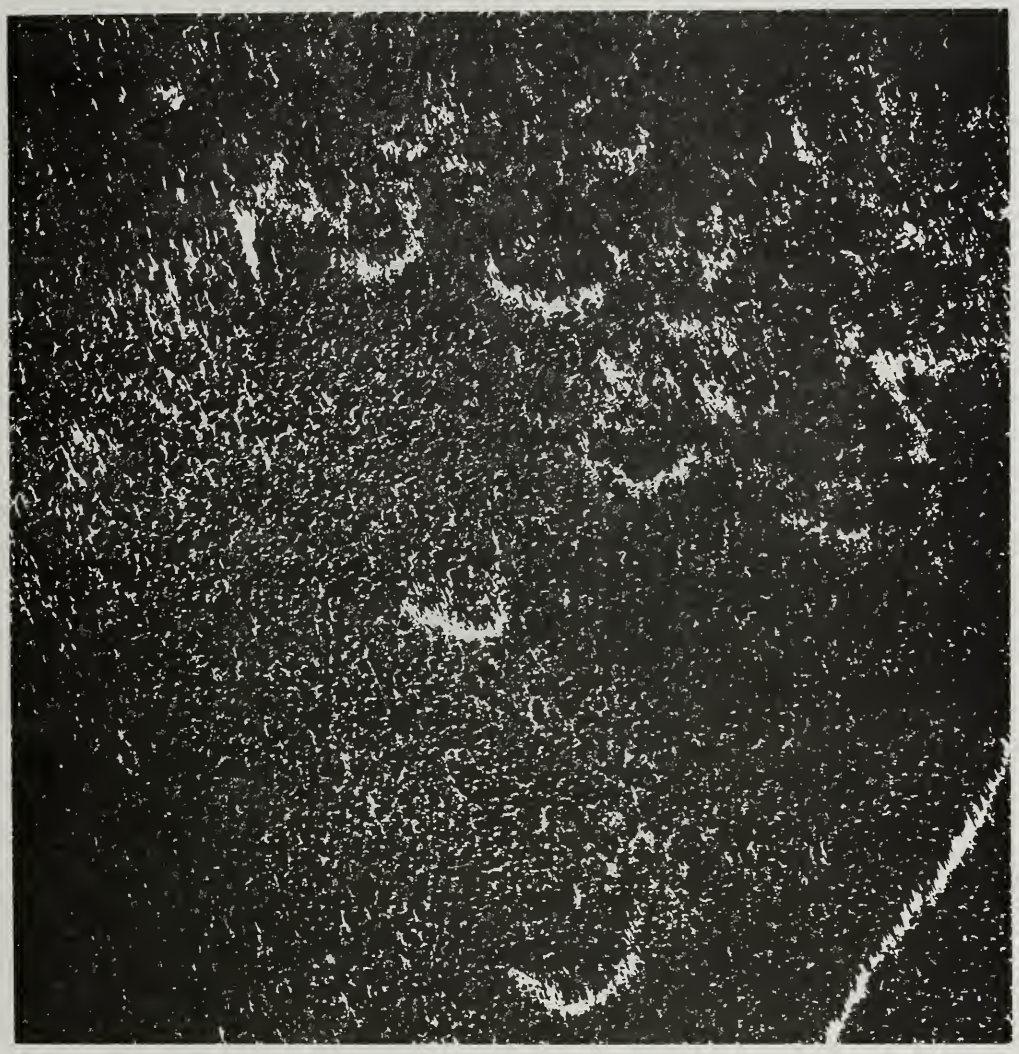

Figure 10. 1:15,840 scale vertical photo of same area.

Figure 11. 1:31,680 scale vertical photo at Waldo Lake Test Site.

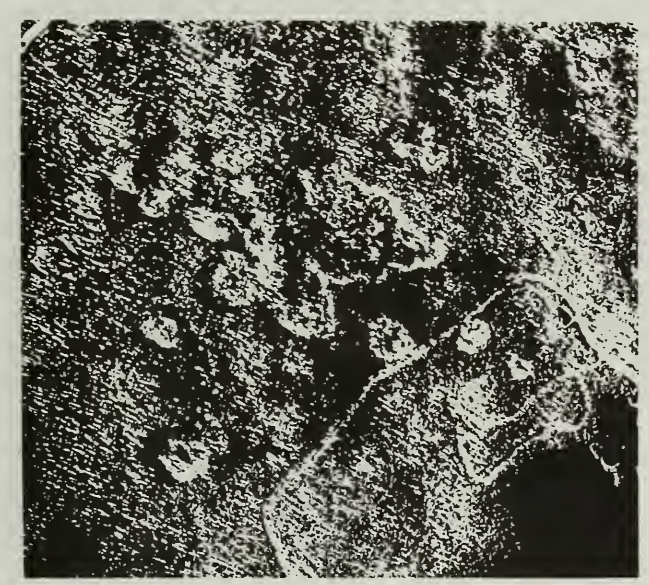

Figure 12. 1:46,000 scale vertical photo of Waldo Lake area.

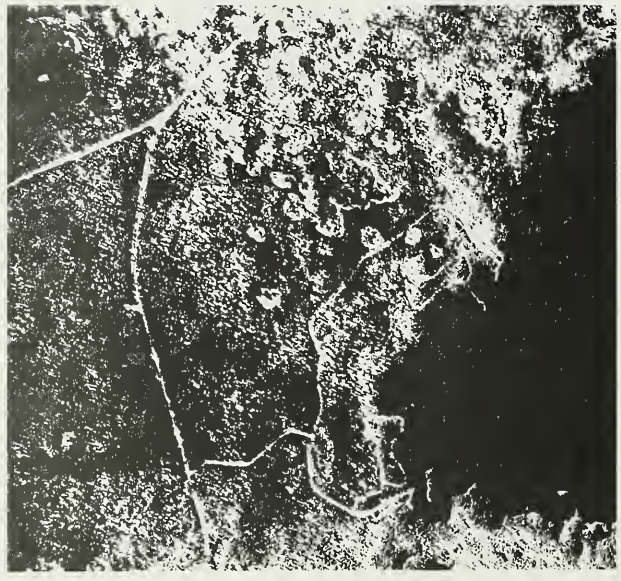

Figure 13. 1:92,000 scale vertical photo of Waldo Lake area. Small centers are quite indistinct at this scale.

Figure 14. 1:184,000 scale vertical photo of Waldo Lake area. Magnification of print is needed to detect small root rot centers (75 to 150 feet across).

ERTS IMAGERY OVERVIEW

The indicated success-ratio likelihood for detecting root rot disease centers on suborbital imagery provides strong potentiality for delineating disease signatures on ERTS imagery. Plans have been made to collaborate with the ERSAL (Environmental Remote Sensing Applications Laboratory) program at Oregon State University to investigate the capabilities of ERTS imagery to identify both insect and disease phenomena. Several bands of the MSS will be made available as well as color enhanced imagery.

LITERATURE CITED

1. Childs, T. W., and K. R. Shea. 1967. Annual losses from disease in Pacific Northwest forests. Resource Bulletin, PNW-20, Pacific Northwest and Range Exp. Sta. U.S. Forest Service. 19 p.
2. Wear, J. F. 1966. The development of spectro-signature indicators of root disease on large forest areas. Annual Progress Report for Earth Resources Survey Program, OSSA/NASA, by the Pacific Southwest Forest and Range Experiment Station.
3. Wear, J. F. 1970. Developing remote sensing techniques for diseased forest trees. Jour. of Remote Sensing, 1(5):6-10.
4. _____ 1967. The development of spectro-signature indicators of root disease on large forest areas. Annual Progress Report for Earth Resources Survey Program, OSSA/NASA, by the Pacific Southwest Forest and Range Experiment Station.
5. _____ 1968. The development of spectro-signature indicators of root disease impacts on forest stands. Annual Progress Report for Earth Resources Survey Program, OSSA/NASA, by the Pacific Southwest Forest and Range Experiment Station.

6. Wear, J. F. and F. P. Weber. 1969. The development of spectro-signature indicators of root disease impacts on forest stands. Annual Progress Report for Earth Resources Survey Program, OSSA/ NASA, by the Pacific Southwest Forest and Range Experiment Station.
7. Weber, F. P. and J. F. Wear. 1970. The development of spectro-signature indicators of root disease impacts on forest stands. Annual Progress Report for Earth Resources Survey Program, OSSA/ NASA, by the Pacific Southwest Forest and Range Experiment Station.
8. Wear, J. F. 1971. Detection of root disease impacts on forest stands by sequential orbital and suborbital multispectral photography. Annual Progress Report for Earth Resources Survey Program, OSSA/NASA, by the Pacific Southwest Forest and Range Experiment Station.

DEVELOPMENT AND FIELD TEST OF AN ERTS-MATCHED FOUR-CHANNEL SPECTROMETER

by

F. P. Weber

The Forest Service research program in remote sensing has become diverse and multifaceted with NASA SR&T support in recent years. Some of the support was directed to studies on the biophysical and physiological characterization of plant communities, especially conifers under physiologic stress. Our research in this area was focused on two problems: (1) Poria weirii damage to Douglas-fir (Pseudotsuga menziesii (Mirb.) Franco) in the Pacific Northwest and (2) mountain pine beetle (Dendroctonus ponderosae Hopk.) damage to ponderosa pine in the Black Hills. In both cases an effort was made to define the spectral signature of trees under stress and to use that information in developing an airborne multispectral detection system. The techniques of making energy budget and water balance analyses were used, in part, for the characterization of the trees under stress as being different from healthy trees. These pursuits led to extensive use and development of biophysical instrumentation for the quantification of plant responses. In this program we used several different radiometers, but none was adequate for measuring spectral response data over long periods of time and in the required spectral bandwidths.

Early in 1971 it became obvious that we would need a precision instrument of some sort to provide closeup spectral radiometric ground truth for our planned ERTS experiment. It was reasoned that we would need a device which would have at least four channels, was lightweight and portable,

would measure spectral irradiance or spectral radiance in four simultaneous bandwidths, and would be inexpensive enough so that we could deploy several such instruments around the country to operate continuously for the duration of the ERTS experiment. We did not find an instrument to fit our requirements, either because existing designs were not rugged for extensive field use or because they were far too expensive. After consultation with instrumentation experts at the University of Michigan Willow Run Laboratories (WRL) we began the design work on a Forest Service field spectrometer in early summer of 1971. It was hoped that our instrument would provide useful quantitative ground truth not only for the proposed ERTS experiment but also for the ongoing Earth Resources Aircraft Program (ERAP).

Being a prototype spectrometer, the RS-2 was somewhat different in design from that of the field spectrometers which are operating today in connection with our ongoing ERTS-1 experiment. However, the detectors and filters are identical. The main difference in the newer models is that they are lighter, and the circuitry is simpler.

The spectral bandpass for the RS-2 channels is defined by four special-order filters which we obtained from Laser Energy, Inc. (Figure 1).[1] They are designed with sideband blocking and peak transmittance of 83 percent. The bandpass of the filter for channel 4[2] extends only to 1.0 micrometer (μm),

[1]Trade names and commercial enterprises or products are mentioned solely for necessary information. No endorsement by the U.S. Department of Agriculture is implied.

[2]In this discussion, channel 1 is 0.5 to 0.6 μm; channel 2 is 0.6 to 0.7 μm; channel 3 is 0.7 to 0.8 μm; and channel 4 is 0.8 to 1.0 μm.

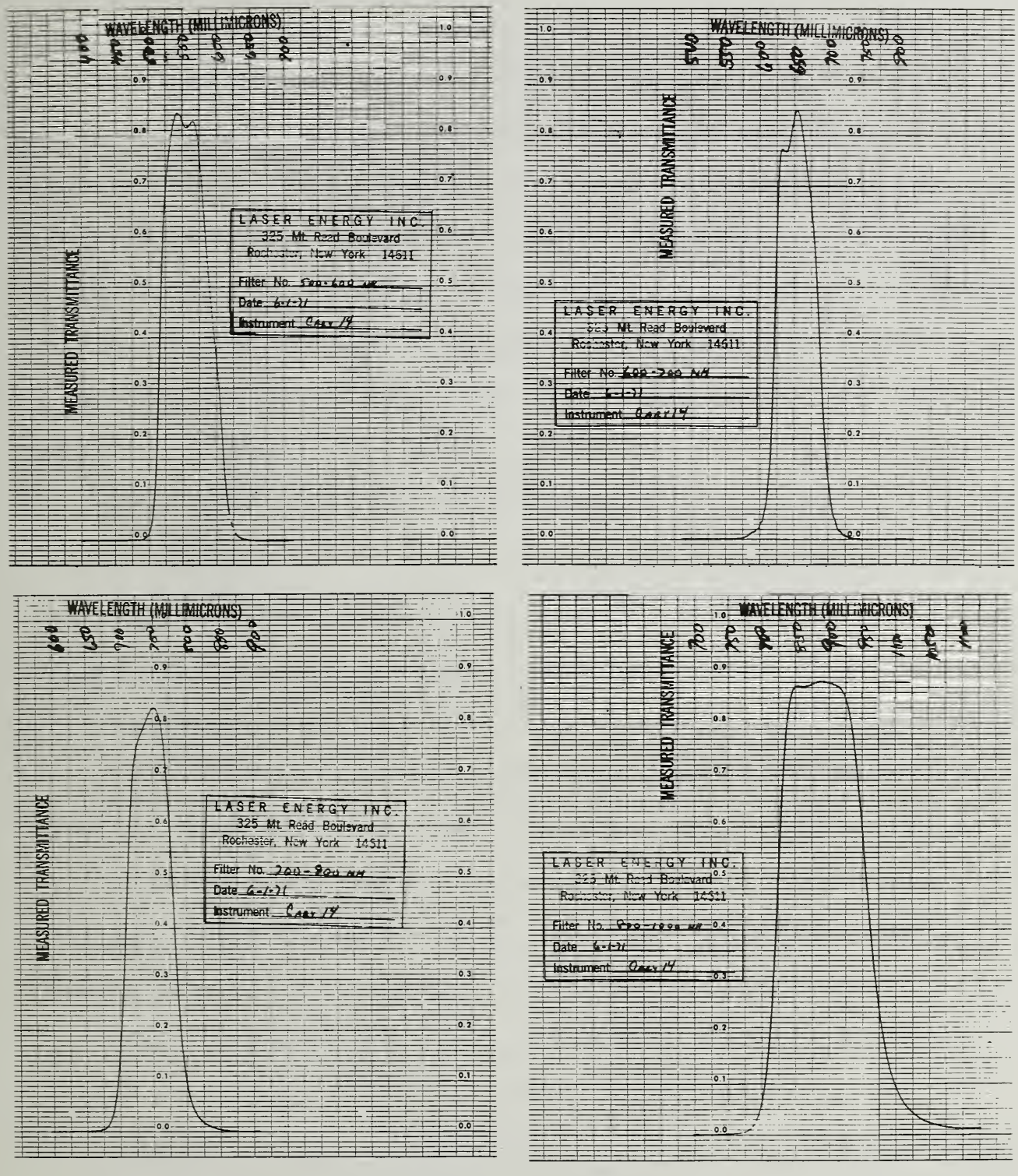

Figure 1. The spectral bandpass and transmittance of the four RS-2 spectrometer filters are shown on the Cary 14 measured spectrophotometer curves provided by Laser Energy, Inc.

but that channel was later refiltered to extend the bandpass to 1.1 μm. Otherwise the bandpass of the RS-2 was designed to match that of the ERTS multispectral scanner (MSS) subsystem.

The field spectrometer uses four United Detector calibrated PiN 10 Schottky photodiode detectors which have an active area of 1.25 cm^2 when the full 45^o field-of-view of the instrument is used. However, we could obtain more precise measurements after restricting the field-of-view to 10^o and using the detectors with an active area of 0.16 cm^2. The spectrometer unit is powered by a rechargeable Gelyte battery which drives the light chopper motor and associated circuitry. The spectrometer was also designed to operate on 115 volts for operation in the laboratory and for recharging the battery. Although the Gelyte battery contributed most of the weight to the prototype RS-2, the high amperage rating provided for 6-1/2 hours of continuous use in the field.

Extensive spectral calibration and light sensitivity tests were run in the laboratory on the field spectrometer. Figure 2 shows the calibrated radiance output at five levels for each detector. Due to the slightly different spectral responsivities of each of the detectors, there is a different calibrated radiance for a given neutral density level.

For the calibration data in Figure 3 we measured the detector response for each channel as a function of changing target exitance. Target exitance may be defined as the energy in watts per unit area of each particular target. To do this we measured the spectral energy reflected off a flat white target illuminated with a 1000-watt standard lamp from a distance of 50 cm. For this test it was necessary to place the light source and the

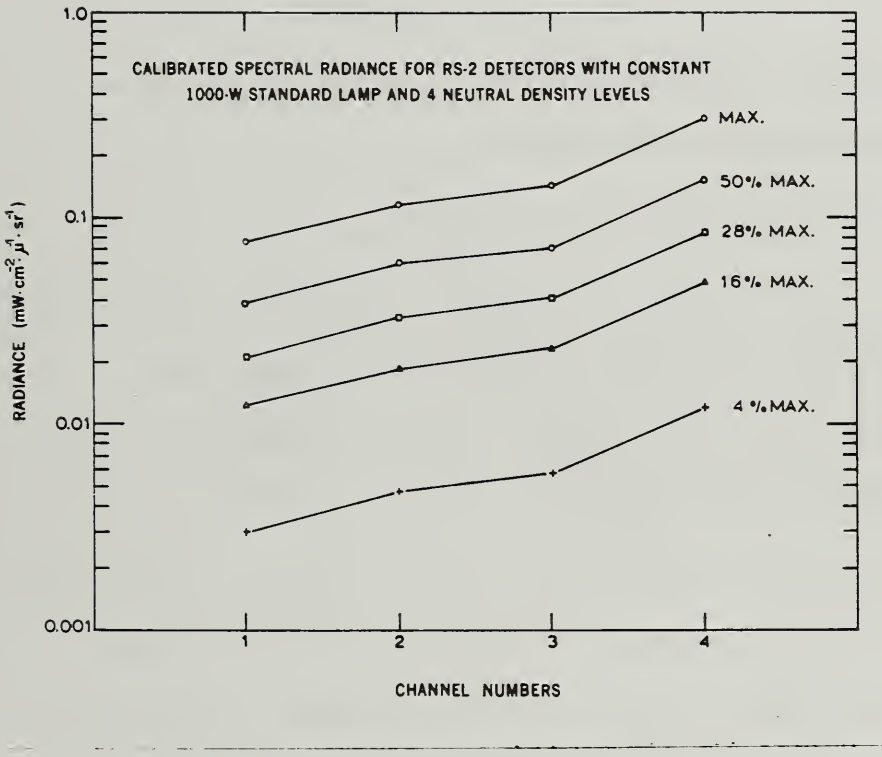

Figure 2. The calibrated spectral radiance for the RS-2 detectors was measured at four neutral density levels and maximum output for a 1000-watt standard lamp.

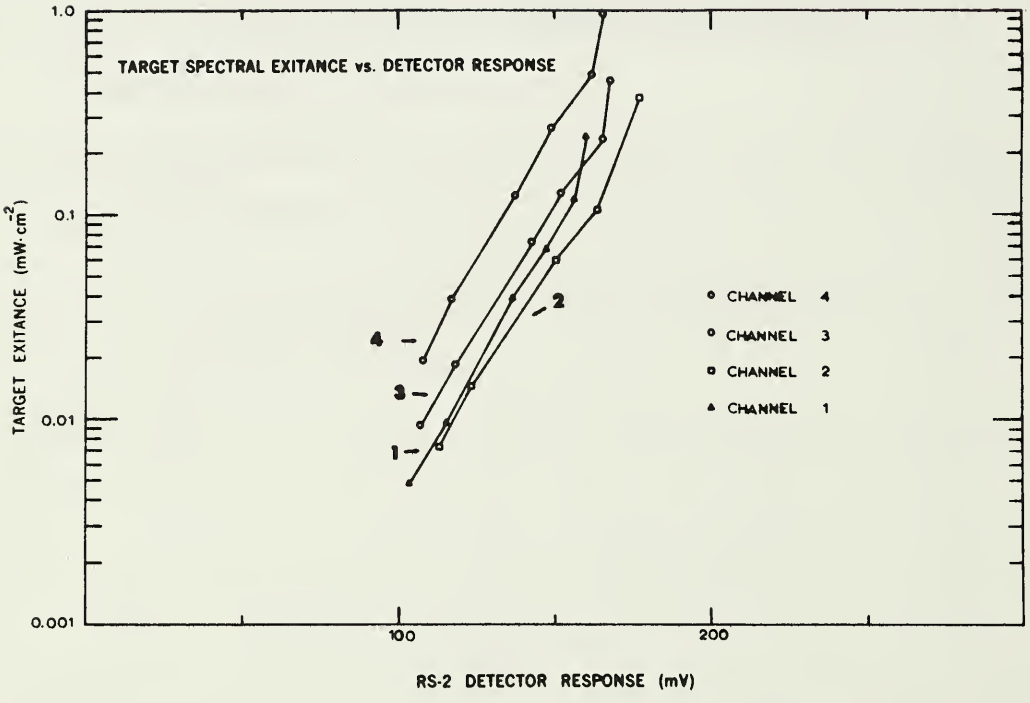

Figure 3. The field spectrometer detector responses (in millivolts) were measured at six different levels of target exitance. The spectral characteristics of the target remained constant; only the exitance level was varied.

detectors in the same vertical plane from the reflecting surface, with the light position slightly higher than the detectors. The detectors were well baffled to prevent direct illumination of the detector surfaces by the light source. The reflecting surface was painted with 3M white paint which is preferred for this type of target exitance calibration because of the reflectance characteristics which produce a flat response for that portion of the spectrum of interest.

The detector response levels shown in Figure 3 are unamplified signals from the small area detector with a 10^{o} field-of-view. The RS-2 was tested for detector response with two different amplifiers. First, the United Detector (UDT-100) FET amplifier was tested. This device seemed like a good compact preamplifier (considered desirable for field applications) because of the small 7.5-volt self-contained battery which provided the constant bias current. The UDT-100 provides a gain of 100 which makes it well suited for the signal conditioning necessary for recording signals directly on a portable chart recorder in the field. For use with targets in the Black Hills for the ERTS experiment, we amplified the output of the RS-2 with Burr Brown 3061/16 instrumentation amplifiers and then recorded the outputs on our Vidar 5403 digital data acquisition system. The 3061/16 amplifiers proved to be somewhat superior in terms of stability of signal and lack of noise interference pickup. However, the instrumentation amplifiers are dependent on a $\pm$ 15 vdc power supply which must be considered in the final application of a field spectrometer.

The last laboratory test for the RS-2 spectrometer was a measurement

and calculation of the spectral responsivities of the detectors (Figure 4). These were calculated for each channel as the ratio of detector output to spectral radiance output for several different levels of target reflectance. In the laboratory, target reflectances were created with neutral density filters attenuating a 100 percent reflectance from a white surface illuminated with a 1000-watt standard light source.

We had an opportunity to field test the Forest Service RS-2 spectrometer in November 1971 (Figure 5) in conjunction with a flight of the University of Michigan M-7 multispectral scanner system over our Atlanta, Georgia, test site (217).[3] In this test we were primarily concerned with the signatures of hardwood and conifer trees, pastures and brushfields, and open water. We were fortunate to have a hydraulic lift available to place the spectrometer and recorder over the tops of the trees and other targets while the Michigan plane was gathering data overhead.

The data in Figure 6 show the four-channel analysis of target exitance for one of the days when the Michigan plane flew. Radiometric relationships of various targets were established throughout the day and were valuable data for preprocessing analysis and optimum channel selection in the multispectral processing of aircraft data at WRL. Figure 6 shows the spectral radiant exitance for pine, hardwood, pasture, and water. These were the targets of principal interest and offered a range of spectral responses. For example, exitance values for pine and hardwood are separated in channel 2

[3]The multispectral scanner test flight is the same one discussed in Section I of this report entitled "Land use classification in the southeastern forest region by multispectral scanning and computerized mapping."

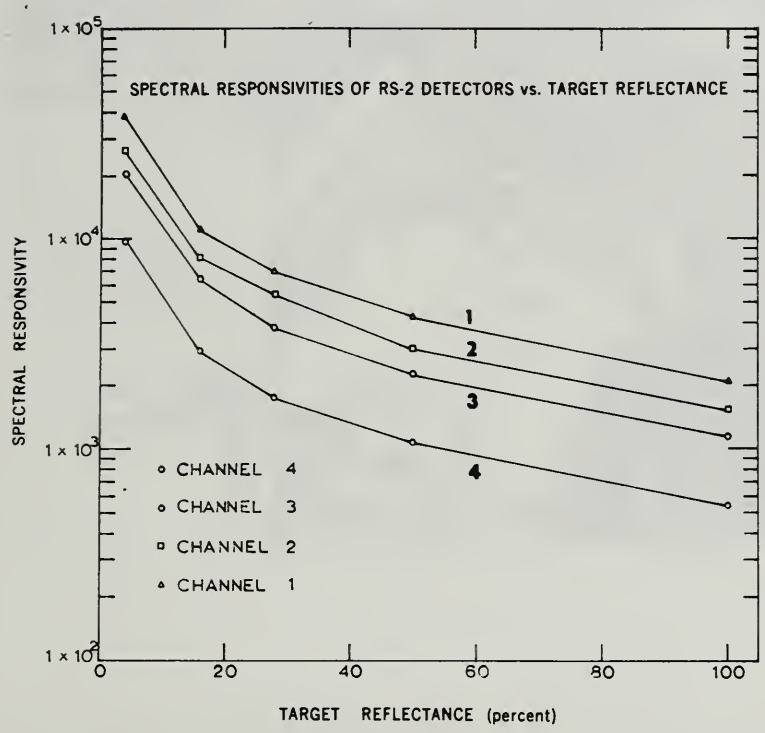

Figure 4. The spectral responsivities of the RS-2 detectors were calculated for five levels of target reflectance.

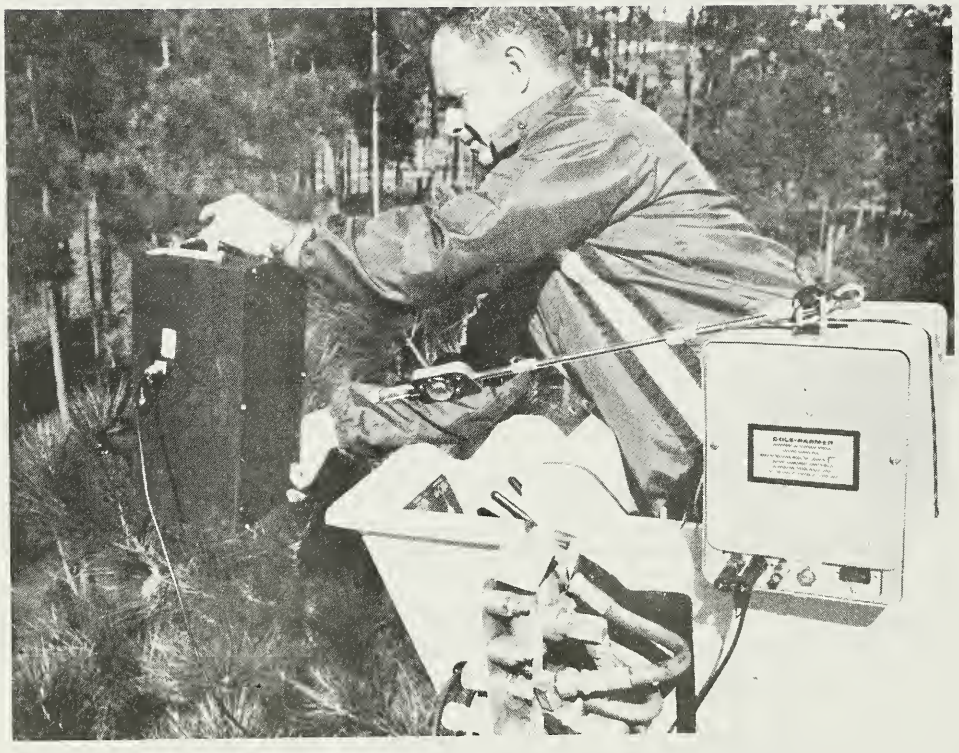

Figure 5. The Forest Service RS-2 field spectrometer was field tested in November 1971 in connection with a multispectral scanner flight over the Atlanta, Georgia, test site (217). Author is holding RS-2 over pine foliage while being supported in the bucket of a cherry picker.

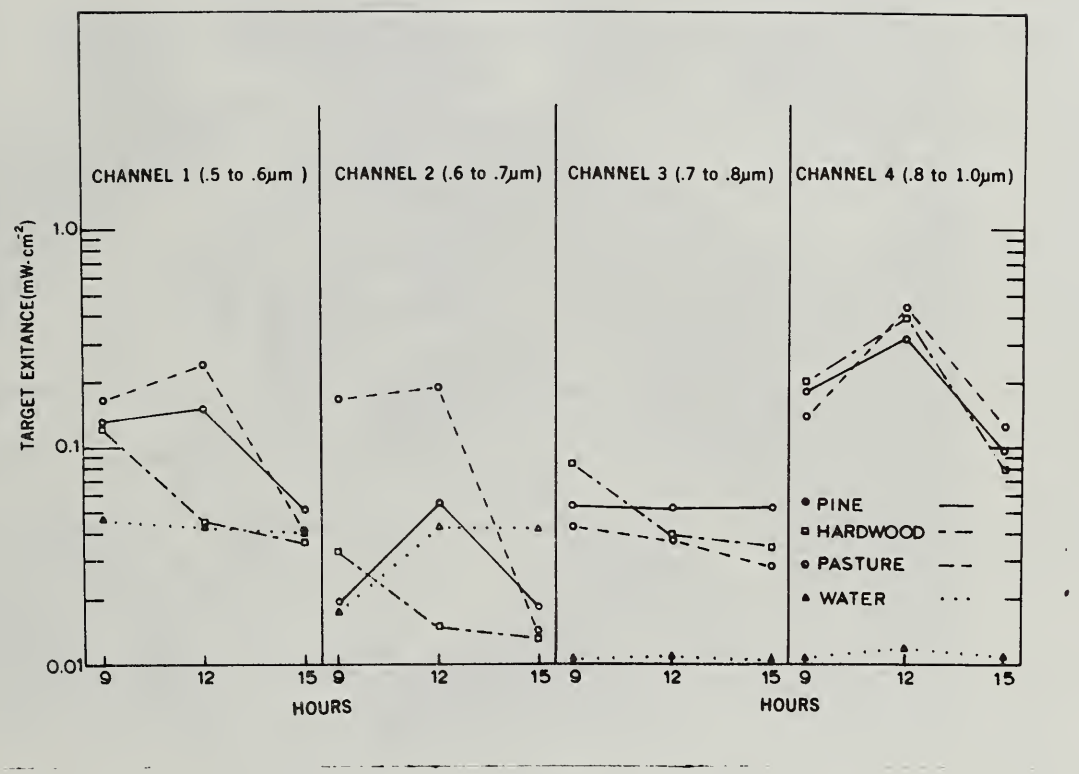

Figure 6. Radiometric data from the field test of the RS-2 spectrometer shows the radiant exitance differences between four targets throughout the day. Data were collected in conjunction with a flight of the M-7 multispectral scanner over the Atlanta, Georgia, test site (217).

in the morning and at midday. Also, pasture had a much higher reading than the other targets on channel 2 in the morning and at midday. Channel 1 was good for separating pine, pasture, and hardwood at midday. Water was very different from other targets at all times of day on channels 3 and 4. The possibility of making this kind of target spectral signature analysis under field conditions and with natural illumination is exactly the reason why the spectrometer was developed.

The field spectrometer operated very well in accordance with its design throughout the three-day field test. However, some problems were obvious with the prototype instrument which required design changes before the spectrometer became useful as a field instrument. Although the RS-2 is compact, it is unnecessarily heavy (6 kilograms) which makes its use from the top of a cherry picker awkward. Certainly the prototype was too heavy to be used suspended from an overhead tramway system as planned. An additional annoyance was that we had a single-channel portable recorder for use in the field so that the output of the RS-2 was wired to sample the channels sequentially (with a rotary switch) rather than simultaneously.

As a result of the successful development and test of the prototype field spectrometer, five new spectrometers were built (Figure 7) and have been installed at our ERTS-1 test site in the Black Hills (226A). Although the new spectrometers were constructed with ERTS money, we would not have been able to build them rapidly and get them deployed to the test site had not the developmental research been supported by the SR&T program.

Figure 7. The interior of one of the five field spectrometers currently operating at ERTS test site 226A in the Black Hills is shown. Redesign of the prototype RS-2 resulted in a weight reduction of 4 kilograms.

CALIBRATION OF FOCAL PLANE SHUTTERS

by

Robert W. Dana and Benno Marx

INTRODUCTION

There are several aspects to the importance of measuring the exposure time of a camera. For an efficient system of film exposure adjustment, the exposure times (or shutter speeds) should be set at values varying by approximately a factor of two, i.e., 1/500 sec, 1/1,000 sec, etc. Cameras used in multicamera systems, from which the imagery is to be analyzed quantitatively, should have exposure times which are well matched or at least well calibrated against one another. In the case of the focal plane shutter with its moving curtain, it is necessary to test for uniformity of motion and, therefore, uniformity of exposure across the image plane.

These properties can be tested photographically using a rotating transparent drum (ANSI, 1952), but a quicker and cleaner method employing electro-optic technology provides savings of time and money. We have devised a technique useful for cameras in general, but designed for focal plane aerial cameras in particular, which includes an intense light source, photodetector with amplifier, and an oscilloscope. An electronic time interval counter provides a worthwhile adjunct.

GENERAL SYSTEM DESCRIPTION

The instrument arrangement is shown mounted on an optical bench for convenient height and distance adjustments (Figure 1). A laser

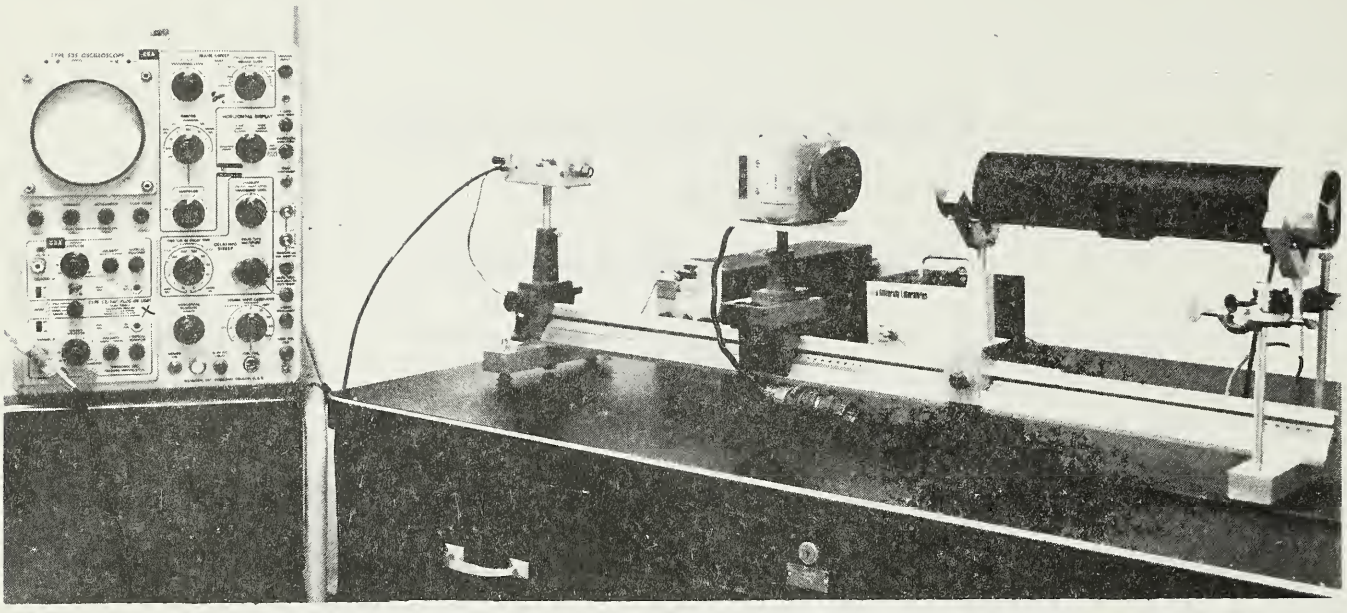

Figure 1. Instrumentation for exposure time measurements for focal plane shutters. The primary components are a general-purpose oscilloscope, fast response detector with amplifier, and a small He-Ne laser.

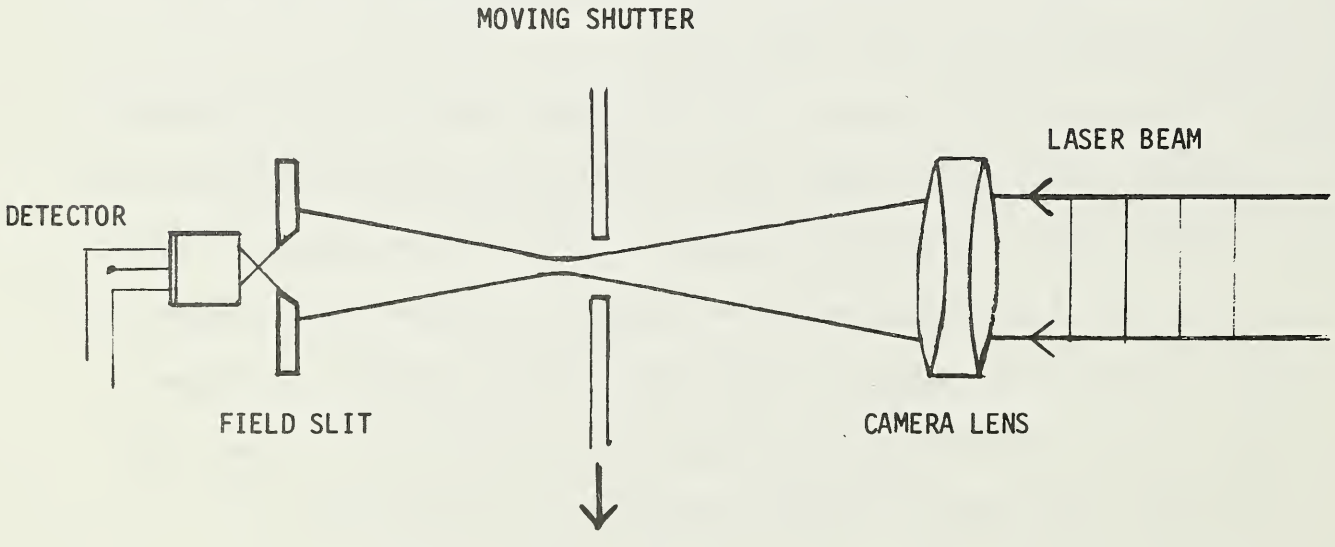

Figure 2. Optical system of exposure time measurement technique for focal plane shutters.

provides high-intensity light in a collimated beam which effectively comes from an infinite point behind the laser. Aerial camera lenses usually have a set infinite focus. Therefore, the collimated beam is converged by the lens to a tiny point at the image plane which is close to the plane of the focal plane shutter. This point of light is smaller than the opening in the shutter curtain.

The principles of geometrical and physical optics that are involved are fairly straightforward, but one must take care to measure light in a manner consistent with the way that it exposes the film. A focal plane shutter can be described as a moving curtain with a rectangular slit which passes just in front of the film plane. The effective exposure time ($\bar{T}$) is given by

$$\bar{T} = \int \frac{H(t)\, dt}{H_{max}} \qquad (1)$$

where $H(t)$ is the time-dependent irradiance and H_{max} is the maximum value of irradiance used as a normalizing factor. The exposure time can also be expressed as the ratio of the slit width to the average curtain velocity. Adjustments in exposure time are generally made by varying this shutter slit width.

When the slit passes across a uniform beam of light with a uniform velocity, the total time that the detector is irradiated is dependent on the widths of both the beam and the slit. But the average time as defined by equation 1 is dependent only on the wider of the two elements. Therefore, it is important that the light beam be focused to a size smaller than the shutter slit width to assure that the time measurements are invariant to beam width. In addition, we place the detector several

centimeters behind the shutter to sample only the center portion of the beam (Figure 2) where it is diverged to a size several times as wide as the detector aperture. Lasers propagating in the TEM_{oo} mode have a gaussian-shaped beam on both sides of the focusing lens (Dickson, 1970), and much of the beam nonuniformity can be removed in this manner. Diffraction patterns from the edges of the slits and lens optical transfer characteristics are negligible in this measurement since the slit width exceeds 1 mm, and we are only attempting about 5 percent accuracy.

ELECTRONICS

Any beam of light chopped by a focal plane shutter has significant rise and fall times representing the time taken for each edge of the shutter slit to traverse the light beam. Ideally, we want only the time required for the focal plane shutter to pass a theoretical point. To do this with a finite size light beam, we have designed a circuit which measures the peak voltage V_p across some photo sensor and then quickly switches a time-measuring circuit whenever a subsequent light pulse reaches some fraction (usually one half) of the peak voltage V_s as shown in Figure 3.

The light sensor chosen for this purpose was a silicon phototransistor. This device is essentially a silicon photodiode integrated with a high-gain npn silicon transistor in the same semiconductor chip. The high gain of the phototransistor permits sensitivities greater than $0.2 ma/mw/cm^2$ at low unit cost. Photo current rise and fall times of a few microseconds are sufficiently fast for shutter speed measurements. The phototransistor response approaches linearity with respect to light

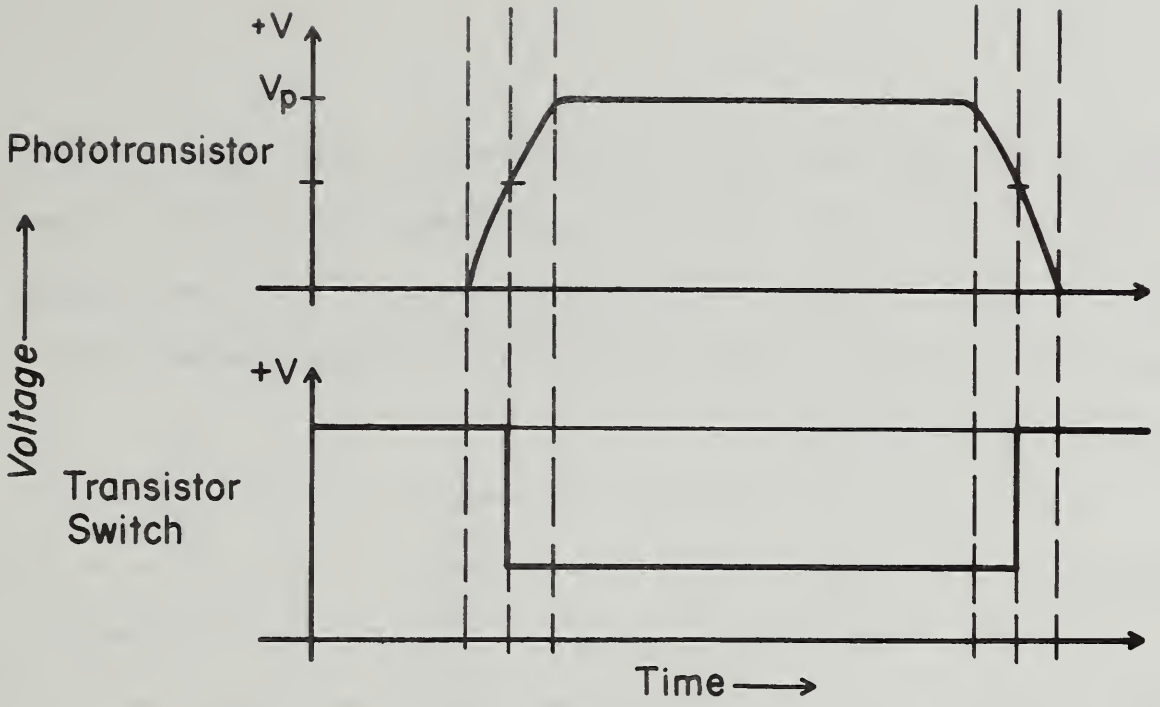

Figure 3. Plot of the phototransistor voltage (proportional to the irradiance of light) and the output voltage of the transistor switch versus time.

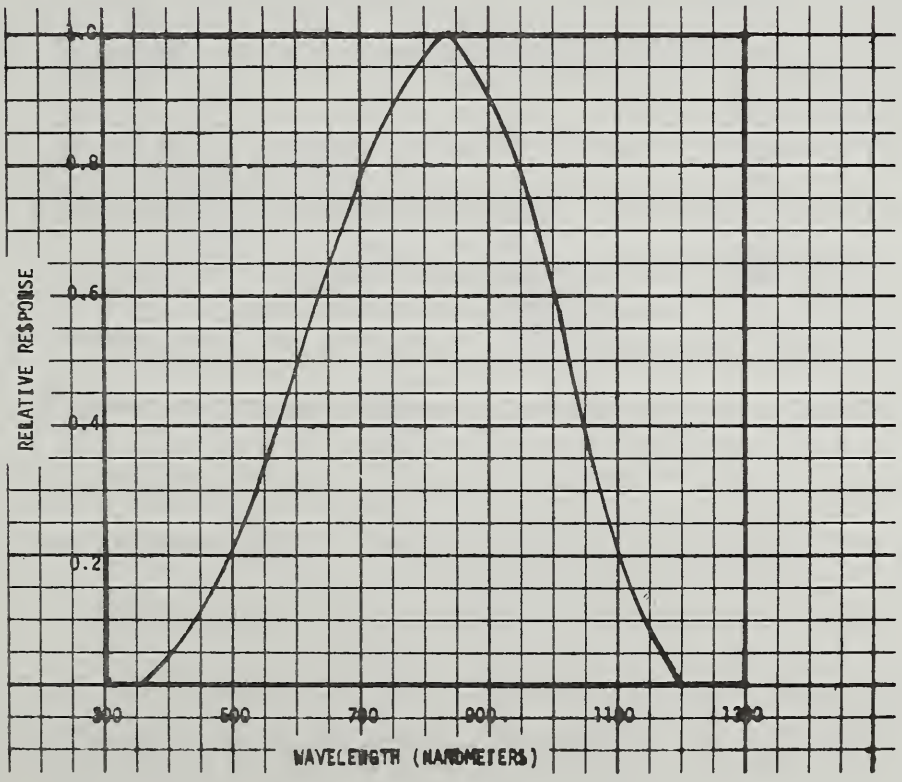

Figure 4. Relative response with wavelength to the Sprague ED401 npn silicon phototransistor.

input for the high light levels achieved with a laser source. As can be seen in Figure 4, the spectral response peaks at about 850 nanometers (nm). In general, silicon phototransistors have a useful wavelength range of 450 to 1050 nm with good sensitivity for helium-neon laser light at 632.8 nanometers.

Figure 5 is a diagram of the pulse-measuring circuit. When a sequence of light pulses is put into it, the first light pulse prepares the circuit for a measurement, and a peak detector samples and holds the peak voltage V_p. An amplifier AR2 then senses the voltage level, driving a simple low impedence voltage divider which produces a level V_s approximately equal to $V_p/2$. The next pulse activates the switching transistor Q1, whose emitter is referenced to the V_s level when the input reaches that level. The output signal is an amplified square wave having a width approximately equal to the input pulse half width. This square wave can trigger an electronic time interval meter efficiently and is easy to measure on an oscilloscope. Simultaneously, the sample and hold circuit readjusts its voltage level to the new impulse.

Due to severe noise problems associated with the electric shutter and motor driven film advance of an aerial camera, a small RC integrator is added directly to the phototransistor's output, while a large capacitor is mounted across the power supply inputs. These precautions were adequate in insuring measurements without interfering noise.

A sensitivity adjustment is provided through the front panel -- its level to be changed until the red light emitting diode (LED) just fails to emit. This assures us of the transistor Q1 triggering at the half

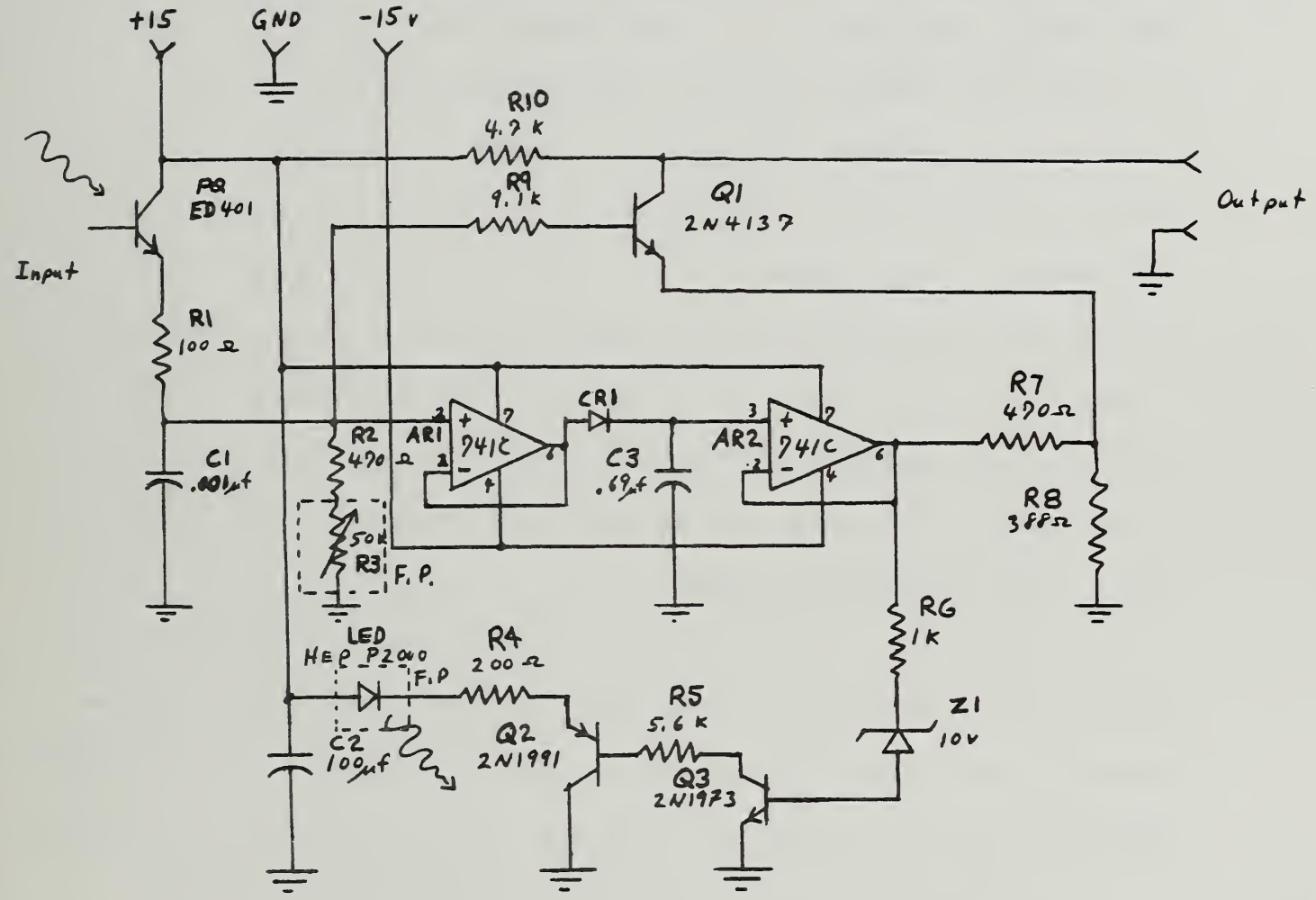

Figure 5. Schematic of pulse-measuring circuit. The symbol F.P. indicates front panel mounting of that component.

amplitude of the input pulse, not at half the power supply voltage -- an event which happens if the sensitivity is too high.

PERFORMANCE

The precision and accuracy of the pulse-measuring circuit can be determined by applying it with a time-variable beam from an infrared emitting diode radiating at a wavelength of 900 nanometers. When driven by a low-voltage sine wave with a diode in series for rectification, the IR LED emits a pulse similar in shape to that of the focal plane shutter. For a pulse width of five milliseconds, a dual trace scope display and a time interval counter revealed an accuracy of four percent for the half width. Although very slight adjustments in the sensitivity were necessary during a four-hour test, the long-term drift in the measured half width and the short-term repeatability were less than 1 percent of the mean value.

Unless the input pulse is a linear ramp up and down, the time between half power points will not equal the mean value of amplitude as defined by the integral in equation 1. The half width will be an adequate approximation of it, however, and the same ratio $\bar{T}/T_{1/2}$ should be obtained for all settings of a focal plane shutter. Values of V_s other than the half power point can be adjusted for a particular pulse shape by changing resistors R7 and R8.

LITERATURE CITED

1. American National Standards Institute, Inc. 1952. Performance characteristics of focal plane shutters used in still cameras. ANSI Standard PH 3.2 - 1952, American National Standards Institute Inc., New York, New York.

2. Dickson, L.D. 1970. Characteristics of a propagating gaussian beam. Applied Optics 9(8):1854-1861.

MATHEMATICAL MODELING OF FILM CHARACTERISTIC CURVES

by

Robert W. Dana and Nancy X. Norick

INTRODUCTION

To facilitate the use of color film calibration data, there was a need for algebraic equations to express the relationship between film density and relative log exposure. Known reflectance differences or contrast ratios of various objects could then be used to predict density differences on film, and conversely, density differences could readily be converted to reflectance differences for more accurate object recognition.

The shape of a characteristic curve of a color reversal film is exhibited in Figure 1, which displays the integral density of Eastman Kodak 2443 color infrared (CIR) film measured with a green filter (red light sensitive layer). The shape of the curve suggests an exponential form encountered often in physics and electronics.

$$D = Ae^{-f(x)} + C, \qquad (1)$$

where

D = density

x = relative $\log_{10}$ exposure

The function $f(x)$ should be monotonically increasing with x so that the constant A takes the value of the maximum density ($D_{max} = 3.2$) at zero exposure, and C takes the value of the minimum density ($D_{min} = 0.1$) at infinite exposure. Functions that are linear in x and quadratic in

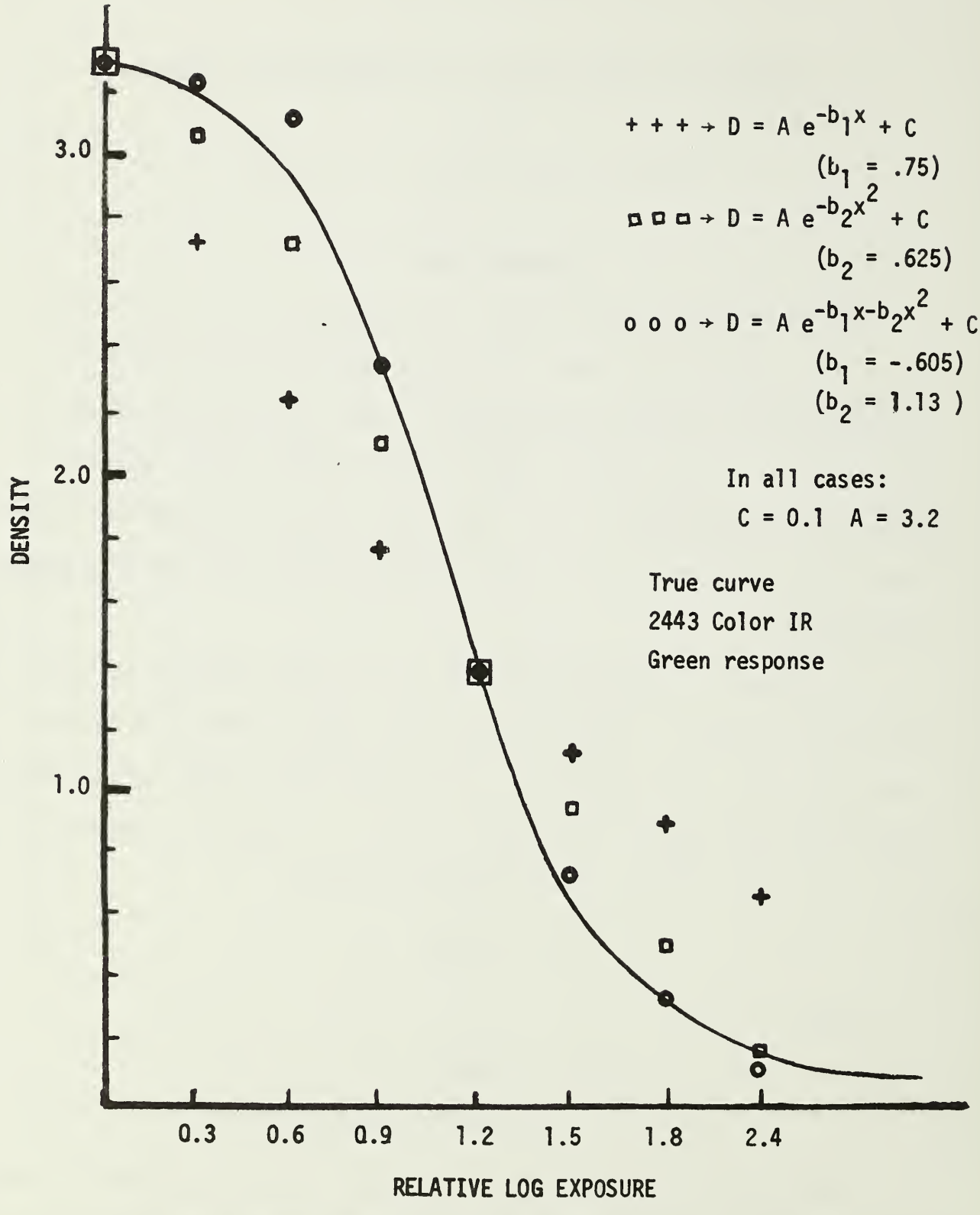

Figure 1. Typical characteristic curve of the green response for CIR film. Several points for three possible models are plotted.

x are shown in a graphic fitting with the point x = 1.2, D = 1.4 used as a constraint. The best fit was for $f(x) = b_1x + b_2x^2$ with nonzero values of b_1 and b_2. One more fitting point ($\log_{10}E = 0.9$, D = 2.35) was required to provide two equations from which the two coefficients b_1 and b_2 were solved. These results were encouraging enough to lead to a more refined computer modeling procedure with a cubic term included in f(x).

COMPUTATIONAL METHODS

Equation 1 can be changed to a more usable form by putting the constant A into an exponential expression and taking the logarithm

$$\ell n\,(D - C) = \beta_o + \beta_1 x + \beta_2 x^2 + \beta_3 x^3 \qquad (2)$$

where

$$\beta_o = \ell nA$$

$$\beta_1 = -b_1$$

$$\beta_2 = -b_2$$

β_3 = another constant

At least-squares fit of equation 2 was performed for 2443 CIR film and the beta values found by regression techniques. Several variables were considered in the computations to assure a good fit of the model to available data. The value intended for the offset constant C was the minimum density of a scan of the sensitometer strip, but we also tried values of $D_{min} + n(.01)$ with n taking integral values between minus 14 and plus 5. Density data were somewhat noisy at the toe of the characteristic curve and above the shoulder, requiring truncation of the density

values used for fitting. Low densities were truncated at D_{min} + .05 density units. Two cases were taken for elimination of high values -- data above D_{max} + 0.10 and data above D_{max} + 0.20. Practical considerations would generally obviate the calibration of density data outside this range of acceptance anyway.

Two different forms of the exponential equation were tested. A quadratic form with β_3 equal to zero was tried as well as the full cubic equation 2.

The film strips were exposed by a Joyce-Geveart model 2L sensitometer on 70 mm film, producing exposures 210 mm in length with a linear variation in relative $\log_{10}E$ of 0 to 4.0. The spectral distribution was approximately that of average daylight (Dana and Myhre 1971). The film was processed in Nikor equipment with E-4 chemicals.

Film strips were scanned by a Photometric Data Systems digital comparator/microdensitometer, such that a density sample was taken at intervals of one mm and recorded on magnetic tape. The effective aperture was 100 micrometers (μm) diameter. One scan down the center of the sensitometer exposure was taken using each of three color filters (red, green, blue), and one scan was taken using no filter (clear).

Limitations in film latitude caused the full range of densities to be located in a scan length of 170 mm. Truncation of the data according to the rules discussed previously brought the size of the working data set to approximately 80 to 95 mm for each scan run. No attempt was made at smoothing the data or averaging several scans together. It was felt that single data sets of this size were sufficient to filter out unwanted noise and prove the validity of the exponential model for CIR film.

RESULTS

The outputs of the film curve modeling program are beta values, correlation coefficients, standard errors of estimate, plots of actual truncated data versus predicted density data, and a listing of the full data set. Some of the results are shown in Figures 2 through 7. Figure 2 is the plot of actual and predicted curves for the best case of the red response (infrared sensitivity) of this film. The fit of the data is very close, and the standard error (i.e., the root mean square deviation between these curves) is 0.023 density units. This is excellent considering the densitometry was done with precision and accuracy of approximately 0.01 and 0.02, respectively. The best fits for the green and clear response curves yield standard errors less than 0.033.

The best case for the blue response of CIR film given by Figure 3 is somewhat poorer. Here the standard error was 0.079. An artifact which appears in all color response curves in this test but is most pronounced with the blue filter curve is a small discontinuity at about 2.0 density. Most analog and digital plots for other film samples have not exhibited lack of smoothness at middle densities. The only explanation offered is that the light beam had a slight nonuniformity at the center of the sensitometer platen at the time these samples were exposed. Variations with wavelength indicate that scattering effects are also present.

The actual data are somewhat noisy at high density, indicating that further truncation of the upper end would permit a better fit of

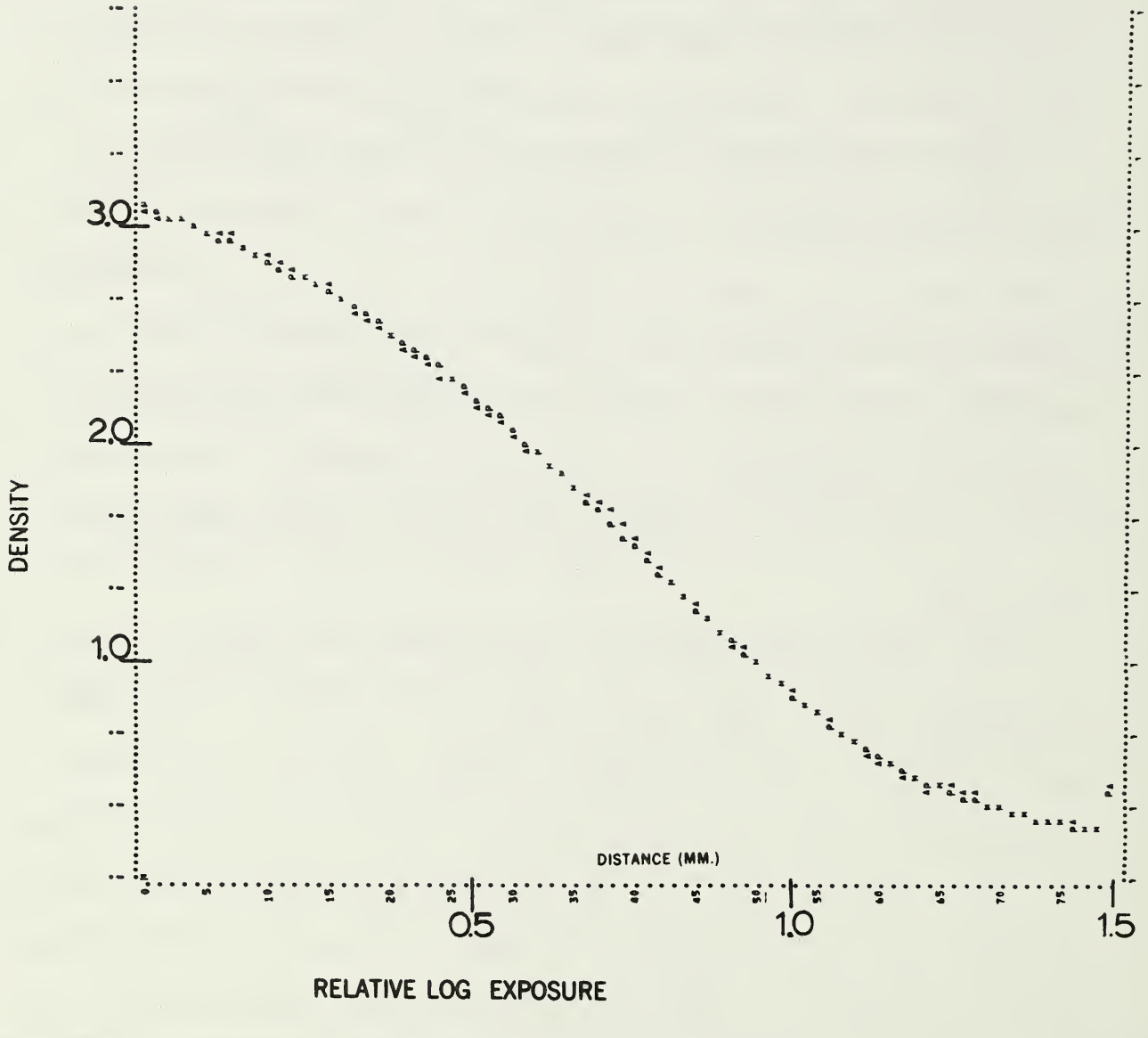

Figure 2. Plot of the best fit for data set no. 1. The symbol A represents actual data; P represents a predicted value; and M represents a coincident point. This case was the cubic model with truncation above D_{max} and C equal to D_{min}.

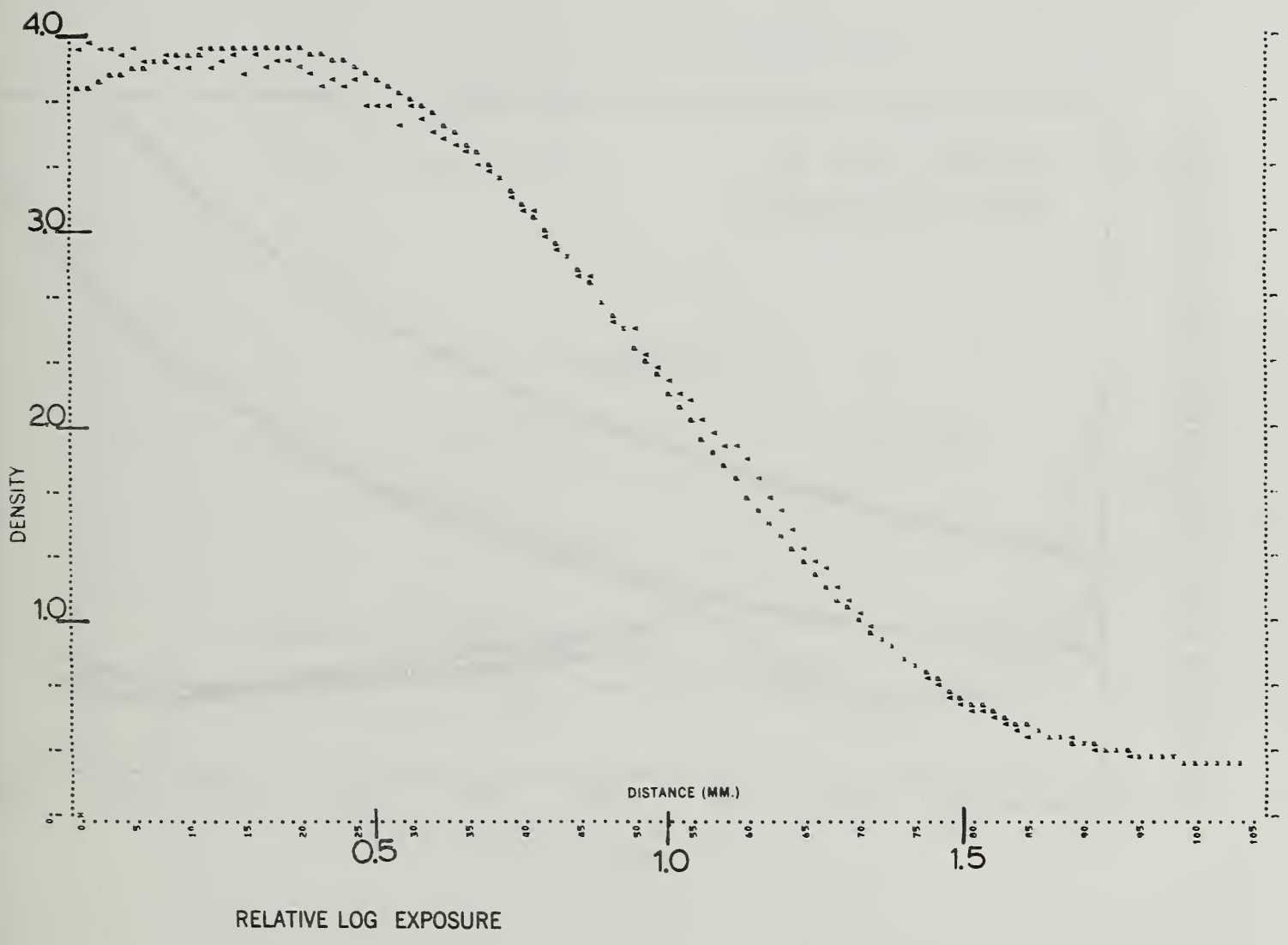

Figure 3. Plot of the best fit for data set no. 3. The symbol A represents actual data; P represents a predicted value; and M represents a coincident point. This case was the cubic model with truncation above D_{max} - 0.1 and C equal to D_{min}.

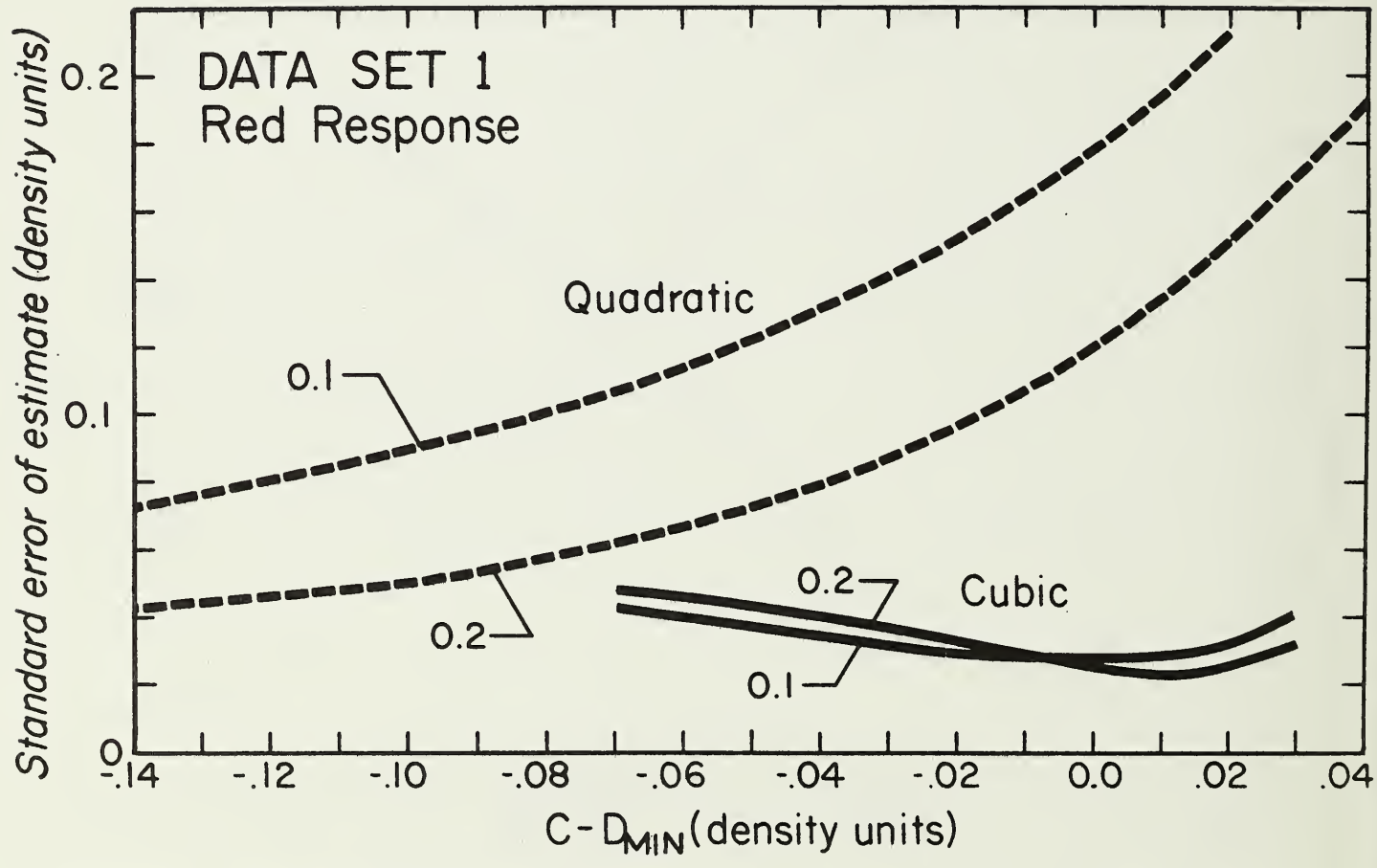

Figure 4. Standard error of estimate for data set no. 1 versus offset constant C. Curves for truncation at D_{max} - 0.1 and D_{max} - 0.2 are shown.

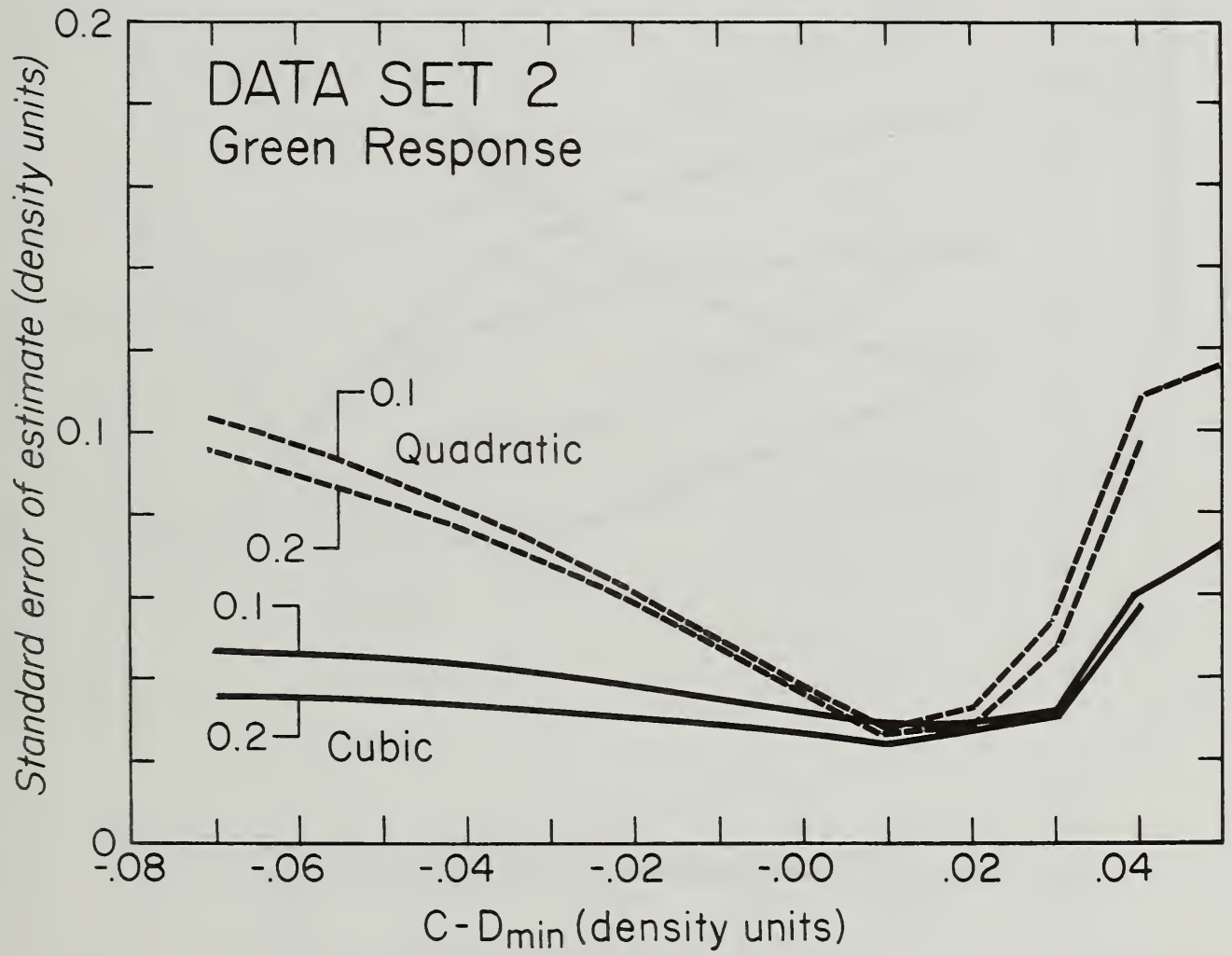

Figure 5. Standard error of estimate for data set no. 2 versus offset constant C. Curves for truncation at D_{max} - 0.1 and D_{max} - 0.2 are shown.

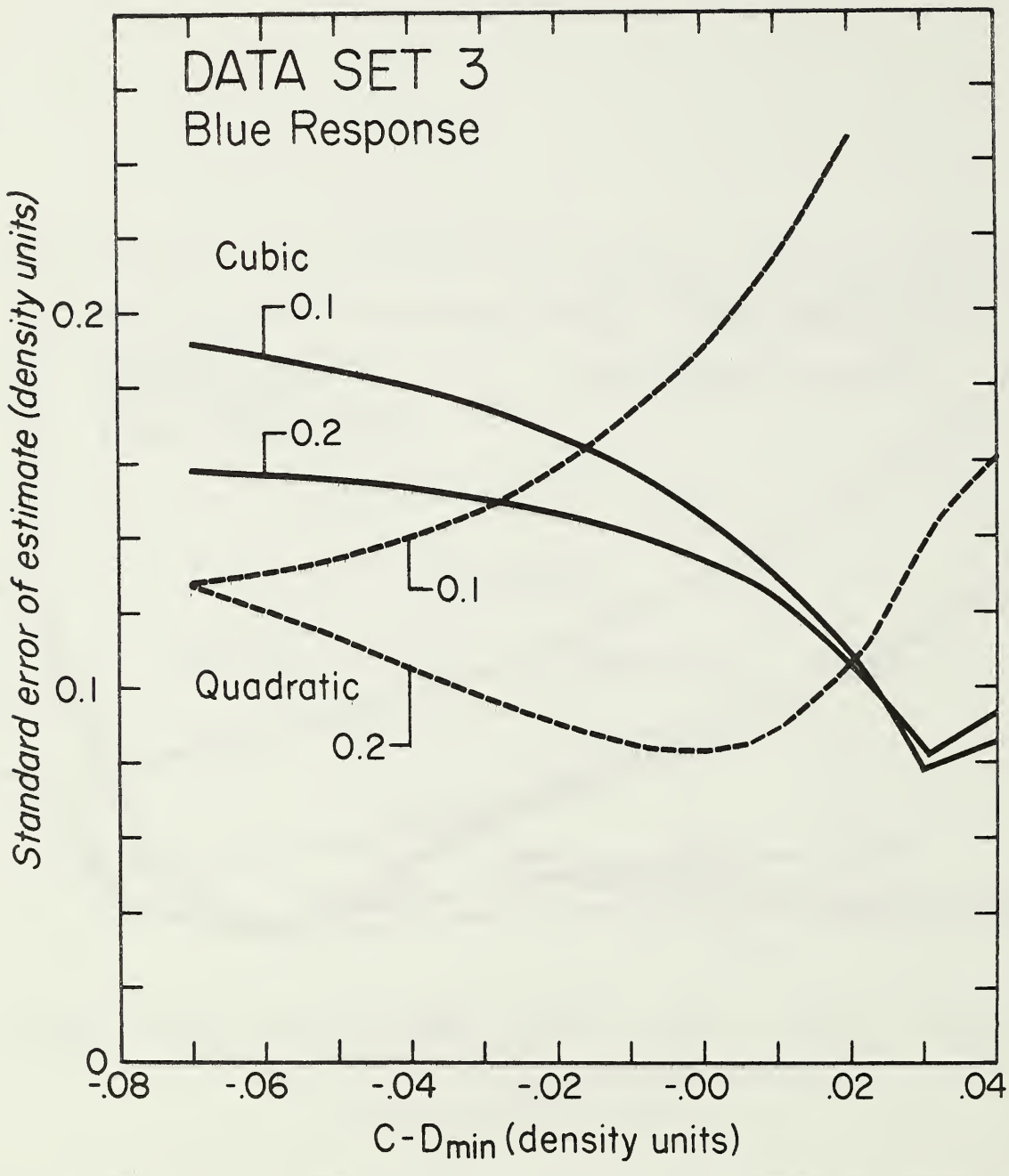

Figure 6. Standard error of estimate for data set no. 3 versus offset constant C. Curves for truncation at D_{max} - 0.1 and D_{max} - 0.2 are shown.

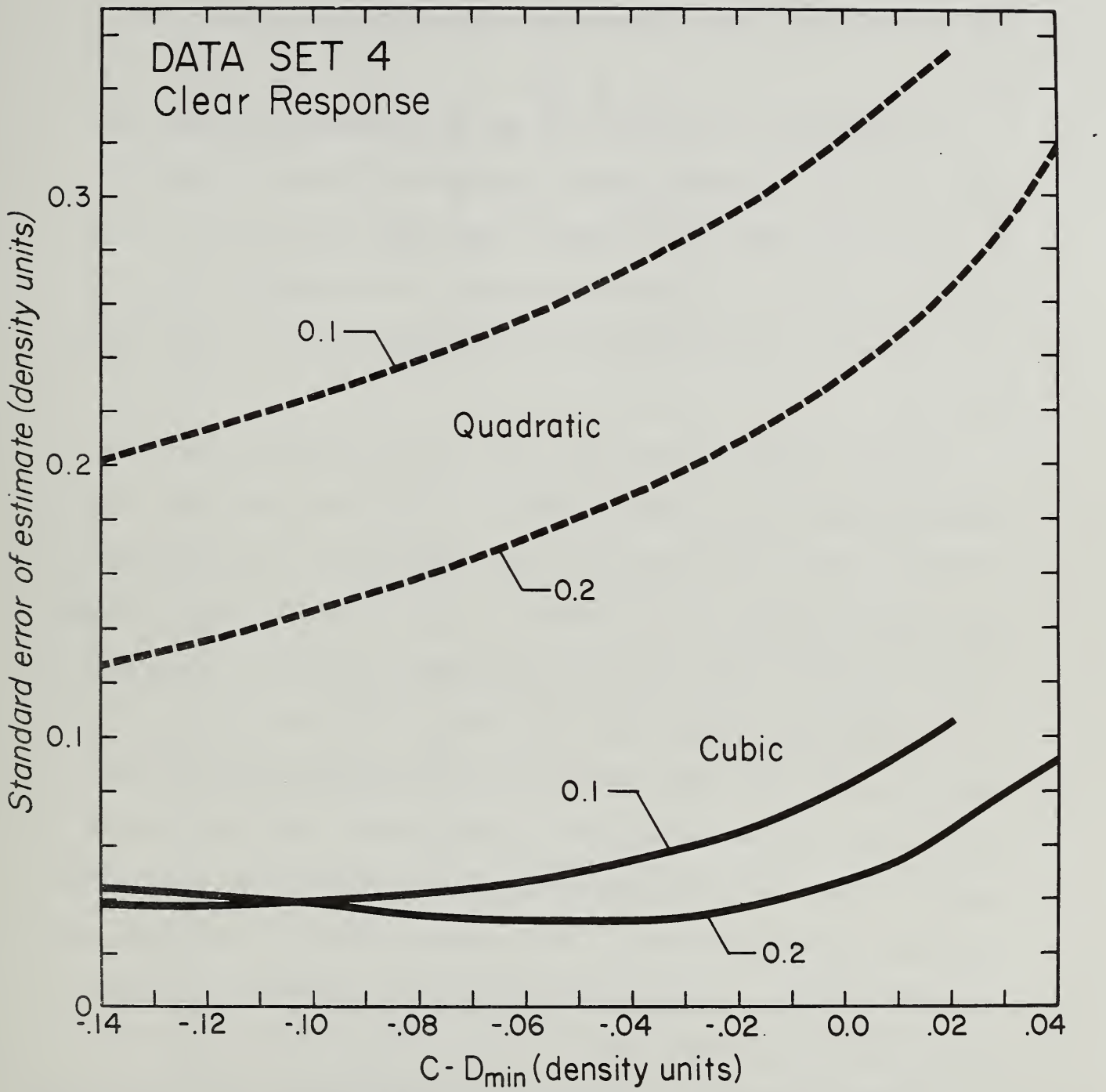

Figure 7. Standard error of estimate for data set no. 4 versus offset constant C. Curves for truncation at D_{max} - 0.1 and D_{max} - 0.2 are shown.

the model. Figure 6, showing the standard error values for all trials with this data set, also suggests more truncation would reduce the error.

An examination of Figures 4, 5, and 7 of standard error for red, green, and clear responses reveals that the cubic model is superior to the quadratic form in that there is much less sensitivity to truncation and to choice of C value. In general, the truncation of D_{min} -0.2 yields superior results to the case of eliminating only the data above D_{min} -0.1.

The beta values for the best cases (lowest standard error) using the cubic equations are given in Table 1 for the four data sets. The variable x used in the computations was the distance in mm along the sensitometer exposure. A difference of 1.0 in relative $\log_{10}E$ is equal to 52.7 mm, and at that value of x the terms of equation 2 are shown. It is notable that there is not a set pattern for the sign of β_1, β_2 and β_3 and that the higher order terms of the series expression are quite large. The series does not converge nicely, and these results suggest the need to test an equation with fourth- and fifth-order terms. We found, incidentally, that at the points on Figures 5 and 6 where the quadratic curves intersected the cubic curves, the value of β_3 was indeed zero for the cubic model.

Figures 4 through 7 also show for the cubic model that a sufficient range of C values has been attempted to find where the minimum error occurs. The curves for the quadratic model do not in all cases reach the minimum point. It is apparent, though, from their decreasing slopes

Table 1. Beta coefficients for the best fit of the cubic model for each of the four data sets. The terms of equation 2 are also computed for x = 52.7 mm (1 unit of $\log_{10}E$).

Data Set	β_0	β_1 (10^{-3} mm^{-1})	β_2 (10^{-4} mm^{-2})	β_3 (10^{-6} mm^{-3})	$\beta_1 x$	$\beta_2 x^2$	$\beta_3 x^3$
1 (Red)	1.08	-8.96	0.42	-7.61	-0.472	0.116	-1.11
2 (Green)	1.08	-3.33	-6.27	0.615	-0.175	-1.740	0.0904
3 (Blue)	1.25	6.62	-1.09	-3.89	-0.348	-0.303	-0.568
4 (Clear)	1.16	-6.34	1.80	-7.14	-0.334	0.500	-1.04

at the lower ends that they will reach minimum values that are higher than those we have obtained in other cases.

CONCLUSIONS

We have exhibited strong evidence that an exponential model which is second or third order in log exposure is accurate for a set of integral density characteristic curves of CIR film. It remains to be seen if the relationship holds for a variety of emulsions and processing runs. Usually one would expect few differences in curve shape -- only differences in speed or absolute value of $\log_{10}E$.

Our next test should include fourth- and fifth-order terms, especially in the case of the blue response curve where the best case gave a standard error of 0.083 density units. Further truncation of the high density data might also reduce the error to the excellent results of about 0.03 obtained for the red, green and clear curves.

LITERATURE CITED

1. Dana, R. W., and R. J. Myhre. 1971. Calibration of Color Aerial Photography. In: Monitoring Forest Land from High Altitude and from Space. Annual Progress Report for Earth Resources Survey Program. OSSA/NASA, by the Pacific Southwest Forest and Range Experiment Station. 48 p., illus.

APPENDIX A

NASA-USDA FORESTRY AND RANGE REMOTE SENSING RESEARCH PROGRAM "REMOTE SENSING APPLICATIONS IN FORESTRY" SERIES

1966 Annual Reports

STAR* No.	Title
N67-19905	Carneggie, D. M., W. C. Draeger and D. T. Lauer. The use of high altitude, color and spectrozonal imagery for the inventory of wildland resources. Vol. I: The timber resource. School of Forestry and Conservation, University of California, Berkeley. 75 pages.
N66-39698	Carneggie, D. M., E. H. Roberts and R. N. Colwell. The use of high altitude, color and spectrozonal imagery for the inventory of wildland resources. Vol. II: The range resource. School of Forestry and Conservation, University of California, Berkeley. 22 pages.
N67-19939	Carneggie, D. M. and R. N. Colwell. The use of high altityde, color and spectrozonal imagery for the inventory of wildland resources. Vol. III: The soil, water, wildlife and recreation resource. School of Forestry and Conservation, University of California, Berkeley. 42 pages.
N66-39304	Heller, R. C. et al. The use of multispectral sensing techniques to detect ponderosa pine trees under stress from insect or pathogenic organisms. Pacific Southwest Forest and Range Experiment Station, U.S. Forest Service, USDA. 60 pages.
N66-39386	Lauer, D. T. The feasibility of identifying forest species and delineating major timber types in California by means of high altitude small scale aerial photography. School of Forestry and Conservation, University of California, Berkeley. 130 pages.
N66-39700	Wear, J. F. The development of spectro-signature indicators of root disease on large forest areas. Pacific Southwest Forest and Range Experiment Station, U.S. Forest Service, USDA. 24 pages.

*Available through NASA Scientific Technical and Information Facility, P. O. Box 33, College Park, Maryland 20740.

STAR No.	Title
N66-39303	Lent, J. D. Cloud cover interference with remote sensing of forested areas from earth-orbital and lower altitudes. School of Forestry and Conservation, University of California, Berkeley. 47 pages.
N66-39405	Weber, F. P. Multispectral imagery for species identification. Pacific Southwest Forest and Range Experiment Station, U.S. Forest Service, USDA. 37 pages.

1967 Annual Reports

N68-17406	Draeger, W. C. The interpretability of high altitude multispectral imagery for the evaluation of wildland resources. School of Forestry and Conservation, University of California, Berkeley. 30 pages.
N68-17494	Lauer, D. T. The feasibility of identifying forest species and delineating major timber types by means of high altitude multispectral imagery. School of Forestry and Conservation, University of California, Berkeley. 72 pages.
N68-17671	Carneggie, D. M., C. E. Poulton and E. H. Roberts. The evaluation of rangeland resources by means of multispectral imagery. School of Forestry and Conservation, University of California, Berkeley. 76 pages.
N68-17378	Wear, J. F. The development of spectro-signature indicators of root disease on large forest areas. Pacific Southwest Forest and Range Experiment Station, U.S. Forest Service, USDA. 22 pages.
N68-17408	Heller, R. C., R. C. Aldrich, W. F. McCambridge and F. P. Weber. The use of multispectral sensing techniques to detect ponderosa pine trees under stress from insect or pathogenic organisms. Pacific Southwest Forest and Range Experiment Station, U.S. Forest Service, USDA. 65 pages.
N68-17247	Weber, F. P. and C. E. Olson. Remote sensing implications of changes in physiologic structure and function of tree seedlings under moisture stress. School of Natural Resources, University of Michigan. 61 pages.

STAR No.	Title
	1968 Annual Reports
N69-16461	Lent, J. D. The feasibility of identifying wildland resources through the analysis of digitally recorded remote sensing data. School of Forestry and Conservation, University of California, Berkeley. 130 pages.
N69-25632	Carneggie, D. M. Analysis of remote sensing data for range resource management. School of Forestry and Conservation, University of California, Berkeley. 62 pages.
N69-16113	Lauer, D. T. Forest species identification and timber type delineation on multispectral photography. School of Forestry and Conservation, University of California, Berkeley. 85 pages.
N72-74471	Driscoll, R. S. and J. N. Reppert. The identification and quantification of plant species, communities and other resource features in herbland and shrubland environments from large scale aerial photography. Rocky Mountain Forest and Range Experiment Station, U.S. Forest Service, USDA. 62 pages.
**	Wear, J. F. The development of spectro-signature indicators of root disease impact on forest stands. Pacific Southwest Forest and Range Experiment Station, U.S. Forest Service, USDA. 27 pages.
N69-16390	Poulton, C. E., B. J. Schrumpf and E. Garcia-Moya. The feasibility of inventorying native vegetation and related resources from space photography. Department of Range Management, Agricultural Experiment Station, Oregon State University. 47 pages.
N71-37947	Heller, R. C., R. C. Aldrich. W. F. McCambridge, F. P. Weber and S. L. Wert. The use of multispectral sensing techniques to detect ponderosa pine trees under stress from insect or pathogenic organisms. Pacific Southwest Forest and Range Experiment Station, U.S. Forest Service, USDA. 45 pages.
N69-12159	Draeger, W. C. The interpretability of high altitude multispectral imagery for the evaluation of wildland resources. School of Forestry and Conservation, University of California, Berkeley. 68 pages.

**STAR number not available.

STAR No.	Title
N72-74472	Langley, P. G. and D. A. Sharpnack. The development of an earth resources information system using aerial photographs and digital computers. Pacific Southwest Forest and Range Experiment Station, U.S. Forest Service, USDA. 26 pages.
N69-15856	Olson, C. E. and J. M. Ward. Remote sensing of changes in morphology and physiology of trees under stress. School of Natural Resources, University of Michigan. 43 pages.

1969 Annual Reports

N70-41162	Olson, C. E., J. M. Ward and W. G. Rohde. Remote sensing of changes in morphology and physiology of trees under stress. School of Natural Resources, University of Michigan. 43 pages.
N70-41164	Heller, R. C., R. C. Aldrich, W. F. McCambridge and F. P. Weber. The use of multispectral sensing techniques to detect ponderosa pine trees under stress from insect or diseases. Pacific Southwest Forest and Range Experiment Station, U.S. Forest Service, USDA. 59 pages.
N70-42044	Langley, P. G., D. A. Sharpnack, R. M. Russell and J. Van Roessel. The development of an earth resources information system using aerial photographs and digital computers. Pacific Southwest Forest and Range Experiment Station, U.S. Forest Service, USDA. 43 pages.
N70-41064	Driscoll, R. S. The identification and quantification of herbland and shrubland vegetation resources from aerial and space photography. Rocky Mountain Forest and Range Experiment Station, U.S. Forest Service, USDA. 55 pages.
N70-41282	Colwell, R. N. et al. Analysis of remote sensing data for evaluating forest and range resources. School of Forestry and Conservation, University of California, Berkeley. 207 pages.
N70-41063	Poulton, C. E., E. Garcia-Moya, J. R. Johnson and B. J. Schrumpf. Inventory of native vegetation and related resources from space photography. Department of Range Management, Agricultural Experiment Station, Oregon State University. 66 pages.

STAR No.	Title
N70-41217	Wear, J. F. and F. P. Weber. The development of spectro-signature indicators of root disease impacts on forest stands. Pacific Southwest Forest and Range Experiment Station, U.S. Forest Service, USDA. 58 pages.

1970 Annual Reports

**	Wilson, R. C. Potentially efficient forest and range applications of remote sensing using earth orbital spacecraft -- circa 1980. School of Forestry and Conservation, University of California, Berkeley. 199 pages.
**	Aldrich, R. C., W. J. Greentree, R. C. Heller and N. X. Norick. The use of space and high altitude aerial photography to classify forest land and to detect forest disturbances. Pacific Southwest Forest and Range Experiment Station, U.S. Forest Service, USDA. 36 pages.
**	Driscoll, R. S. and R. E. Francis. Multistage, multiseasonal and multiband imagery to identify and quantify non-forest vegetation resources. Rocky Mountain Forest and Range Experiment Station, U.S. Forest Service, USDA. 65 pages.
**	Personnel of Forestry Remote Sensing Laboratory. Analysis of remote sensing data for evaluating vegetation resources. School of Forestry and Conservation, University of California, Berkeley. 171 pages.
**	Meyer, M. P., D. W. French, R. P. Latham and C. A. Nelson. Vigor loss in conifers due to dwarf mistletoe. School of Forestry, University of Minnesota. 21 pages.
N71-36770	Langley, P. G., J. Van Roessel, D. A. Sharpnack and R. M. Russell. The development of an earth resources information system using aerial photographs and digital computers. Pacific Southwest Forest and Range Experiment Station, U.S. Forest Service, USDA. 32 pages.
N72-28321	Weber, F. P. and J. F. Wear. The development of spectro-signature indicators of root disease impacts on forest stands. Pacific Southwest Forest and Range Experiment Station, U.S. Forest Service, USDA. 46 pages.
**	Heller, R. C., F. P. Weber and K. A. Zealear. The use of multispectral sensing techniques to detect ponderosa pine trees under stress from insects or diseases. Pacific Southwest Forest and Range Experiment Station, U.S. Forest Service, USDA. 50 pages.

**STAR number not available.

STAR No.	Title
N72-27375	Olson, C. E., W. G. Rohde and J. M. Ward. Remote sensing of changes in morphology and physiology of trees under stress. School of Natural Resources, University of Michigan. 26 pages.

1971 Annual Reports

N71-32815	Dana, R. W. Calibration of color aerial photography. Pacific Southwest Forest and Range Experiment Station, U.S. Forest Service, USDA. 14 pages.
N72-28327	Driscoll, R. S. and R. E. Francis. Multistage, multiband and sequential imagery to identify and quantify non-forest vegetation resources. Rocky Mountain Forest and Range Experiment Station, U.S. Forest Service, USDA. 75 pages.
N72-28328	Amidon, E. L., D. A. Sharpnack and R. M. Russell. The development of an earth resources information system using aerial photographs and digital computers. Pacific Southwest Forest and Range Experiment Station, U.S. Forest Service, USDA. 7 pages.
N72-28324	Personnel of the Remote Sensing Research Work Unit. Monitoring forest land from high altitude and from space. Pacific Southwest Forest and Range Experiment Station, U.S. Forest Service, USDA. 179 pages.
N72-28326	Poulton, C. E., D. P. Faulkner, J. R. Johnson, D. A. Mouat and B. J. Schrumpf. Inventory and analysis of natural vegetation and related resources from space and high altitude photography. Department of Range Management, Agricultural Experiment Station, Oregon State University. 59 pages.
N72-28325	Meyer, M. P., D. W. French, R. P. Latham, C. A. Nelson and R. W. Douglass. Remote sensing of vigor loss in conifers due to dwarf mistletoe. School of Forestry, University of Minnesota. 40 pages.
N72-28037	Olson, C. E., W. G. Rohde and J. M. Ward. Remote sensing of changes in morphology and physiology of trees under stress. School of Natural Resources, University of Michigan. 77 pages.
**	Personnel of Forestry Remote Sensing Laboratory. Analysis of remote sensing data for evaluating vegetation resources. School of Forestry and Conservation, University of California. 195 pages.

**STAR number not available.

STAR No.	Title
	1972 Annual Reports
**	Driscoll, R. S. and R. E. Francis. Multistage, multiband and sequential imagery to identify and quantify non-forest vegetation resources. Rocky Mountain Forest and Range Experiment Station, U.S. Forest Service, USDA. 42 pages.
**	Amidon, E. L., D. A. Sharpnack and R. M. Russell. The development of an earth resources information system using aerial photographs and digital computers. Pacific Southwest Forest and Range Experiment Station, U.S. Forest Service, USDA. 23 pages.
**	Poulton, C. E. Inventory and analysis of natural vegetation and related resources from space and high altitude photography. Range Management Program, Agricultural Experiment Station, Oregon State University. 48 pages.
**	Personnel of the Remote Sensing Research Work Unit. Monitoring forest land from high altitude and from space. Pacific Southwest Forest and Range Experiment Station, U.S. Forest Service, USDA. 200 pages.
**	Olson, Jr., C. E. Remote sensing of changes in morphology and physiology of trees under stress. School of Natural Resources, University of Michigan. 26 pages.
**	Personnel of the Forestry Remote Sensing Laboratory. Analysis of remote sensing data for evaluating vegetation resources. School of Forestry and Conservation, University of California, Berkeley. 245 pages.
**	Douglass, R. W., M. P. Meyer and D. W. French. Remote sensing applications to forest vegetation classification and conifer vigor loss due to dwarf mistletoe. College of Forestry, University of Minnesota. 86 pages.

**STAR number not available.